

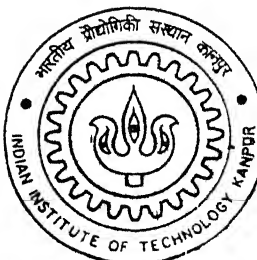
Y010110

AN EXPERIMENTAL STUDY OF LEAN PREMIXED TURBULENT FLAME BASED COMBUSTOR

By

R. KANNAN

TH
AE/2002/M
K133e



DEPARTMENT OF AEROSPACE ENGINEERING

Indian Institute of Technology Kanpur

FEBRUARY, 2002

**AN EXPERIMENTAL STUDY OF LEAN PREMIXED
TURBULENT FLAME BASED COMBUSTOR**

A Thesis Submitted
in Partial Fulfillment of the Requirements
for the Degree of

Master of Technology

by

R.KANNAN



to the
DEPARTMENT OF AEROSPACE ENGINEERING
INDIAN INSTITUTE OF TECHNOLOGY
KANPUR-208016
FEBRUARY-2002

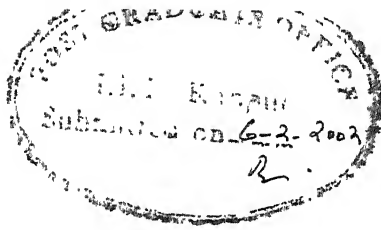
/AF

पुस्तकालय
भारतीय विद्योपीठ विश्वविद्यालय कानपुर
ब्राह्मि नं 3.7903.....



A137903

CERTIFICATE



It is certified that the work contained in the thesis entitled "An Experimental Study of Lean Premixed Turbulent Flame Based Combustor", by Mr. R.Kannan, has been carried out under my supervision and this work has not been submitted elsewhere for a degree.

D.P.Mishra

(Dr. D.P.Mishra)

Department of Aerospace Engineering,
Indian Institute of Technology,
Kanpur-208016.

5th February 2002

ACKNOWLEDGEMENTS

I express my deep sense of gratitude to my guide Dr. D.P.Mishra, for his overwhelming support, constructive criticism and guidance. I am very grateful to my guide for his personal as well as technical guidance during my M.Tech Programme.

I am thankful to Mr.J.B.Mishra, Mr.Ramanuj, Mr.V.K.Shrivastava, Mr.S.S.Chauhan, Mr.Ganveer, Mr.Suresh Mishra, and Mr.Sharad for their help at various stages of my work. I express my appreciation and deep sense of gratitude to all of my friends who apart from helping me in this work also have made my stay at Kanpur very pleasant and memorable.

Finally but not least I am so grateful to the Almighty God and Guru who gave me so much of courage and enthusiasm to do the job very efficiently.

R.KANNAN

Dedicated to two divine souls
my Father and Mother
who inspired me to do this.

Abstract

The growing world wide concern for emissions from aircraft gas turbines engines, stationary power plants, furnaces, boilers, and other combustion devices has motivated us to the study of the turbulent of lean premixed flame based combustor. The combustion process in the lean combustor is studied with help of coaxial burner. Both bluff body and vane swirler flame stabilizers are employed in stabilizing the turbulent lean premixed flame. The partially premixed fuel injection strategy has been adopted to enhance the stability limits.

The lean stability and emission analysis for bluff body stabilized flames are investigated in details for two flame holder location, $H/D_{core} = 0.61 \text{ & } 5.0$. The stability limit is measured for a wide range core velocity of 4-20 m/s. The lean stability limit for coflow air stream is found to be improved for $H/D_{core} = 5.0$ due to the improved mixing of coflow with core flow streams. But there is an increase of the NO emission for $H/D_{core} = 5.0$, which may be due to the higher combustion gas temperature due to improved mixing between the coflow and core flow. On the contrary, the CO emission level is reduced considerably, which this may be attributed to the presence of excess coflow air. In order to reduce the emission level, the fuel-air mixture is injected in the coflow stream instead of air. The stability limit is improved marginally for $H/D_{core} = 5.0$ when the premixed mixture is used in the coflow stream. Interestingly, this partially premixed fuel injection in the coflow stream although reduces the NO emission level, but produces little more CO emission.

The lean flame stability and emission level are studied for swirl generated in the coflow with use of vane swirlers. The effects of swirl numbers (0.13 & 0.67) on the lean stability and emission levels are studied for two different coflow air. It has been found that there is an improvement of the stability limit and CO emission level for high swirl number (0.67) case as compared to low swirl number (0.13). On the contrary, the NO emission level is increased considerably due to the higher temperature prevailing in the burner. An attempt is also made to inject fuel premixed mixture to the coflow stream. For lower coflow velocity, the stability and CO emission level for lower swirl number show slight improvement due to presence of improved fuel distribution. The CO emission level is increasing in the case of lower swirl number with higher coflow velocity ($V_{cf} = 2.56$). In the case of low swirl number, the NO emission is improved with addition of fuel-air mixture to the coflow. But, the NO emission does not show any significant change in the higher swirl number. However, the CO emission level is improved for the case of higher swirl number with higher coflow velocity. Besides this, efforts are made to measure overall sound pressure level using microphone based sound level meter for both cold and reacting flow. Interestingly, the sound level is increased significantly when combustion takes place. With increase in coflow velocity, the sound level decreases significantly particularly at higher core flow velocity. However, it seems that the swirl number does not have much effect on the sound level.

CONTENTS

1. INTRODUCTION	1
1.1. Introduction	1
1.2. Diffusion Flame Based Combustor	2
1.3. Premixed Flame Based Combustor	3
1.3.1. Its Applications	5
1.3.2. Design Aspects of Premixed Flame Based Burners	5
1.4. Flame Stabilization	6
1.4.1. Bluff Body Flame Stabilizer	7
1.4.2. Swirler	8
1.4.3. Opposed Reacting Jet	11
1.5. Conclusion	11
2. LITERATURE SURVEY	12
2.1. Experimental Aspects of Lean Premixed Combustion	12
2.2. Scope of Work	17
3. EXPERIMENTAL SETUP	18
3.1. Introduction	18
3.2. Experimental Setup Facility	18
3.2.1. Air System	18
3.2.2. Fuel System	20
3.2.3. Coaxial Burner	21
3.2.4. Swirl Burner	23
3.3. Measurement Methods	23
3.3.1. Air Flow Measurement	23
3.3.1.1. Flow Meter	23
3.3.1.2. Calibration of Flow Meter	23
3.3.2 Temperature Measurement	26

3.3.3. Emission Measurement	26
3.3.4. Sound Pressure Level Measurement	26
3.4. Experimental Precautions and Safety Measures	26
3.5. Experimental Procedure	27
3.5.1. Co-axial Burner	27
3.5.2. Swirl Burner	27
3.5.3. Sample Calculation	28
3.6. Validation of Experimental Setup	29
3.7. Concluding Remarks	29
4. RESULT AND DISCUSSION	31
4.1. Introduction	31
4.2. Bluff Body Stabilized Flame With Coflow Air	31
4.2.1. Lean Stability Limits	31
4.2.2. Flame Structure	35
4.2.3. Exit Gas Temperature	38
4.2.4. Exhaust Gas Emission Characteristics	38
4.2.4.1.Exhaust Gas Oxygen Content	38
4.2.4.2.Exhaust CO Emission	42
4.2.4.3.Exhaust CO ₂ Content	44
4.2.4.4.Exhaust NO Content	46
4.3. Bluff Body Stabilized Flame With Fuel-Air Coflow Mixture	49
4.3.1. Lean Stability Limit	49
4.3.2. Combustion Gas Exit Temperature	51
4.3.3. Exhaust O ₂ Content	53
4.3.4. Exhaust CO Content	53
4.3.5. Exhaust CO ₂ Emission	56
4.3.6. Exhaust NO Emission	56
4.3.7. NO _x Emission	60
4.4. Swirl Stabilized Flame Analysis	60
4.4.1. Lean Stability Limits	60
4.4.2. Exit Temperature Distribution	64
4.4.3. Exhaust Gas O ₂ Content	64
4.4.4. Exhaust Gas CO Emission	67

4.4.5. Exhaust CO ₂ Emission	70
4.4.6. Exhaust NO Emission	70
4.4.7. Overall Sound Pressure Level Measurements	74
4.5. Uncertainty Analysis	75
4.6. Concluding Remarks	78
4.7. Suggestion For Future Work	79
REFERENCES	80

LIST OF FIGURES

1.1.	A schematic of a typical gas turbine combustor	3
1.2.	A schematic of a thermal profile through a laminar premixed flame	4
1.3.	A schematic of a flashback suppression in a premixed combustion system	6
1.4.	A schematic of turbulent flame stabilization by a bluff body	8
1.5.	A schematic of recirculation zone created by swirl flow	9
1.6.	A schematic diagram of opposed reacting jet	10
3.1	A schematic diagram of experimental setup	19
3.2	A schematic of the coaxial burner	21
3.3a	A schematic diagram of swirl burner	22
3.3b	A schematic of swirler with guide vane assembly	22
3.4	A schematic of the flow meter calibration setup	24
3.5	Calibration chart for nozzle flow meter	25
3.6	Calibration chart for orifice flow meter	25
3.7	Validation of experimental setup	29
4.1	Lean stability limit for $H/D_{core} = 0.61$ with coflow air only	32
4.2	Lean stability limit for $H/D_{core} = 5.0$ with coflow air only	32
4.3	Schematic of mixing geometry between the core and coflow for the flame holder located within the potential core	33
4.4	Schematic of mixing geometry between the core and coflow for the flame holder located above the potential core	35
4.5	Schematic of recirculatory flow behind wedge flame holder	36
4.6	Schematic of bluff body stabilized flame structure for different core velocity	36
4.7a	Exit gas temperature distribution for $H/D_{core} = 0.61$ with a coflow velocity of 1.28 m/s	39
4.7 b	Exit gas temperature distribution for $H/D_{core} = 5.0$ with a coflow velocity of 1.28 m/s	39

4.8	Average exit temperature for $H/D_{core} = 0.61$ with coflow air only	40
4.9	Average exit gas temperature for $H/D_{core} = 5.0$ with coflow air only	39
4.10	Exhaust gas O_2 content for $H/D_{core} = 0.61$ with coflow air only	41
4.11	Exhaust gas O_2 content for $H/D_{core} = 5.0$ with coflow air only	41
4.12	Exhaust gas CO emission for $H/D_{core} = 0.61$ with coflow air only	43
4.13	Exhaust gas CO emission for $H/D_{core} = 5.0$ with coflow air only	43
4.14	Exhaust gas CO_2 content for $H/D_{core} = 0.61$ with coflow air only	45
4.15	Exhaust gas CO_2 content for $H/D_{core} = 5.0$ with coflow air only	45
4.16	Exhaust gas NO emission for $H/D_{core} = 0.61$ with coflow air only	47
4.17	Exhaust gas NO emission for $H/D_{core} = 5.0$ with coflow air only	47
4.18	Exhaust gas NO_x emission for $H/D_{core} = 0.61$ with coflow air only	48
4.19	Exhaust gas NO_x emission for $H/D_{core} = 5.0$ with coflow air only	48
4.20	Lean Stability limit for $H/D_{core} = 0.61$ with coflow air velocity = 1.28 m/s	50
4.21	Lean Stability limit for $H/D_{core} = 5.0$ with coflow air velocity = 1.28 m/s	50
4.22	Exit gas temperature distribution for $H/D_{core} = 0.61$ with coflow velocity = 1.28 m/s & $\phi_{cf} = 0.596$	51
4.23	Average combustion gas temperature for $H/D_{core} = 0.61$ with coflow fuel premixed with air	52
4.24	Average combustion gas temperature for $H/D_{core} = 5.0$ with coflow fuel premixed with air	52
4.25	Exhaust gas O_2 for $H/D_{core} = 0.61$ with coflow air velocity = 1.28 m/s	54
4.26	Exhaust gas O_2 for $H/D_{core} = 5.0$ with coflow air velocity = 1.28 m/s	54
4.27	Exhaust gas CO for $H/D_{core} = 0.61$ with coflow air velocity = 1.28 m/s	55
4.28	Exhaust gas CO for $H/D_{core} = 5.0$ with coflow air velocity = 1.28 m/s	55
4.29	Exhaust gas CO_2 for $H/D_{core} = 0.61$ with coflow air velocity = 1.28 m/s	57

4.30	Exhaust gas CO ₂ for H/D _{core} = 5.0 with coflow air velocity = 1.28 m/s	57
4.31	Exhaust gas NO for H/D _{core} = 0.61 with coflow air velocity = 1.28 m/s	58
4.32	Exhaust gas NO for H/D _{core} = 5.0 with coflow air velocity = 1.28 m/s	58
4.33	Exhaust gas NO _x for H/D _{core} = 0.61 with coflow air velocity = 1.28 m/s	59
4.34	Exhaust gas NO _x for H/D _{core} = 5.0 with coflow air velocity = 1.28 m/s	59
4.35	Lean stability for the Swirl No. 0.13 with coflow air or fuel premixed with air	61
4.36	Effect of Core equivalence ratio for the Swirl No. 0.13 with coflow velocity of 1.5 m/s	61
4.37	Effect of Core equivalence ratio for the Swirl No. 0.13 with coflow velocity of 2.56 m/s	62
4.38	Lean stability for the Swirl No. 0.67 with coflow air or fuel premixed with air	62
4.39	Effect of Core equivalence ratio for the Swirl No. 0.67 with coflow velocity of 2.56 m/s	63
4.40	Exhaust gas combustion temperature for the Swirl No. 0.13 with coflow air or fuel premixed with air	65
4.41	Exhaust gas combustion temperature for the Swirl No. 0.67 with coflow air or fuel premixed with air	65
4.42	Exhaust gas O ₂ for the Swirl No. 0.13 with coflow air or fuel premixed with air	66
4.43	Exhaust gas O ₂ for the Swirl No. 0.67 with coflow air or fuel premixed with air	66
4.44	Exhaust gas CO for the Swirl No. 0.13 with coflow air or fuel premixed with air	68
4.45	Exhaust gas CO for the Swirl No. 0.67 with coflow air or fuel premixed with air	68
4.46	Exhaust gas CO ₂ for the Swirl No. 0.13 with coflow air or fuel premixed with air	69

4.47	Exhaust gas CO ₂ for the Swirl No. 0.67 with coflow air or fuel premixed with air	69
4.48	Exhaust gas NO for the Swirl No. 0.13 with coflow air or fuel premixed with air	71
4.49	Exhaust gas NO for the Swirl No. 0.67 with coflow air or fuel premixed with air	71
4.50	Exhaust gas NO _x for the Swirl No. 0.13 with coflow air or fuel premixed with air	72
4.51	Exhaust gas NO _x for the Swirl No. 0.67 with coflow air or fuel premixed with air	72
4.52	Overall Sound Pressure Level for Swirl No. 0.13 with coflow velocity of 1.5 m/s	73
4.53	Overall Sound Pressure Level for Swirl No. 0.13 with coflow velocity of 2.56 m/s	73
4.54	Overall Sound Pressure Level for Swirl No. 0.67 with coflow velocity of 2.56 m/s	74

NOMENCLATURE

Q_{A_2}	Coflow airflow rate (lpm)
Q_{F_1}	Core fuel flow rate (lpm)
Q_{F_2}	Coflow fuel flow rate (lpm)
Q_{A_1}	Core airflow rate (lpm)
α	Coefficient of Diffusivity (m^2/s)
μ	Dynamic Viscosity ($N\ s/m^2$)
α_1	Vane angle
ϕ_{cf}	Coflow equivalence ratio
ϕ_{core}	Core equivalence ratio
$(F/A)_{stoich}$	Stoichiometric fuel-air ratio
ϕ_{ov}	Overall equivalence ratio
ρ	Density of air (kg/m^3)
F/A	Fuel-air ratio
G_ϕ	Axial flux of angular momentum
G_x	Axial flux of linear momentum
Pe	Pecklet Number
Re	Reynolds Number
SN	Swirl number
V_{av}	Average Velocity (m/s)
V_{cf}	Coflow Velocity (m/s)
V_{core}	Core Velocity (m/s)

CHAPTER-1

Introduction

1.1 Introduction

The growing world wide concern for emissions from the aircraft gas turbines engines, stationary power plants, furnaces, boilers, and other combustion devices has motivated several researchers to investigate them thoroughly during last two decades. To mitigate this perennial problem, several researchers have undertaken both experimental and numerical investigations of the combustors to understand the mechanism of combustion processes and find out better cost effective methods to minimize the emission level from such devices. Although, over the years considerable progresses have been made in reducing the emission level, but there is a lot more to be done for further reduction of emission level. Hence, it is believed that more research effort will also continue into future.

The design of modern combustor is more dictated by the stringent environmental constraints. Because, the emissions from combustion devices can cause immense harm to both human beings and vegetation. It has been reported that high pollutant level in atmosphere can enhance more chances of morbidity and mortality in human beings in future. The major pollutants from the combustion devices are CO, CO₂, NO_x, SO_x, unburnt hydrocarbons (UHC), particulates and etc, which increase the pollution level in air. The green house gases like NO_x, CO, soot, and unburnt hydrocarbons are the main cause for global warming [1]. Of course the local increase in pollution level is mainly caused by the automotives particularly in urban areas. It has been reported in literature that sustained exposure to the carbon monoxide and oxides of nitrogen can affect the health of human being considerably. The photochemical smog is caused by the combination of hydrocarbon with oxides of nitrogen. The vegetation is extensively affected by the phototoxicants SO₂, peroxyacetyl nitrate (PAN), C₂H₄ and others. The very chlorophyll of the leaves is being destroyed by these phototoxicants that may lead to disruption of photosynthesis. It must be kept in

mind that the photosynthesis is one of the main processes, which sustains the life in the whole universe. Hence, the disruption of photosynthesis may threaten even the very existence of life in this earth. Of course, such kind of damage can be caused by pollutants in the troposphere, which is polluted by land based combustion devices. But the stratosphere region of the atmosphere is also affected adversely due to the increase of emissions level in recent time particularly by high-speed aircraft engines. The oxides of nitrogen and sulphur on reacting with the ozone layer destroy the ozone level, which would lead to increase in ultraviolet radiations to the earth's surface. It has been reported recently that there is a significant increase in skin cancers in human beings due to ozone layer depletion. Hence, there is growing concern for designing and developing eco-friendly combustion devices, which is the main motivation of the present investigation.

1.2 Diffusion Flame Based Combustors

Generally the combustion in most of practical combustors such as gas turbine, diesel and industrial furnaces are carried out employing the diffusion flames due to its inherent better stability conditions in the combustion devices over the whole range of their operations. For example, in jet engines as shown in Fig 1.1, a liquid fuel spray is introduced by injection into air before combustion can occur. The fuel, air and combustion products must interdiffuse through each other to form a uniform mixture. This is an example of diffusion flame (non-premixed flame) based combustor. The flame structure achieved in case of diffusion flame by means of burning gaseous fuel or the burning wake of a vaporizing fuel droplet, which cannot be influenced by the rate of reaction. These flames can provide less combustion intensity and combustion efficiency. And also, it generates automatically maximum level of pollutants. Because, the combustion in such devices generally takes place around stoichiometric fuel and air ratio where the flame temperature and NO_x formation reaches their maximum level. As a result, large amounts of NO_x are formed due to the very high temperature in the reaction zone. At the same time, the fuel is approaching the flame in the absence of oxygen leads to soot formation and incomplete combustion products, emitting large amount of CO and unburnt hydrocarbon. The inability of controlling the NO_x formation, unburnt hydrocarbons (UHC) adequately in a diffusion flame combustor led to development of new types of combustors. In recent times, there

is growing consensus among combustion engineers to design and develop premixed flame based combustor, which is expected to improve the characteristics of combustor. The lean premixed flame based combustor is preferred because the burning of a rich mixture causes the control of UHC emissions to be more difficult. Consequently, efforts are being underway by several researchers to design and develop pre-vaporized lean premixing combustor. Although there will be considerable decrease in NO_x level but the levels of carbon monoxide increases considerable when the combustor is operated under lean fuel-air condition [1]. Another problem it poses is the flame stability. The success of such kind of technology will be mainly dependent on the judicious design of the combustor by which better stabilization of flame can be achieved with minimum emission level. The present investigation is basically meant to address such problems of lean premixed combustor. In order to study the premixed flame characteristics, some fundamental concepts and terminology are required and these are discussed below.

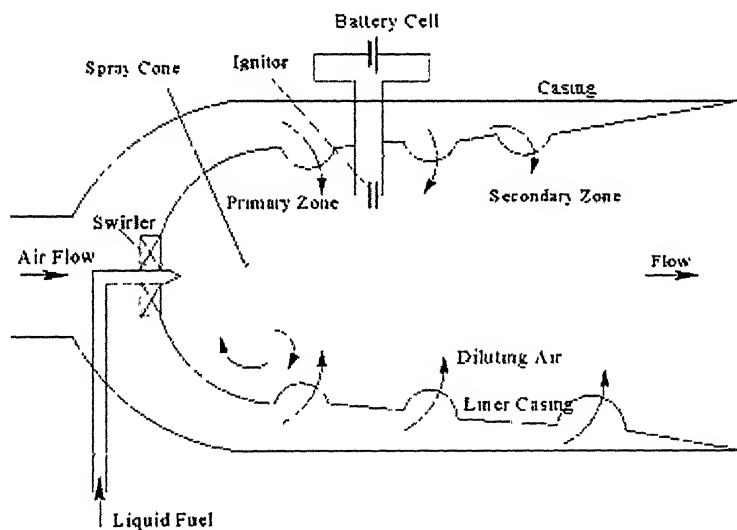


Fig 1.1 A Schematic of f a typical gas turbine combustor.

1.3. Premixed Flame Based combustor

Premixed flame is a combustion wave in an explosive medium in which both fuel and oxidizers are mixed at molecular level before the actual combustion is being taken place. Examples of the premixed flame are Bunsen burner flame in a laboratory, the flame in a jet engine afterburner and etc. In the Bunsen burner, gaseous fuel is injected into a tube open at the bottom, allowing air to be drawn in

by the fuel jet. In premixed combustor, not only gaseous fuel but also liquid and solid fuel can be utilized. The afterburner is also example of premixed flame based combustor in which liquid fuel is injected into hot turbine exhaust gases. The liquid droplets vaporize and mix with the air to form a premixed explosive mixture. Further downstream of the fuel injection, it is ignited near the flame stabilizer to which premixed flame is anchored. In the case of liquid rocket engine, the fuel and oxidizer are mixed at the molecular level before actual combustion could take place. The solid fuels can be burned by mixing fuel-oxidizer, for example in the solid rocket engine, molecular level mixing is also attained establishing premixed flames in the rocket motor.

In a premixed flame, the fuel and air are essentially premixed to form a mixture that is uniform in composition and temperature. Combustion occurs by the propagation of a flame front separating unburnt mixture from fully burnt mixture. In combustion chamber, the flame front is affected by the turbulence already present in the flow or generated by the combustion process. The premixed

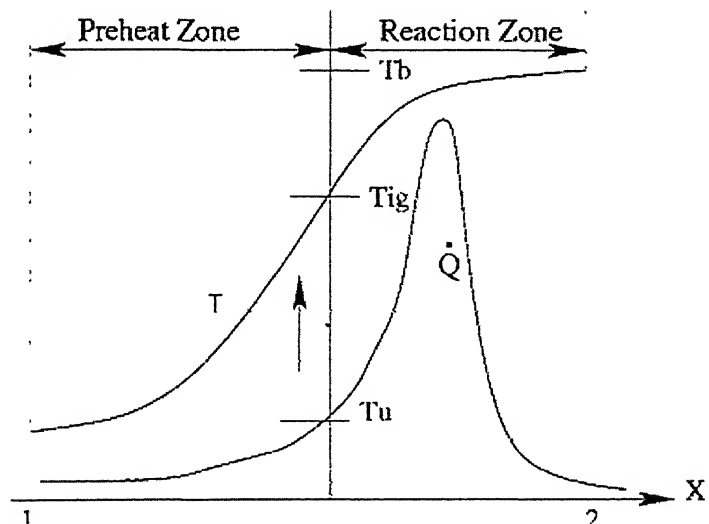


Fig 1.2. A schematic of thermal profile through a laminar premixed flame

flame can be divided into regions [2] as shown in Fig 1.2, one in which the intense exothermic reactions take place and the other which receives its temperature rise by thermal conduction from the hot zone. The temperature at that point dividing the two zones is generally closer to the ignition temperature, T_{ig} , the temperature

at which vigorous reaction starts. In the case of premixed explosive mixture, the occurrence of flash back is very common. Flash back occurs where the flame would propagate into the burner tube (see Fig 1.3) and leads to a dangerous situation. Flash back occurs when the laminar flame speed is greater than the velocity of the mixture. To avoid this, generally flash back suppressor is used in the laboratory experiments. The typical diagram of the flash back suppressor is shown in the Fig 1.3. Another problem faced by the premixed flame based burner is the blow off that occurs when the flame is driven away from the burner tip. Blow off occurs when the local flow velocity is greater than the flame speed. This can be avoided by choosing appropriate flame stabilization methods such as bluff body, swirler, opposed reacting jet, and etc. The stability of the premixed flames in the combustor will be discussed in details in subsequent sections.

1.3.1. Its Application

Premixed flames find a lot of applications in the field of thermal engineering due to the requirement of energy efficient combustion systems both in industries and home. Some of the applications of premixed flames are listed below:

1. Gas turbine engine, for power generation
2. I Bunsen burner in laboratory and homes.
3. Spark-ignition engine.
4. Modern gas-fuelled gas turbine engine.
5. Jet engine afterburners
6. Rocket motors
7. Explosives.

1.3.2. Design Aspects of Premixed Flame Based Burners

In premixing flame based combustor, fuel and air are mixed very well even to the molecular level before the actual combustion take place which helps in reducing unburnt hydrocarbon and CO formation. However, the premixed flame burner has two main problems such as flash back and blow off as mentioned earlier, which are very challenging problems to be tackled by the combustion engineers particularly from the point of view of safety as well as efficient combustion. The flash back should be avoided by using perforated plate or wire mesh. In order to avoid blow off, certain flame stabilization methods should be considered while designing a premixed flame combustor. By altering the mixture composition and

temperature, one can achieve the whole range of control over the premixed flame properties like burning velocity, ignition temperature and stability criteria. Hence, it is important to consider the above points while designing a premixed flame based combustor. Some of the flame stabilization methods are discussed briefly in the flowing sections.

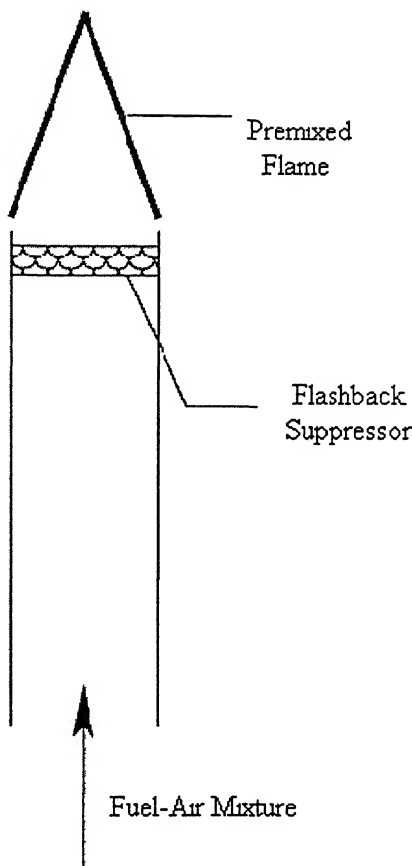


Fig 1.3. Schematic of flashback suppression in a premixed combustion system (Bunsen burner).

1.5 Flame Stabilization Methods

Premixed flame based combustor face several problems related to the stabilization of flame in the combustion chamber during its operation due to both lean and rich limit combustion operations. Hence, methods must be devised to stabilize the flame inside the combustor. Besides this, provision must be made particularly for jet engine such that in case of the blow out of the flame from the jet engine afterburner needs some kind of method to reignite the combustor. The accidental blow out of a flame in industrial devices can lead to discharge of raw fuel and

oxidizer with explosion hazards. The flow in most of the practical combustors is turbulent in nature. Normally turbulent flows are unsteady, but in many cases time averages of fluid properties like velocities, temperatures, etc. do exist. Due to unsteady and chaotic motion, the transport rates of heat, mass and momentum are greater in turbulent than in a laminar flow. Beside this turbulent flame speed is one order magnitude higher than the laminar flame speed. Normally turbulent flame speed of hydrocarbon-air mixture would be at most a few hundred centimeters per second. However, in many practical devices, such as ramjet and turbojet combustors in which high volumetric heat release rates are necessary, the flow velocities of the fuel-air mixture are of the order 50 m/s. Hence, a stabilization method is to be considered, for creating low velocity zone such that flame can be stabilized easily. The flame can be stabilized easily by creating a shear layer in the flow. Such kind of method is used in Bunsen burner. But, in practical systems, flame cannot be stabilized by similar methods. Rather, the flame stabilization is accomplished by causing some of the combustion products to recirculate and to continually ignite the fuel-air mixture. This is the primary requirement for flame stabilization. Of course, the continuous ignition could be obtained by inserting small pilot flames. Since pilot flames are an added inconvenience and by themselves can blow out, they are generally not used in fast flowing turbulent streams. Recirculation of combustion products can be obtained by inserting solid obstacles in the stream as pursued in ramjet technology (bluff body stabilization); by directing part of the flow or one of flow constituents, usually air opposed or normal to the main stream, as in gas turbine combustion chambers (aerodynamic stabilization); or by step in the wall enclosure, as in the so called dump combustors.

1.5.1. Bluff Body Flame Stabilizer

There are many methods to stabilize premixed flames in turbulent flows, but common method used in ramjets and afterburners is the use of bluff bodies inserted into the flow field. Because of finite viscosity, the fluid flow can't follow the body smoothly in the rear half section and the flow will separate from the body. This causes a recirculatory flow behind a circular cylinder (the bluff body) as shown in Fig 1.4, which helps in stabilizing the flame. It has been reported in literature [2] that the size of the recirculation zone does not change much with the

variation of upstream flow conditions as long as the flow is turbulent. However, there is slight change in the circulation zone in combustion situation as compared to cold flow condition. However, some of the combustible carried into the recirculation zone by turbulent mass transport and may be burned in the low velocity region. By the same way of mass transport, the products of combustion may exit from the recirculation zone. The heat transfer can take place from the hot recirculation zone to the in-coming combustible streams, rising the temperature toward the ignition condition. A schematic diagram of flow field and turbulent flame stabilization behind a circular cylindrical is shown in Fig 1.4. Generally, the flame is anchored little away from the bluff body while inclining to the incoming fresh mixture stream away from the wake region as shown in Fig 1.4. In the case of bluff body flame stabilization, there will be obstruction due to solid body which cause pressure loses in flow. This pressure loss increases with increase in the blockage ratio due of the bluff body flame stabilizer.

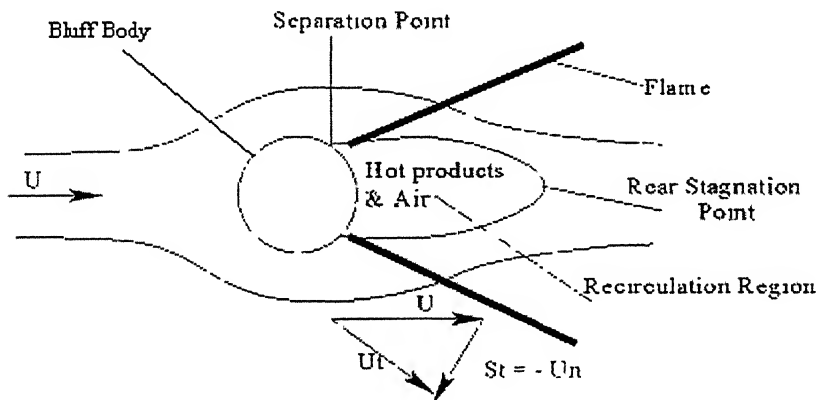


Fig 1.4. Schematic of turbulent flame stabilization by a bluff body [2].

1.5.2. Swirler

Swirlers are used in traditional combustion systems such as gas turbine engines, industrial burners, etc to improve and control the mixing rate between fuel and oxidizer, which helps in improving the flame stability in combustion chamber as shown in Fig 1.5. The aerodynamic behavior of swirling turbulent jet combines with the characteristics of rotating motion and the free turbulence phenomena encountered in jets and wake flows. Normally swirling turbulent flows are divided

into the following groups; such as turbulent swirling jets with weak swirl strongly swirling jets with internal recirculation and buoyant turbulent jets in rotating flow

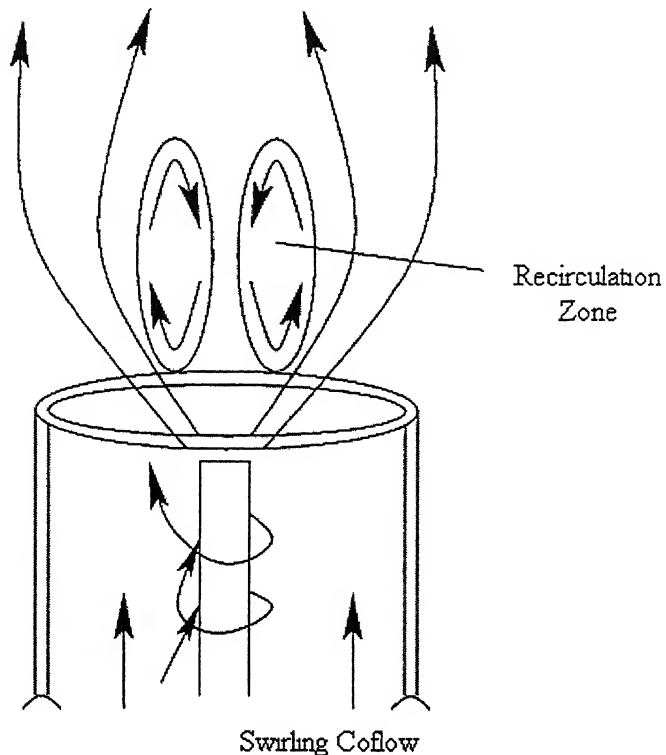


Fig 1.5. Schematic of the recirculation zone created by swirl flow

fields. When air is introduced tangentially into a burner, it is forced to change swirl angle, the flow can be either termed as weak or strong swirl. The swirl is characterized in terms of non-dimensional number, called swirl number,

$$\text{Swirl number, } \text{SN} = \frac{G_\phi}{G_x R} [3]$$

$$\text{Axial flux of angular momentum, } G_\phi = \int_0^R (\omega r) \rho U (2\pi r) dr = \text{constant}$$

$$\text{Axial flux of linear momentum, } G_x = \int_0^R \rho U^2 (2\pi r) dr + \int_0^R P (2\pi r) dr = \text{constant}$$

R= exit radius of the burner

Where

U, W and P are the axial and tangential components of the velocity and static pressure respectively in any cross section of the jet.

There are three methods for creating swirl flows:-

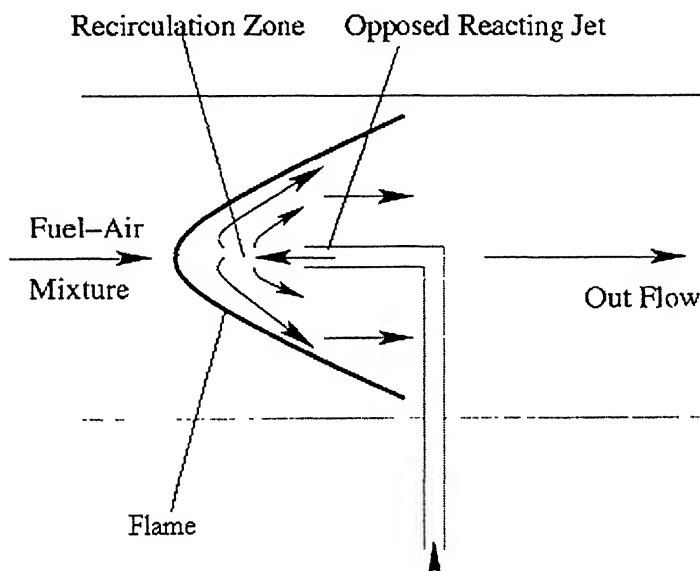
- a) tangential entry of the fluid stream
- b) the use of guide vanes in axial tube flow
- c) rotation of mechanical devices, which import a swirling motion to the fluid passing through it.

Due to the difficulty in measuring accurate velocity and static pressure distributions in a cross section of the swirling jets, one can redefine tangible swirl number by neglecting the static pressure term in the above equation. Then the modified swirl number becomes;

$$\text{Swirl number, SN} = \frac{G_\phi}{G_x R}$$

$$\text{Where, } G_x = 2\pi \int_0^R \rho U^2 r dr$$

At moderate level of swirl flow, an internal recirculation zone can be created, which allows high rate of heat release and helps in stabilizing the flame. This even provides stable and compact flame in adverse condition.



Fuel Premixed With Air or Air Only

Fig 1.6. A schematic of an opposed reacting jet flame stabilizer

1.5.3. Opposed Reacting Jet (ORJ)

The ORJ has several advantages, which make it adaptable to an investigation of the elementary processes governing pollutant formation. These are due to the simplified geometry as shown in Fig 1.6 and flow field provided by it. In the complex combustor configuration, the separation of fluid mechanical and chemical kinetics aspects of the combustion process is extremely difficult. The ORJ has greater control over the pollutant formation, equivalence ratio, inlet temperature, and recirculation zone size. The recirculation zone flow field in the ORJ is also having the characteristic of most conventional gas turbine combustors [4]. The ORJ is easy to study the pollutant formation when compared to the practical combustor.

1.6. Conclusion

A brief account about the types of combustors has been provided in this chapter. The need for better eco-friendly technologies for modern combustion devices has been adequately emphasized. Generally two types of combustor concepts such as diffusion flame based burner, and premixed flame based burners, are being discussed briefly. The recent trend is to design and develop lean premixed flame based combustor such that both the problems of pollutant emissions and energy crisis can be addressed at one stroke. Several types of flame stabilization techniques and their respective applications are discussed extensively in this chapter. This is the main motivation of the present investigation to study experimentally the flame stability and emission problems in a lean premixed flame based combustor. In the next chapter, the literatures related to turbulent lean premixed flame based burners are explored.

CHAPTER-2

LITERATURE SURVEY

In the present chapter, an extensive literature survey regarding the stability and emission control of lean premixed flame has been carried out. The literatures covering both experimental numerical studies are discussed separately in two following sections.

2.1. Experimental Aspects of Lean Premixed Combustion

Schefer and Sawyer [4] employed opposed reacting jet using propane as fuel in order to demonstrate the very lean stable combustion even equivalence ratio as low as 0.45. They achieved a very low NO_x as compared to conventional gas turbine engine. But CO level was higher due to lower residence time available for combustion as mentioned in this paper. Williams et al. [5] studied experimentally the flame stabilization as well as flame propagation in a high velocity stream. The experiments are done in a Bunsen burner with the help of different types of flame holders. They observed that the mechanism of flame stabilization behind bluff objects is different from that of Bunsen flames. Because the eddy region behind the bluff stabilizers is being filled with hot combustion products, which continuously ignite the approach gases. The effects of stabilizer's shape on the stability limit are negligible for several flame stabilizers such as rod, 30 open and closed edge gutters and flat plates. They observed that heating or cooling of the stabilizer greatly influences the stability limits. Heating extends the stability limits considerably while cooling narrows it down. Increasing of turbulence intensity decreases the stability limits. Later, the flame spreading from bluff-body flame holder was studied by Wright et al [6] to define the influence of certain chemical and fluidynamic parameters on the spreading of a simple flame in a duct. They found out by conducting series of experiments that the rate of flame spreading from a bluff body is slow and is remarkably independent of approach stream speed, temperature, fuel-air ratio and fuel type as long as the flame is turbulent and the flow is everywhere subsonic.

Zukoski et al [7] studied the wake transition effect in the bluff bodies flame stabilization process. They found that the blow off velocity of a bluff body flame holder increases, as the square root of the characteristic flame holder dimension over a substantial range of mixture ratios in presence of wake transition. But, they couldn't provide any convincing explanation to qualify the above statement. Bovina [8] investigated a study of heat exchange between the recirculation zone behind the flame holder and the outer flow since the stability of the flame is greatly dependent on the amount of heat received by the fresh mixture from the re-circulation zone. He devised a new method to find out the residence time of gas in the recirculation zone behind the flame holder for both cold and reacting flows by introducing and photoelectric recording of the luminous particles in the recirculation zone.

In 1960, Jeff [9] carried out extensive studies on can type combustors. He investigated several methods of controlling flow patterns within the can type combustors by designing appropriate mixing injection arrangements. The above effects were studied for three types of can combustors namely single row, shrouded cone and pepperpot can. In single row can type combustors, he observed that excellence flame stability can only be achieved at the expense of combustion efficiency. On further investigation, it was found that the lower efficiency is caused due to the formation of slow burning core of mixture surrounded by the burned material that was generated by flow reversal. Hence it was concluded that proper fuel-air mixing is essential for improved and uniform heat release rate. In another studies, Filippi and Mazza [10] employed a single cylindrical rod of 5mm dia in a rectangular chamber to stabilize the flame. In order to enhance the stability limit further, they tried to inject small quantity of fuel in the recirculation zone. During their studies, they used several flame holder configurations with various fuels as injecting fuels. It was observe that the injection of fuel in the flame holder wake had no significant effect on enhancing the flame stability limit. Since bluff body flame stabilizer obstructs the flow and reduced by the stream of higher-pressure loss.

Winterfield [11] described the process of the turbulent exchange of mass, momentum and energy behind the flame holder. He found that the spreading of

the flame is occurring by the turbulent transport of heat from the flame at the boundary of the recirculation zone to the adjacent unburnt gas. He also observed that the turbulent exchange is mainly attributed to the geometry of the recirculation zone and the residence time of the gas particles within the recirculation zone. The effect of various degree of swirl such as weak, moderate and strong ranges over an axisymmetric free turbulent jet was carried out experimentally by Chigier and Chervinsky [12]. Axial and swirl velocities, static pressure, and jet width at axial stations upto 15 orifice diameters were measured for cold flow with the help of five hole pitot probe. They found that jet width and rate of entrainment for strong swirl were almost twice those for the non-swirling jet.

In another interesting study, Syred et al [13] introduced the concept of creating recirculation zones of swirl using for flame stabilization. They used larger diameter swirl generator in which air is introduced through eight tangential ports. They indicated that there is a similarity in size and shape of the recirculation zone between the cold and reacting flows. Hence it may be sufficient to use cold flow studies to predict the size and shape of the reacting flow of an actual combustor. Later, Syred and Beer [14] came with concept of precessing vortex core (PVC) in which a naturally three-dimensional time dependent turbulent motion occurs, which is effected by combustion. They considered three types of flame configuration, such as flame produced by premixed fuel-air, flame produced by tangential air and axial fuel entry through the base plate, and flame produced by tangential fuel entry. Apparently, they found that flame produced by tangential air with axial fuel was more efficient without suppressing the precessing vortex core. The high intensity combustion of premixed air and kerosene in high-speed swirling flow was studied by Mestre and Benoit [15]. In this case, the flame is stabilized by means of several flame holders. They have attributed the increase in combustion intensity to the centrifugal force field, the more rapid dilution and the greater stability of the cooling film on the outer wall.

André Mestre [16] studied the efficiency and pollutant formation of a swirl flow combustor. He observed that the preheated air with better fuel spray in a swirl combustor gave more homogeneous mixture, which produces low CO and NO_x mission with higher combustion temperature and efficiency. Later, the

combustion of fuel jet in lean gaseous fuel-air mixture environment was studied by Karim et al [17]. They investigated the burning characteristics as well as the flammability limits for both coflowing and contra-flowing fuel air mixture in presence of pilot jet diffusion flame. They observed that there was an increase in the flame thickness and its height with enhanced stabilization considerably in the presence of small concentration of lean fuel-air mixture in the surroundings of the jet diffusion flame. Interestingly, they could achieve low lean limit even beyond flammability limit.

Negish [18] investigated the flame stability in a three port coaxial burner. The interaction between inner and the other coaxial flame was studied experimentally using CH₄-air system. They basically found minimum equivalence ratio, ϕ_m over a wide range of average velocity. Flame stabilization was achieved with help of ultra lean pilot flame. It was demonstrated that this type burner was free from thermal inertia, pressure loss and blow off problems. Later Yukio Mizutani and Satomura [19] studied the effective burning of ultra lean fuel-air mixture below the flammability limits in a heat recirculation type cyclone furnace system. From their observations, the surface temperature of the refractory was the main factor for governing combustion process and flame stability. Due to heat recirculatory furnace system, the preheated test mixture was attained approximately the adiabatic flame temperature calculated from the inlet temperature and composition of the preheated mixture.

Later, the improvement in fuel-air mixing was reported by Chen and Driscoll [20] from the vortex generated by swirl flame recirculation. In their experiments, jet of fuel from the central tube was injected into the swirl (toroidal vortex) created by tangential and axial air stream. Due to toroidal vortex in the swirl flow, fuel-air mixing rate five times than the simple jet flame was achieved. Thomas Fric [21] studied experimentally the effect of fuel-air unmixed ness on NO_x emissions. The NO₂ Laser induced fluorescence (LIF) technique is used to quantify unmixed ness levels at the flame holder. He found that the temporal unmixedness or concentration fluctuations were significantly contributing to higher NO_x formation. But at same time, his studies did not show the role of

mixing in the down stream of the flame holder. In another studies, Rokke et al [22] investigated the unconfined straight tube into quiescent air at atmospheric pressure and temperature. They proposed a correlation for lift-off height for partially premixed propane-air flames. Later Yoshiaki Onuma et al [23] reported an experimental investigation of a cyclone combustor in which they generated toroidal flame with forced recirculation flow. They studied extensively the process involved in the stabilization of lean premixed flame. Another studies, Wataru Fujisaki et al [24] investigated the combustion characteristics of a two-stage lean premixed combustion technique for gas turbine combustors. They studied the oxidation behavior of CH₄ and CO in the second stage where the primary hot combustion products mix with the secondary ultra lean premixture. It was observed that if the secondary stage temperature was higher than approximately 900-1000 ° C, the secondary ultra lean premixture could be achieved successfully for a wide range of operating condition, even if it was less than the flammability limit.

In a separate study, in order to investigate the mechanism of NO_x formation, lean turbulent premixed CH₄-air and H₂-air combustion were established by Xie et al [25] using an impinging jet. It was reported hat, the turbulent intensity does not affect much in NO_x emission, rather, and they attributed higher NO_x emissions to be proportional to the reactor residence time and combustion gas temperature. It was observed that the NO_x was formed by nitrous oxide mechanism without hydrogen-nitrogen path. In order to study fluid dynamics behavior of vortex interactions, Shu et al [26] studies a time dependent axisymmetric reacting flow model by the way of injecting a fuel rich (CH₄-air) annular jet was connected between a central air jet on the central core and co-flowing air on the outside. They discussed dynamic flame structure and flame-vortex interactions for different Froude number. Numerical as well as experimental studies were carried out to obtain a correlation between the Strouhal number (S), which is associated with vortex roll up, and the Froude number (Fr).

In another interesting studies, Hermanson et al [27] used a co-annular premixed configuration for improving lean stability for natural gas-air system for which an axisymmetric bluff body flame holder string is mounted either at the

inlet or at the exit of the combustor. They found that flame in inlet mounted flame holder combustor was more stable than the exit mounted flame holder combustor. A very low NO_x (12ppm) has been achieved by their burner. Later J.M.Samaniego and Mantel [28] observed the interaction of a two-dimensional vortex with V-shaped laminar premixed flame stabilized on a heated wire in a constant area square-duct. They investigated the effects of Lewis number, radiative heat loss, and unsteadiness on the interaction. Schlieren and smoke flow visualization provide significant details of the flame-vortex interactions. They also studied the heat release rate in terms of Lewis and Damkohler numbers and neglected the effect of radiative heat loss.

2.2. Scope of Work

The present literature review reveals that the flame stability and emission of LPG-air combustion has not been addressed adequately. Based on the literature review, the present work is intended to study experimentally the stability and emission characteristics of a lean premixed LPG-air combustor. The emission studies are done by Gas analyzer. The exit temperature is measured with Platinum and 13% Rhodium thermocouple probe. Here two methods are considered for flame stabilization such as flame stabilization with bluff body and flame stabilization with a swirller in the coflow. The following studies have been undertaken as part of this work.

1. Lean stability limit is studied for different core velocity from 0-20m/s lean stability limit studied for $H/D_{core} = 0.61$ and 5.0. The effect of lean stability limit on coflow air or fuel premixed with air is found out for the above H/D_{core} locations.
2. The temperature at the exit of the burner is measured for all the above cases.
3. The emission levels are measured with KM900 hand-held Combustion Analyser for all the above cases.

Subsequently, in the next chapter, the experimental setup and procedure involved in these studies are explained. The fourth chapter is devoted to discuss about the result obtained in the present work.

CHAPTER-3

EXPERIMENTAL SETUP

3.1 Introduction

In this chapter a complete description and fabrication process of the experimental setup have been presented. The measurement method, calibration process of flow measuring instruments and the experimental procedure with necessary precautions have also been described in detail. The experimental set up is also validated by comparing the present data with available data reported in open literature. The chapter has been presented with the following headings.

1. Experimental setup
2. Measurement methods
3. Experimental procedure
4. Experimental precautions
5. Validation of experimental setup
6. Summary and conclusion

3.2 Experimental Setup

In order to investigate the characteristics of lean combustion, a coaxial burner with bluff body flame stabilization has been developed in our laboratory. A complete schematic diagram of the experimental set up is shown in Fig.3.1. The section has been discussed under the following sub-headings.

1. Air system
2. Fuel system
3. Co-axial Burner
4. Swirl Burner

3.2.1 Air System

The air for conducting experiments is taken from a large storage system, as shown in Fig.3.1. The air pressure in these tanks is around 15atm. The compressed air is

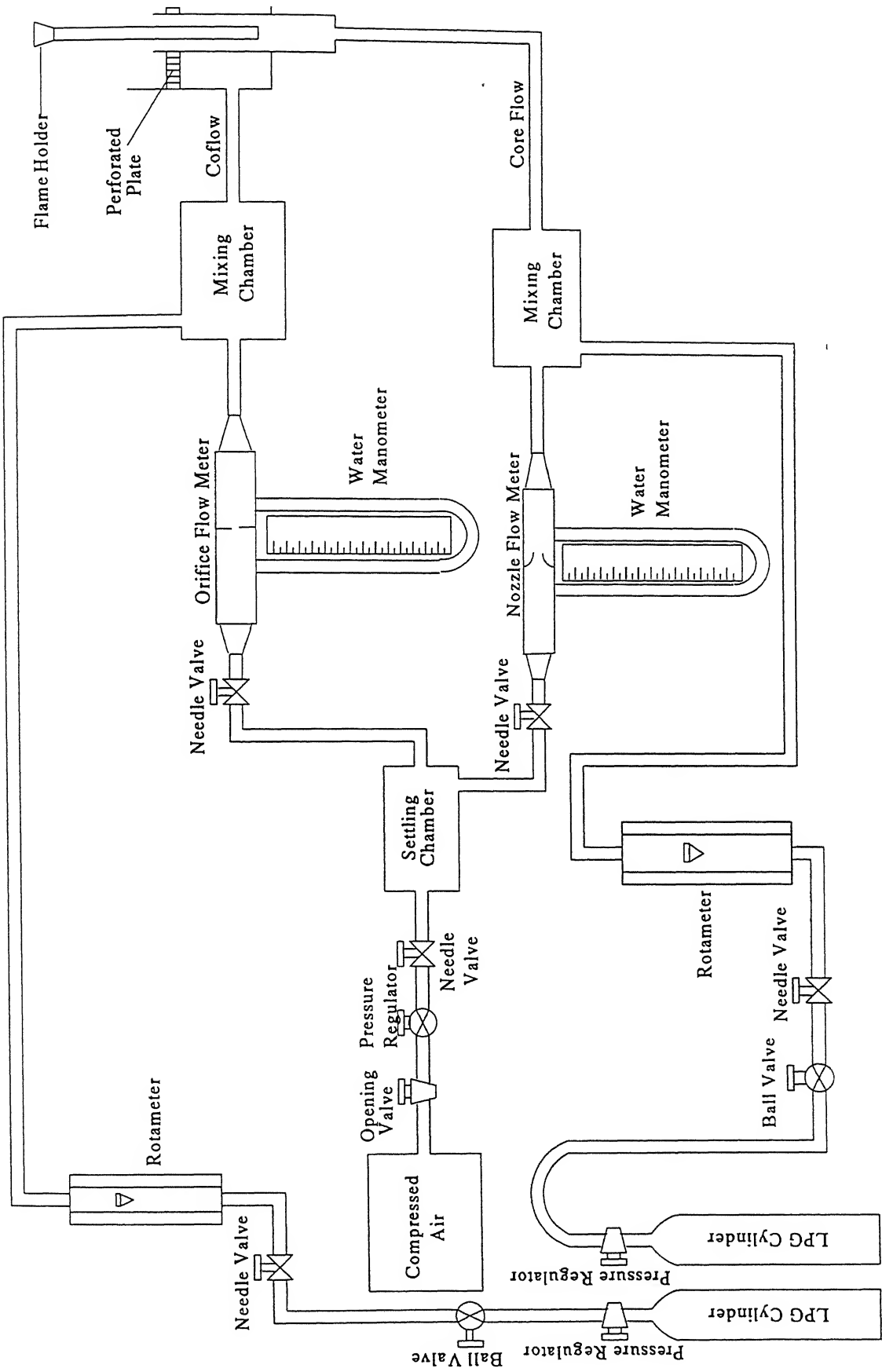


Fig 3.1. A schematic of the experimental setup

metered with the help of precalibrated nozzle flow meter and orifice flow meter. Pressure regulator valve and needle valve controls are provided before flow meter for controlling the flow. Then the air is allowed to enter into the settling chamber, which is made of 120mm long cylindrical pipe of 70mm diameter, as shown in Fig.3.1. From the settling chamber, air is separated through two tapings, one for coflow and another one for core flow.

3.2.2 Fuel System

The experiments are done with Liquefied Petroleum Gas, (LPG) as a fuel, which is stored in a commercially available cylinder. Two separate LPG cylinders are used for coflow as well as core flow. The fuel flow rate is measured with standard calibrated rotameter available in the market. The use of a high-pressure industrial LPG regulator valve instead of normal regulator rectifies backpressure problem created due to high-pressure air.

3.2.3 Coaxial Burner

The energy efficient combustion of LPG-air premixed gas is conducted on a coaxial burner, as shown in Fig.3.2. The present burner has been designed and fabricated in our laboratory. The burner is having one core nozzle and surrounding coflow channel as shown in the Fig.3.2. The core flow nozzle of 18.1 mm diameter is supplied with gaseous fuel premixed with air. The coflow with 49 mm diameter is supplied with either fuel premixed with air or air only. A perforated plate is used to reduce the upstream turbulence. Airflow rates are measured using precalibrated flow meters. Fuel flow rates are measured using standard calibrated rotameter. The flame is stabilized using a bluff-body flame holder as shown in Fig 3.2. This is an inverted truncated cone flame holder with 10mm diameter with 10mm height, (see Fig 3.2). This flame holder is mounted from the combustor inlet (bottom-mounted see Fig 3.2) with the help of a lead screw in order to move the position of the flame holder easily. The premixed fuel-air overall equivalence ratio is calculated from the fuel and airflow rates. The fuel and air are premixed in a mixing chamber as shown in the Fig.3.1. The combustion zone is enclosed by a

circular quartz window with a 50mm diameter and 300mm height for visual observation to find out the stability limit.

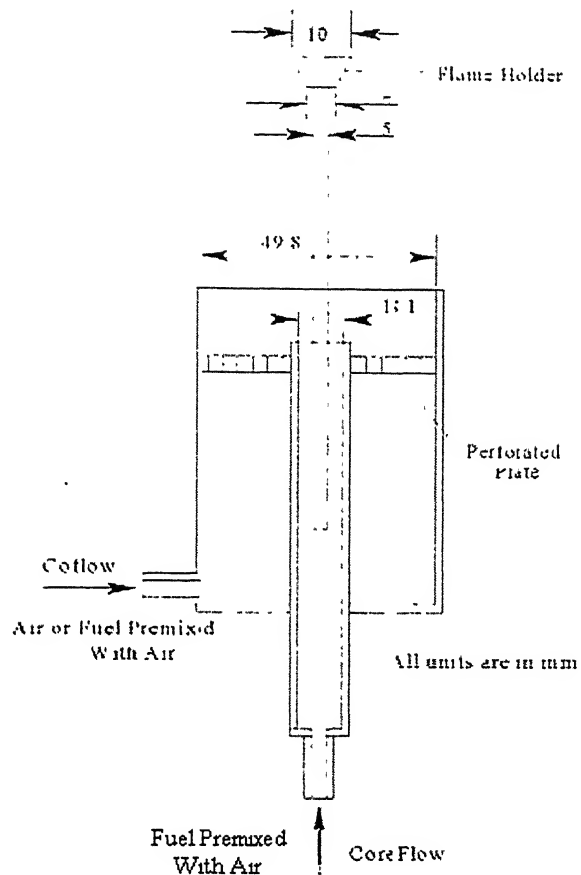


Fig 3.2. A schematic of the coaxial burner

3.2.4. Swirl Burner

The energy efficient and low NO_x combustion of LPG-Air premixture is also studied in a swirl burner. The present co-axial burner has been re-designed and fabricated in our laboratory. The swirl burner is having one core nozzle and surrounding coflow channel as shown in Fig 3.3a. The same core flow nozzle with diameter of 18.1 mm is supplied with LPG premixed with air. The vaned swirler is placed at the exit of coaxial flow port to impart swirler to the coflow. The details of swirler are shown in Fig 3.3b in which total number of vanes with

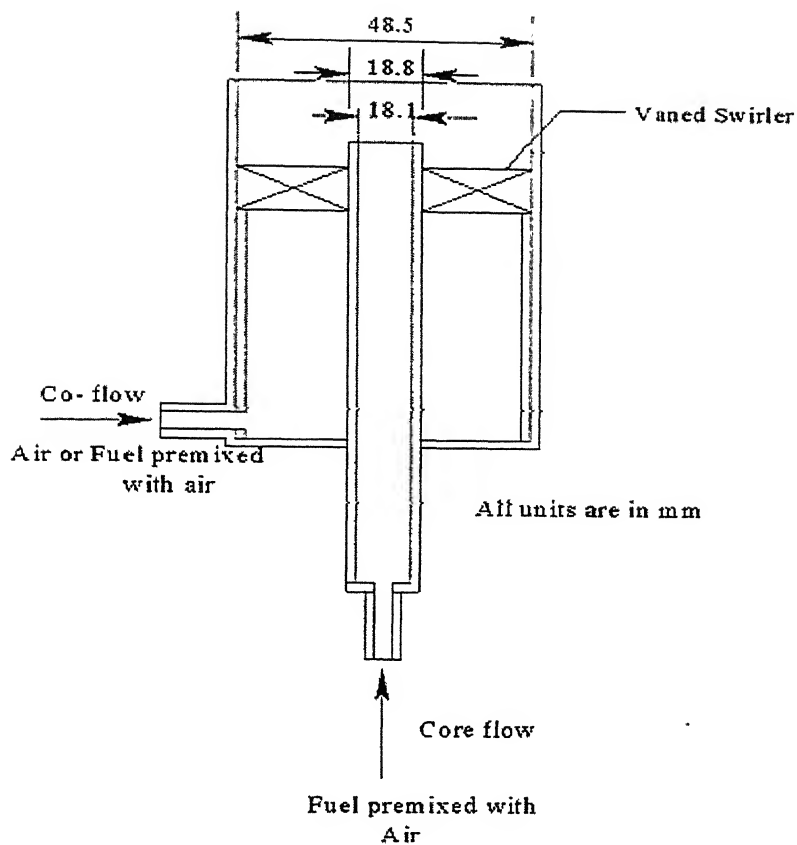


Fig 3.3a. A schematic of the swirl burner

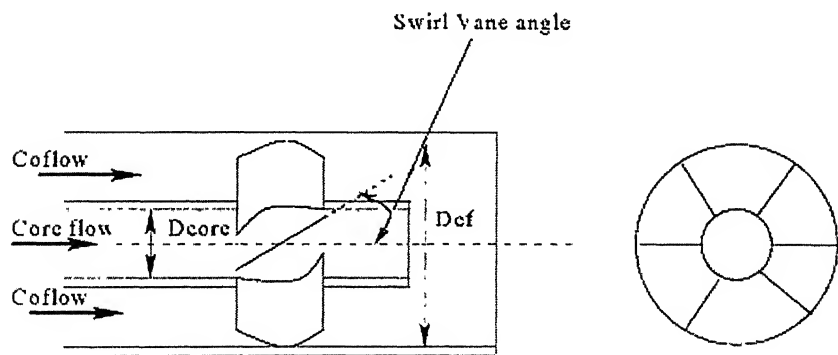


Fig 3.3b. A schematic of the swirler with guide vane assembly [3]

wall thickness of 2 mm. Two swirler with two different vane angles such as 10° and 40° are being used to study the effects of swirl number on the combustion characteristics. The air or fuel premixed with air is allowed to pass through vaned swirler. The swirl coflow creates the recirculation zone, which helps in stabilizing the flame.

3.3 Measurement Methods

3.3.1 Airflow Measurement

3.3.1.1. Flow Meter

The airflow is measured with the help of a nozzle flow meter and an orifice flow meter. The nozzle as well as orifice plate is designed as per ASME standards. The throat diameter of nozzle and orifice plate is 6 ± 0.01 mm and 9 ± 0.01 mm respectively. The flow meter is fixed between the flange ends of two equal internal diameter of 26 mm SS pipe. To have fully developed flow, 1-meter length pipe is provided before the flow-obstructing nozzle or orifice plate. For the smooth airflow at the exit and entrance, conical adapters are provided at both inlet and outlet of the flow meter. The flow meters are calibrated with help of a pitot tube as explained below.

3.3.1.2 Calibration of Flow Meters

A schematic diagram of the flow meter calibration setup is shown in Fig.3.3. For nozzle flow meter calibration, another convergent nozzle of diameter 5 ± 0.01 mm is employed and for orifice flow meter, 6.5 ± 0.01 mm diameter nozzle is used the nozzle is fitted at the exit of the flow meter. These nozzles are used for getting one dimensional velocity profile. A Pitot probe is used to measure the total head associated with the flow at the exit of the nozzle. Total head pressure is measured with the help of mercury manometer. The probe is aligned properly with the direction of the flow at the exit. The differential pressure across the nozzle as well as orifice is measured with two-meter arm length water manometer. Air is allowed to flow through the flow meter. For the corresponding fixed water manometer reading, mercury manometer (water manometer reading in the case of Nozzle flow

meter) reading is noted carefully. From the manometer reading, the jet velocity of the air is calculated. The product of nozzle exit area and jet exit velocity is the actual flow rate. Similar readings are taken for different values of water manometer readings. The nozzle flow meter and orifice flow meter are calibrated separately using above procedure. A calibration curve is plotted between the actual flow rate of air and corresponding water head manometer across the obstructing device. The calibration curves for nozzle flow meter as well as orifice flow meter are shown in Fig 3.4 and 3.5.

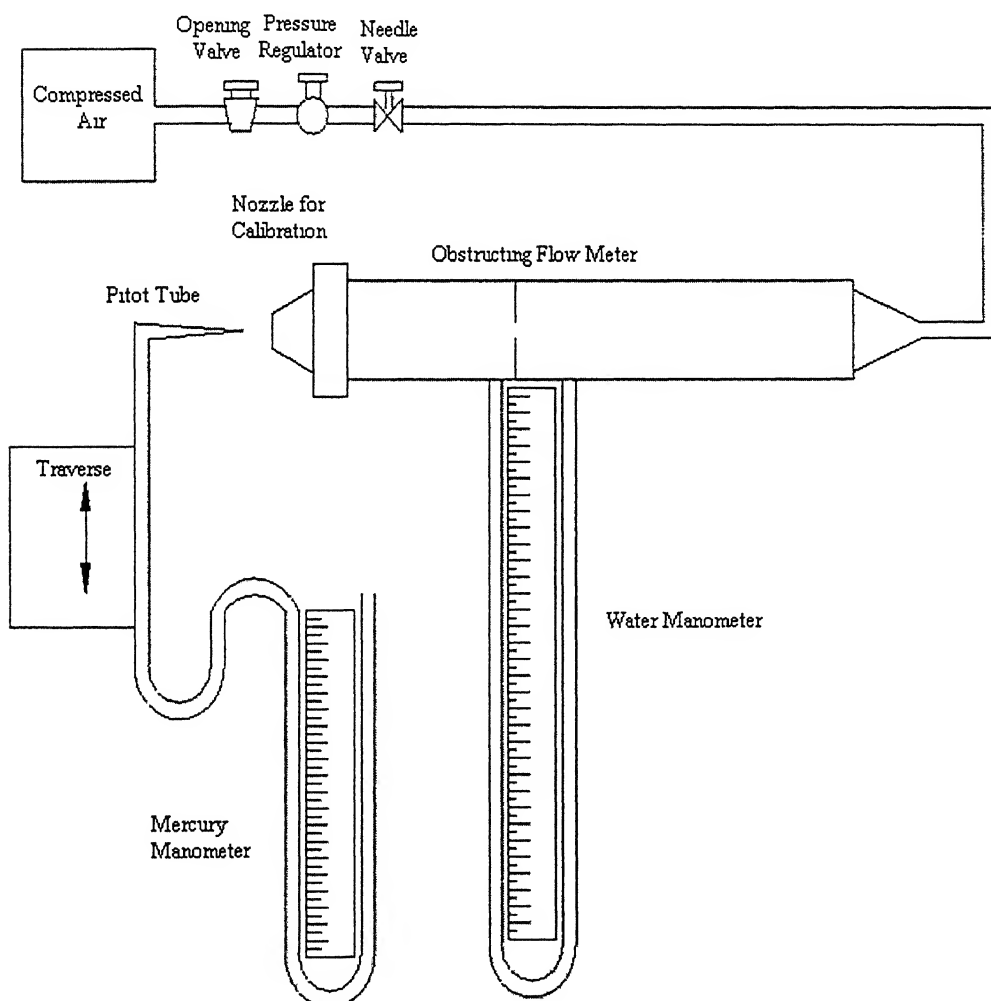


Fig 3.4. Schematic of the flow meter calibration setup

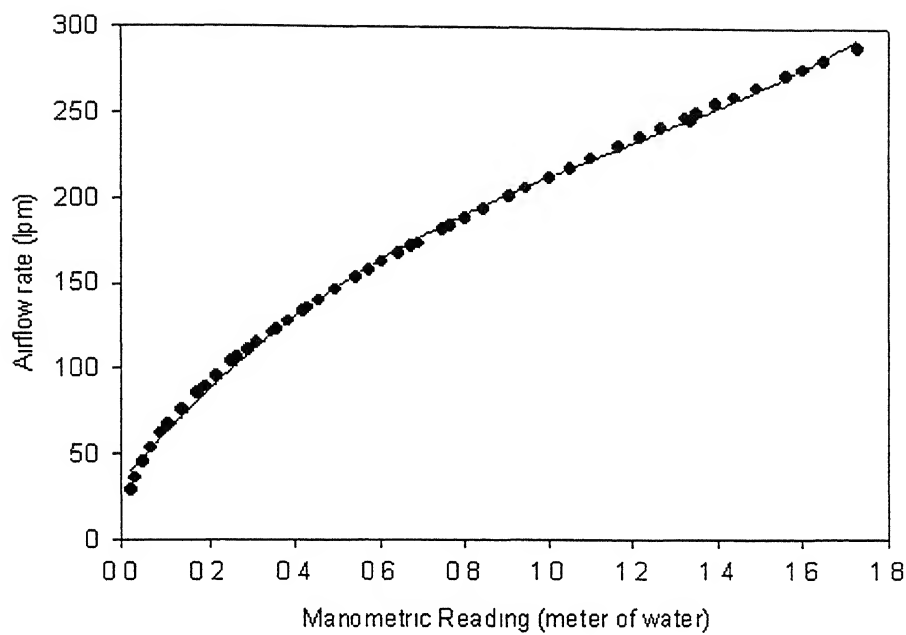


Fig 3.5. Calibration chart for nozzle flow meter

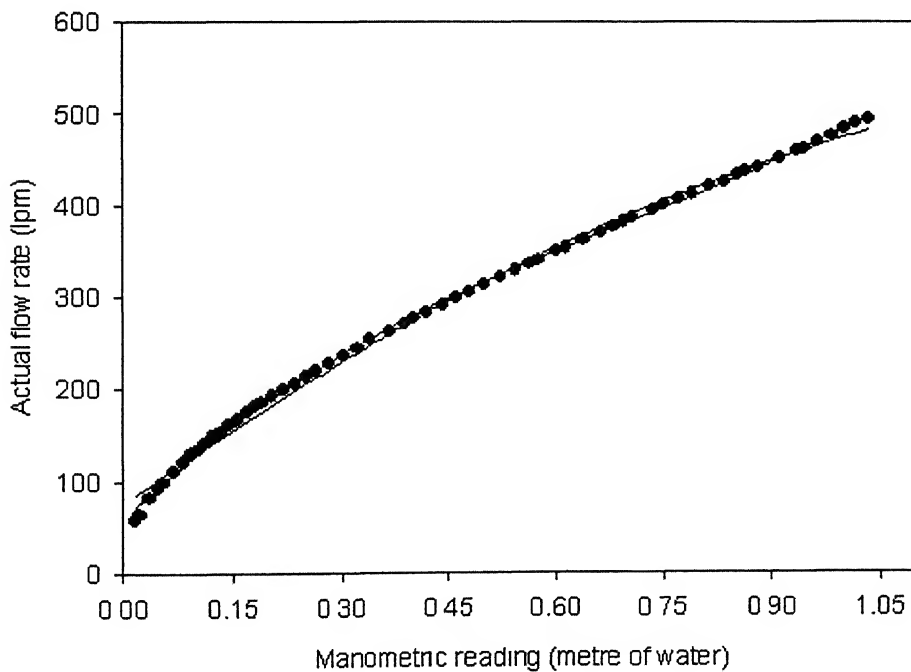


Fig 3.6. Calibration chart for orifice flow meter

3.3.2 Temperature Measurement

Temperature distribution at the exit of the burner is studied with the help of Platinum-13% Rhodium vs. Platinum thermocouple. This temperature probe is useful in avoiding losses due to radiation effects.

3.3.3 Emission Measurement

The pollutants like NO_x, CO and CO₂ are measured with KM900 Hand-Held Combustion Analyzer. All the emission measurement calculations are done for 15% O₂ reference. Analyzer is having auto-calibration setup at every start up. It is also having facility to store the data.

3.3.4 Sound Pressure Level Measurement

Overall sound pressure level measured with help of 800dB model Precision Integrating Sound Level Meter, which is having 1/8" tip Microphone (B & K made). The sound pressure level is taken from the range of value given in the display

3.4. Experimental Precautions and Safety Measures

1. Leakage test is performed before starting the experiment in order to make the set up completely free from leakages even at high velocities.
2. The experimental set up is placed in a large room with ambient temperature.
3. The flame is allowed to reach steady state before every set of readings.
4. Before every experiment, the flame holder is fixed and aligned properly to the centerline of the model.
5. In any case of accident, separate ball valve fitted in the line fuel line is closed. Subsequently LPG regulator is closed.
6. Airflow pressure is maintained at constant value in order to avoid the pressure interference.
7. Before starting the experiment, a bucket of water and fire extinguisher is placed nearer to the experimental set-up

8. In any case of Flash back in the burner, the ball vale fitted in the fuel line is closed and lot of air is opened through the burner.

3.5. Experimental Procedure

The experimental procedure adopted for present study can be explained as follows:

3.5.1. Coaxial Burner

Before starting the experiment, the flame holder location is fixed at particular height in terms of ratio between the flame holder height and core nozzle diameter (H/D_{core}). At first, a rich mixture of fuel and air in the core stream is used to establish a flame. The core fuel flow rate is measured with rotameter while the core airflow is measured with the help of nozzle flow meter. For a fixed core fuel flow rate, the core airflow is allowed to increase till the flame attains the lean stability limit. Lean stability is visualized through circular quartz glass chimney. The above mentioned procedure is repeated for different core fuel flow rate. Now the coflow air is varied and the similar procedure is maintained. For premixed co flow studies, the coflow equivalence ratio is fixed below the flammability of LPG-air mixture. The above similar procedure is repeated for obtaining lean stability limit. In each case, the flue gas temperature and emission level of species such as NO_x, CO and CO₂ are measured with thermocouple and Gas analyzer respectively. The above similar procedure is repeated for two different flame holder locations (H/D_{core}).

3.5.2. Swirl Burner

The swirl guide vanes are perfectly placed before starting the experiment. The fuel and air in the core flow are opened to establish the flame. For a particular coflow air velocity, the lean stability is visualized through glass chimney by varying core airflow rate for a particular fuel flow rate. The above same procedure is repeated for another air velocity and two different fuel premixed with air in the coflow. The emission levels and temperature are measures for all cases. The above same procedure is repeated for next swirl number.

3.5.3. Sample Calculation

The airflow rates are calculated from the nozzle flow meter as well as orifice flow meter calibration plot equation. The equivalence ratio is calculated as shown below.

$$\text{Equivalence ratio, } \phi = \frac{F/A}{(F/A)_{\text{stoich}}}$$

F/A = Fuel flow rate/Airflow rate

$(F/A)_{\text{stoich}}$ = Stoichiometric fuel-air ratio

The overall equivalence ratio

$$\phi_{ov} = \frac{(\mathcal{Q}_{F_1} + \mathcal{Q}_{F_2})}{(\mathcal{Q}_{A_1} + \mathcal{Q}_{A_2})} / 0.0647517$$

Where,

\mathcal{Q}_{F_1} = Core fuel flow rate

\mathcal{Q}_{F_2} = Coflow fuel flow rate

\mathcal{Q}_{A_1} = Core fuel flow rate

\mathcal{Q}_{A_2} = Coflow fuel flow rate.

The swirl number is calculated from this formula [3]

$$\text{Swirl Number, SN} = \frac{G_\phi}{G_x R} = \frac{2}{3} \left[\frac{1 - \left(\frac{R_h}{R} \right)^3}{1 - \left(\frac{R_h}{R} \right)^2} \right] \tan \alpha$$

Where,

G_ϕ = Angular momentum

G_x = Linear momentum

R_h = Radius of hub

R = Radius of outer tube

α = Vane angle

3.6 Validation of Experimental Setup

In order to validate the experimental setup, the lean stability limit data obtained in the present study is compared with similar data reported by Hermanson et al [27]. The comparison data between the two results is shown in the Fig.3.7. The comparison is made at $H/D_{core} = 0.61$ with same blockage ratio 4.23.

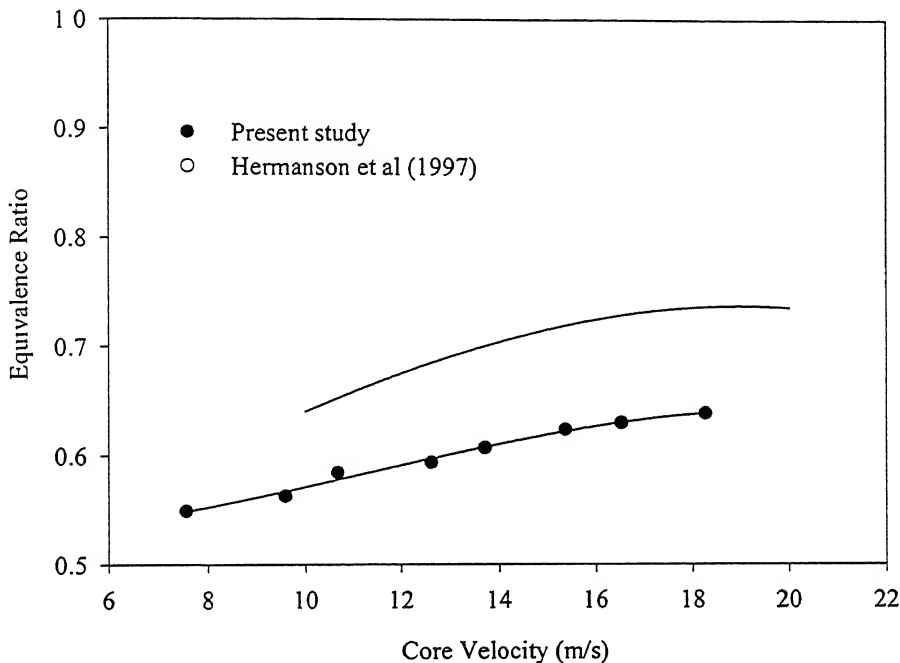


Fig 3.7. Validation of experimental setup

Graphs plotted between core velocity and equivalence ratio for the two cases are having similar trends. It can be noted that the lean stability limit is improved in the present case as compared to the results of Hermanson et al [27] due to the different flame holder diameter and fuel. Hence, the validation results obtained are quite convincing and setup is working properly.

3.7 Concluding Remarks

In the current chapter, the experimental setup for the low NO_x and lean stability co axial burner is discussed. The design procedure for this experimental set-up carried out in the propulsion laboratory is discussed. The fabrication details of the coaxial burner, flame holder with sting, and measuring device like orifice flow

meter are described in detail. The procedures for calibration of orifice flow meter and nozzle for calibrating orifice flow meter have been enumerated in this chapter. The detailed procedure for conducting experiments is highlighted which also includes the necessary safety measures. The lean stability limit of the coaxial burner is found out by direct visualization of the flame through the quartz window. This lean stability limit data obtained in the present experiment is compared with the similar kind of data obtained by the Hermanson et al [27] in order to validate the present experimental set-up. Although there is a slight difference in the results of lean stability limit, but the present results indicate similar trends that of previous studies. After validating the experimental setup, the experiments are conducted for different flame holder locations (H/D_{core}). The results obtained for these studies are discussed in the upcoming chapter in details

RESULT AND DISCUSSION

4.1. Introduction

The literature survey on turbulent premixed combustion reveals that mixing of the fuel and air plays a vital role in determining the lean stability limit, emission characteristic and occurrence of hot spots inside the combustor. The occurrence of hot spot, which affect the emission level very much, can be avoided by several ways. One way is to use the coaxial air, which is found to be helpful in improving lean stability limit. In the present study the flame is stabilized with the help of bluff body in most of the cases. The geometry of the bluff body plays a vital role in improving the flame stability limit. Increase in geometry of the flame holder leads to increase in pressure loss due to the blockage effect. The turbulence of incoming flow stream can be controlled by using a perforated plate and wire mesh. The presence study is aimed at investigating the effects of coflow air and premixed with air on lean stability limit and its emission level. The experiments are conducted for a wide range of Reynolds Number ($Re = \rho V_{av} D_f / \mu = 1749.398 - 7193.6458$) as well as Pecklet Number ($Pe = V_{av} D_f / \alpha = 1244.2246 - 5116.336$). Efforts are being made to operate the combustor at fuel lean condition with higher stability limit. At the same time lean fuel premixed mixture is also used as the coaxial flow apart from only air to reduce emission level.

The results of the present studies reported in terms of flame structure, lean stability limit, emission levels and temperature distributions for two flame holder locations with coflow air or fuel premixed with air.

4.2. Bluff Body Stabilized Flame With Coflow Air

4.2.1 Lean Stability Limits

Several experiments are conducted to find out the limits of stability at lean mixture under which the flame can be stabilized well. The lean stability data of the present coaxial combustor is obtained experimentally using bottom mounted flame holder as described earlier in the Fig 3.2. It can be recalled that the core velocity is varied and the corresponding equivalence ratio is obtained at which the

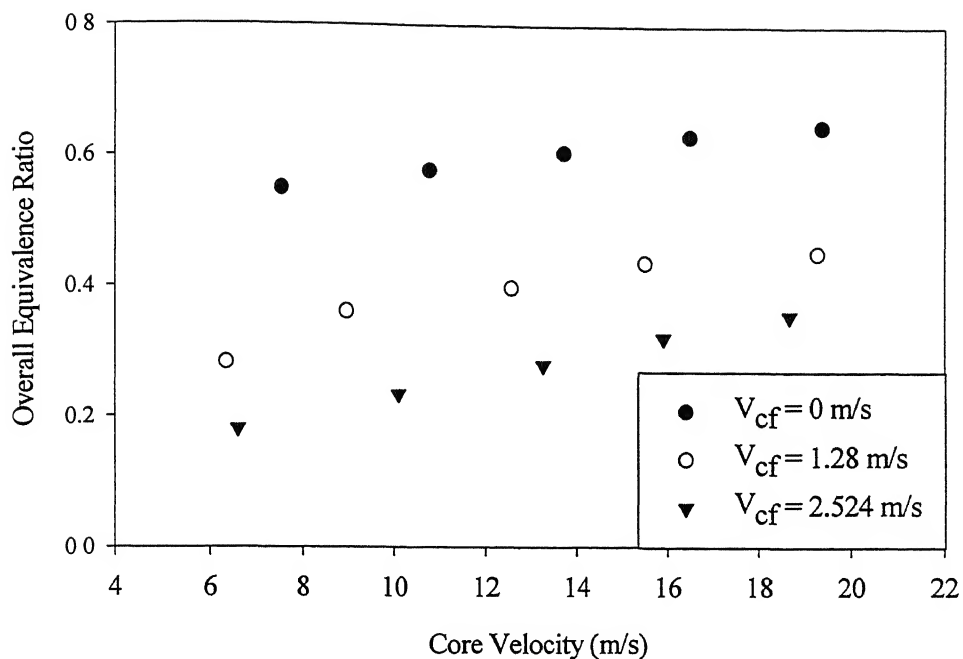


Fig 4.1. Lean stability limit for $H/D_{core} = 0.61$ with coflow air only

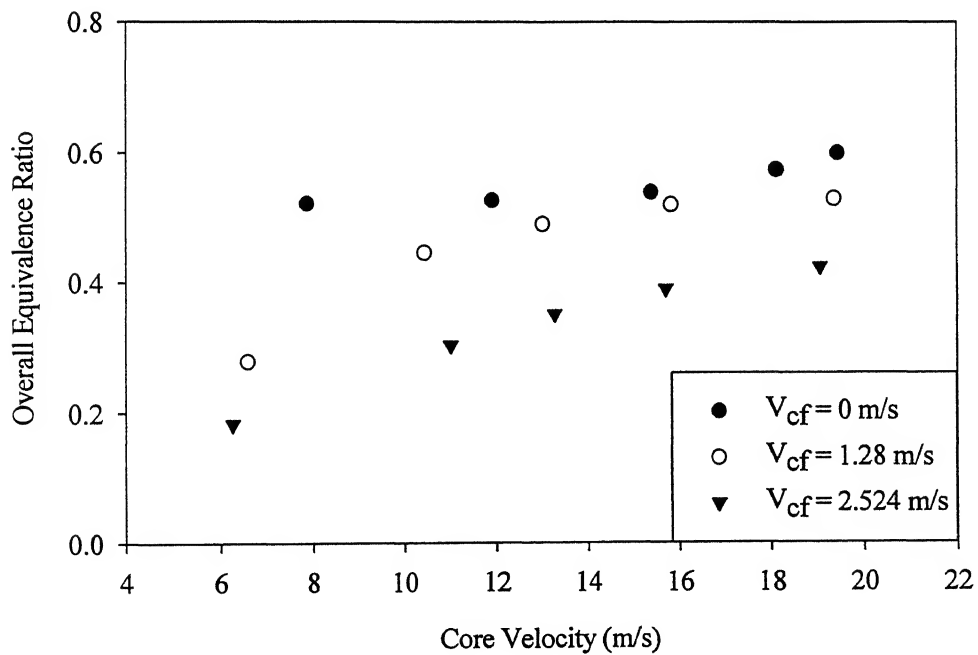


Fig 4.2. Lean stability limit for $H/D_{core} = 5.0$ with coflow air only

flame will be about to blow off. This stability limit is obtained from direct visualization of extinction of the flame. The results of lean stability limits are showed in Fig.4.1 in terms of variation of overall equivalence ratio, ϕ_{ov} (for its definition see Sec: 3.1) with core velocity, V_{core} for flame holder locations of $H/D = 0.61$ with three different coflow velocities. The air is used as a coflow for all cases mentioned in Fig 4.1. It can be seen that overall equivalence ratio for all three cases is increasing with increase in core velocity. The trend of these results can be explained as follows, as the velocity increases the recirculation zone behind the inverted cone bluff body decreases, which provide less residence time for the mixture to stay in the recirculation zone. Besides this, the temperature of the recirculation zone will decrease further due to high convective heat transfer.

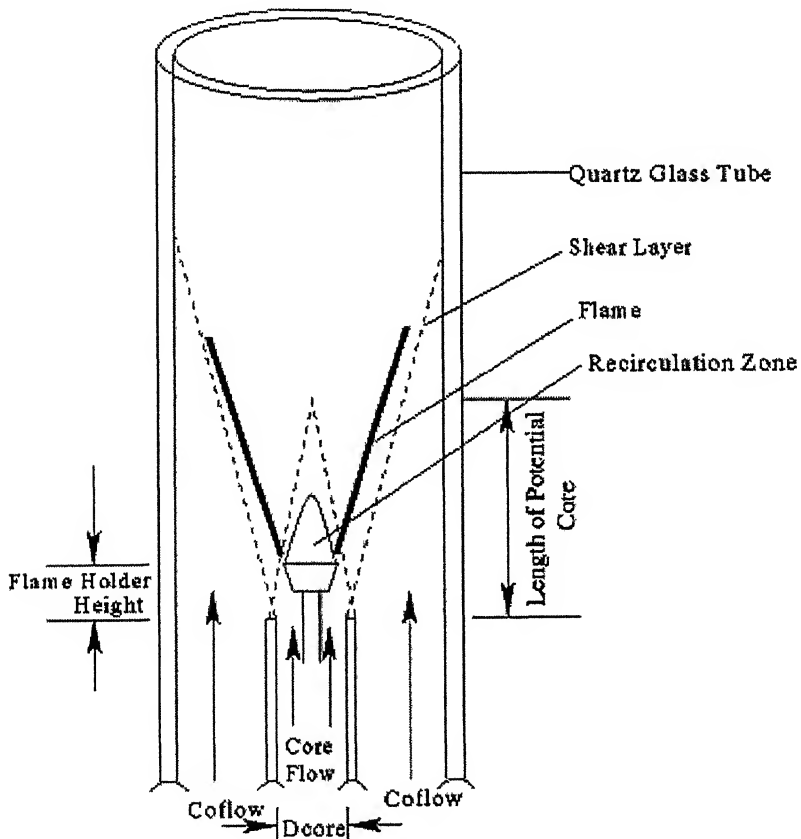


Fig 4.3. Schematic of mixing geometry between the core and coflow for the flame holder located within the potential core

As a result the fuel-air mixer would be ignited at higher equivalence ratio with increase in core flow velocity. Hence one has to enhance equivalence ratio at higher core velocity such that temperature of recirculation zone increases to provide enough amount of heat for the mixture to attain ignition temperature and the flame can be stabilized easily. In order to study the effect of coflow velocity on the lean stability limit, air is added to the coflow, whose velocity is also varied. The results of lean stability limits for two coflow velocity such as $V = 1.28$ m/s and $V = 2.52$ m/s are shown in Fig. 4.2. It is interestingly to note from Fig 4.1 that there is an improvement of stability limits with increase in coflow velocity while maintaining the similar trend that of zero coflow velocity. For example, with coflow velocity of 1.2 m/s, the stability limit has been extended even upto equivalence ratio 0.28 for a core flow velocity of 6.3 m/s.

In order to study the effects of flame holder position on the lean stability limit the flame holder is moved to $H/D_{core} = 5.0$. Similar procedure as mentioned earlier is followed for finding out the stability limit for this case. The results for the case, of $H/D_{core} = 5.0$ is plotted in Fig. 4.2 in terms of overall equivalence ratio against core velocity for three coflow velocities. It can be seen from Fig.4.2 that lean stability limits have similar trend that of earlier case ($H/D_{core} = 0.61$). However, it seems that there is marginal increase in stability limit for $H/D_{core} = 5.0$ case. This improvement of stability limit may be attributed to decrease in velocity at the flame holder owing to boundary of the sting. Besides this, there will be a chance of preheating the upstream mixture of the flame holder by heat transfer via support sting.

The effect of coflow air velocity and the stability limit is studied by varying the velocity of coflow. The results for stability limits is shown in Fig.4.2 which reveals that there is a shift in lean stability limit due to coflow air being very small in comparison to the same case for $H/D_{core} = 0.61$. Since the flame holder is situated outside the potential core zone of the core jet as shown in Fig 4.4, there is a greater chance for better mixing of fuel and air. Hence, the mixing of the core and coflow is occurring in the upstream of the flame holder. As a result, the stability limits for lower range of coflow velocity, the stability limits

closer to one another. However, there is shift of stability limit curve for higher velocity as can be seen in Fig 4.2.

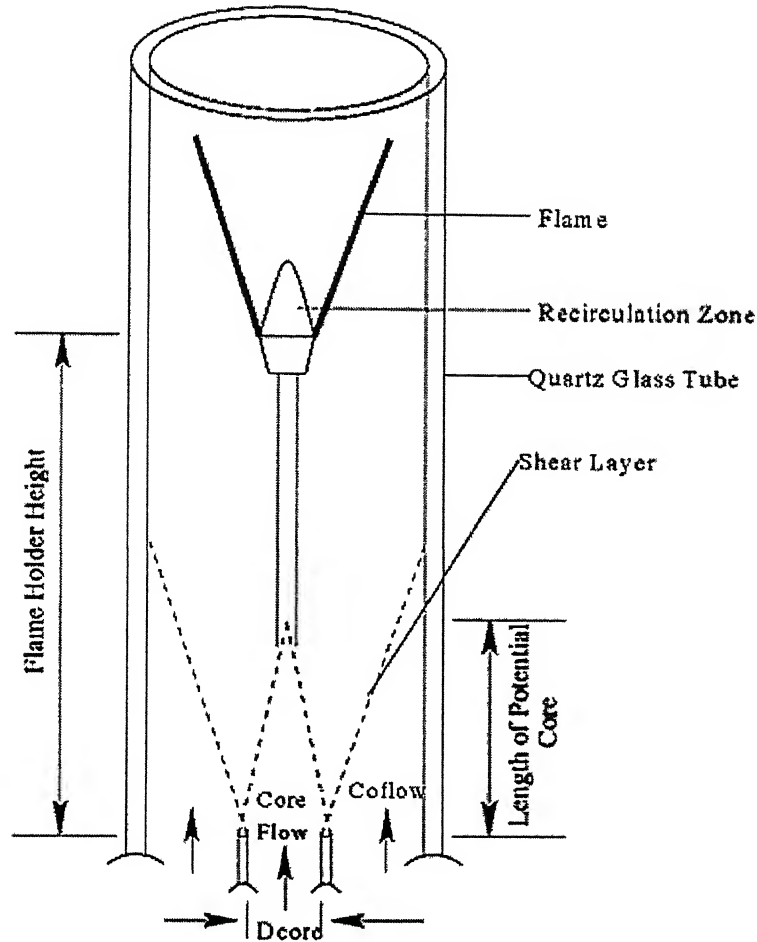


Fig 4.4. Schematic of mixing geometry between the core and coflow for the flame holder located above the potential core

4.2.2. Flame Structure

The structure of a bluff body stabilized flame may be divided into two zones: the immediate wake or recirculating zone and propagating flame. The actual structure of a flame stabilized by an inverted bluff body is shown in Fig 4.5. The free stream combustible gas is ignited as it follows by the hot recirculation zone and the flame is established by this manner in the downstream of the bluff body. When the gas doesn't have sufficient residence time to ignite in spite of the heat transfer

from the wake, the flame does not propagate downstream and blow off takes place.

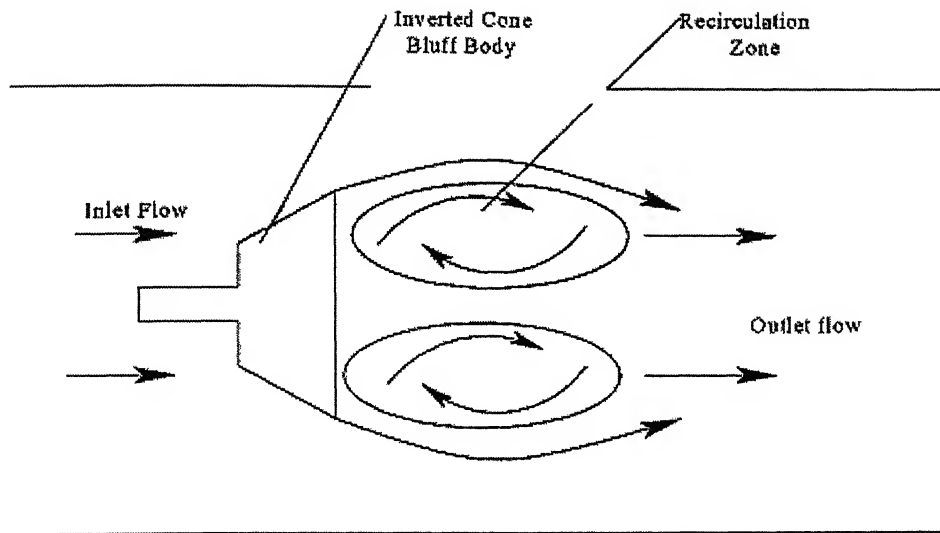


Fig 4.5. Schematic of recirculatory flow behind wedge flame holder

The flame structure is visualized using still photography for a particular core fuel with varying its velocity. The flame photographs for three cases are shown in Fig 4.6. The pictures basically provide certain idea about the mechanism of blow off and stability limit. It can be noted from Fig 4.1a, that the recirculation zone is broader and which may provide enhanced residence time of mixture inside the higher recirculation wake zone behind the body due to $\phi_{ov} = 0.706$ is mainly accounted for the presence of higher turbulent diffusion exchange from the hot recirculation zone to the outer flow. While clearly observing the picture from Fig 4.6a to 4.6c, the recirculation zone size is decreasing with increase in core velocity for a particular fuel flow rate. The amount of time required for igniting the fresh mixture approaching near the flame holder hot wake is decreasing from Fig 4.6a to 4.6c. This will lead to blowing off the flame. In order to avoid this, a small amount of fuel is added to make the stable flame.

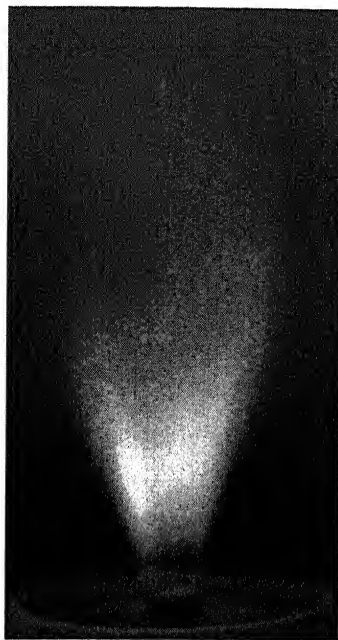


Fig 4.6a.
 $V_{core} = 5.93 \text{ m/s}$, $\phi_{ov} = 0.706$



Fig 4.6b.
 $V_{core} = 6.59 \text{ m/s}$, $\phi_{ov} = 0.633$



Fig 4.6c.
 $V_{core} = 7.46 \text{ m/s}$, $\phi_{ov} = 0.556$

Fig 4.6. Bluff body stabilized flame structure for different core velocity

4.2.3. Exit Gas Temperature

The exit gas temperature is measured at the exit of the burner using Pt-Rh thermocouple. The exit temperature distribution is plotted with radial location (y/R) as shown in Fig 4.7. The exit average gas temperature is calculated by mass averaging method. The exit gas temperature is increasing with an increase in core velocity for all cases of $H/D_{core} = 0.61 \& 5.0$ as shown in Fig 4.8 & 4.9. In the case of $H/D_{core} = 0.61$ as shown in Fig 4.9, the exit temperature is decreasing with addition of air to the coflow. Hence, this curve is depicted to the absence of mixing between the coflow and core flow due to the presence of flame holder within the potential core as shown in Fig 4.3. While going through the exit gas temperature curve for flame holder location, $H/D_{core} = 5.0$ as shown in Fig 4.9, the exit temperature is increasing with addition of air to the coflow for a coflow velocity of 1.28 m/s than that of the case with no air in the coflow. This curve is attributed to the presence of mixing between the coflow and core flow streams due to the presence of flame holder outside the flame holder as shown in Fig 4.4. Further increase in air to the coflow ($V_{cf} = 2.52$ m/s), the exit temperature is decreasing than that of the case with no air in the coflow. This is due to the presence of quenching of hot combustion gas with excess air present in the coflow.

4.2.4. Exhaust Gas Emission Characteristics

The emissions of several species in the exhaust gas of the present co-axial combustor are obtained using combustion gas analyzer at lean stability limit as described earlier. The emission characteristics are reported in terms of variation of emission level of individual species with core velocity for two flame holder locations with three different coflow air velocities. These reported emission level represents average value of emissions obtained from three locations of the burner exit.

4.2.4.1. Exhaust Gas Oxygen Content

The variation of flue gas oxygen content data are reported in Fig.4.10 for $H/D_{core} = 0.61$ against core velocity for two flame holder locations. It can be seen in Fig.4.5 that the flue gas oxygen content is decreasing with increase in core velocity for the case $H/D_{core} = 0.61$ with no air in the coflow. With increase in

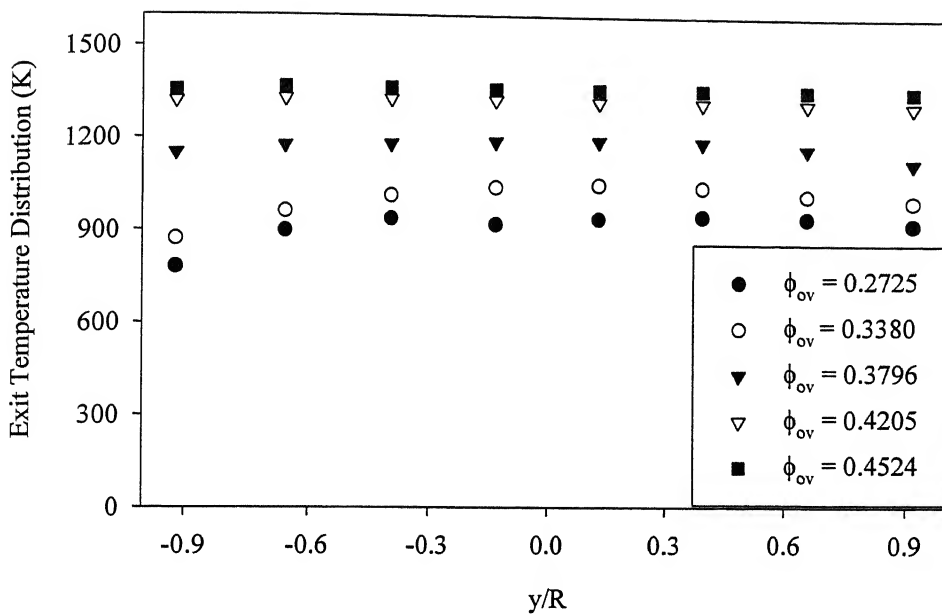


Fig 4.7a. Exit gas temperature distribution for $H/D_{core} = 0.61$ with coflow air only (velocity = 1.28 m/s)

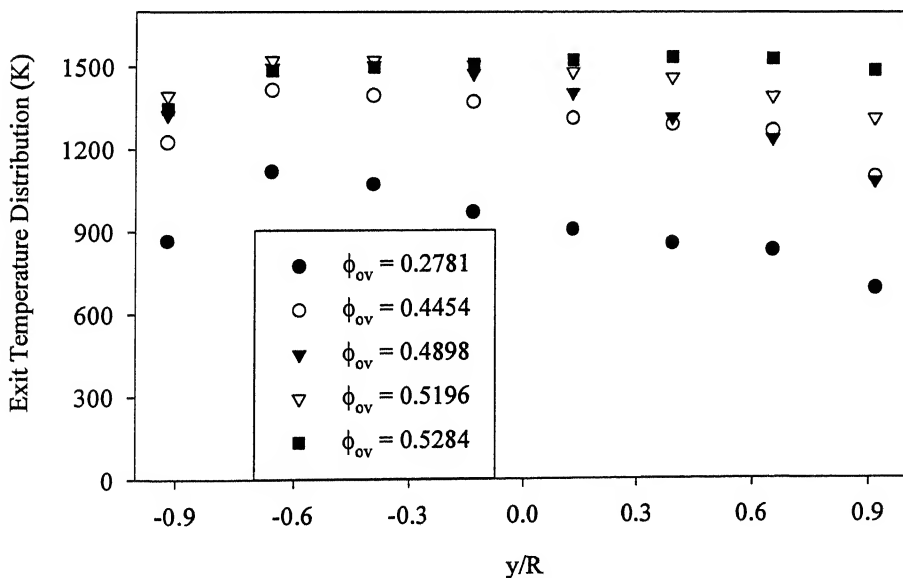


Fig 4.7b. Exit gas temperature distribution for $H/D_{core} = 5.0$ with coflow air only (velocity = 1.28)

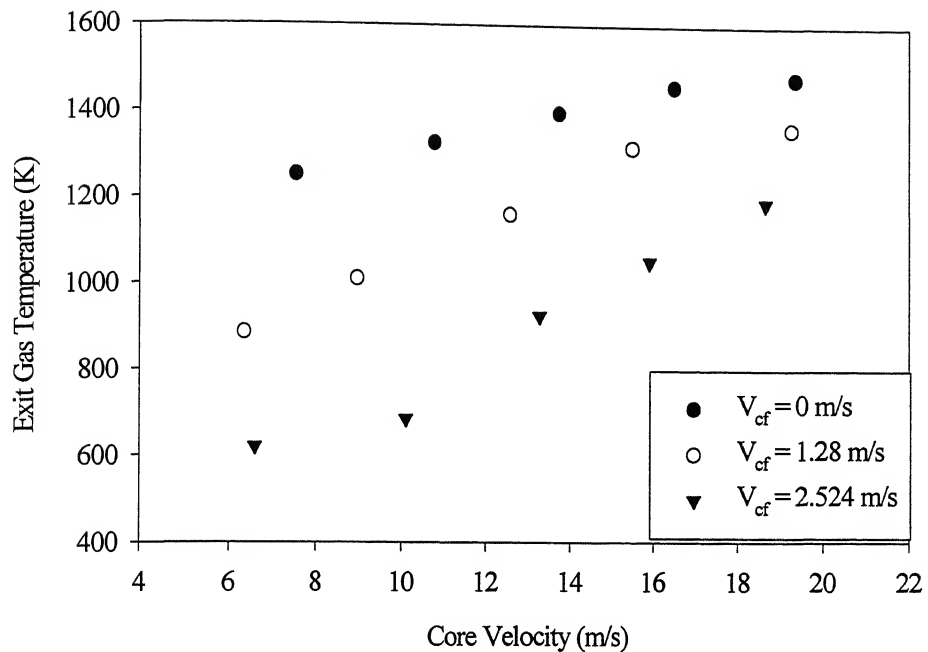


Fig 4.8. Average exit gas temperature for $H/D_{\text{core}} = 0.61$ with coflow air only

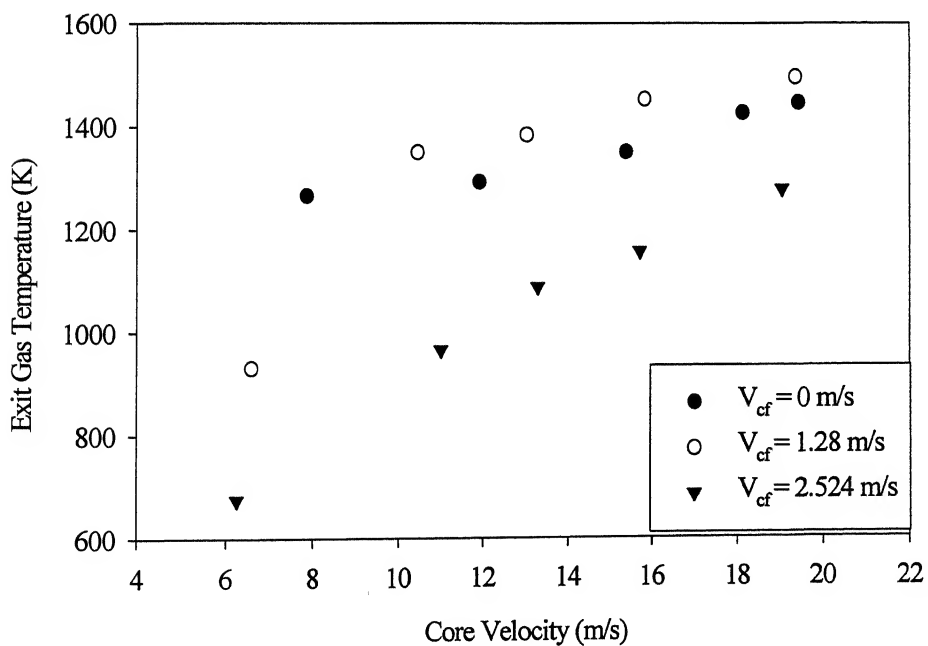


Fig 4.9. Average exit gas temperature for $H/D_{\text{core}} = 5.0$ with coflow air only

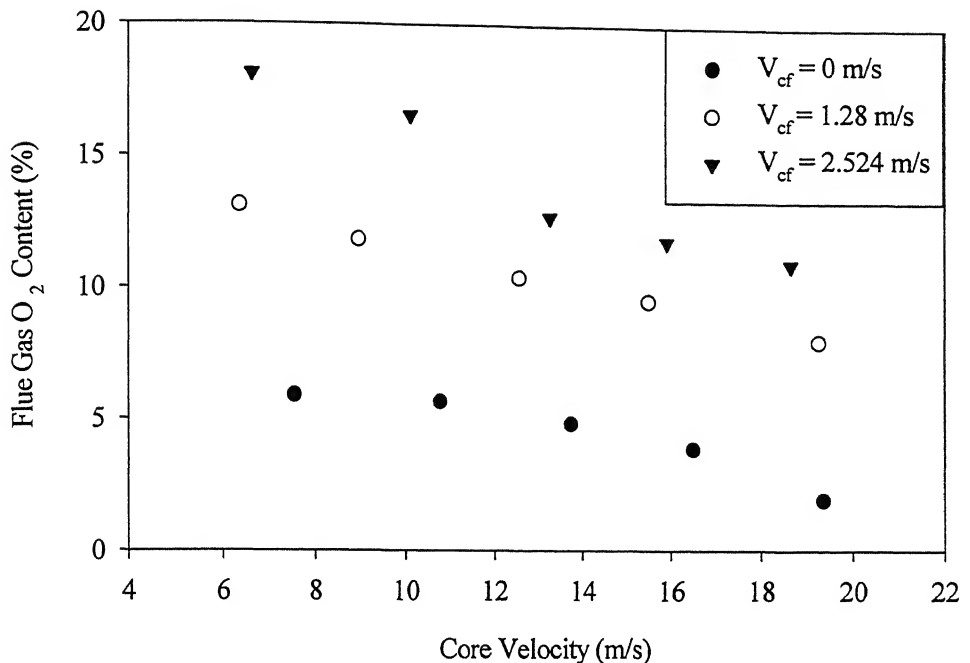


Fig 4.10. Exhaust gas O₂ content for $H/D_{core} = 0.61$ with coflow air only

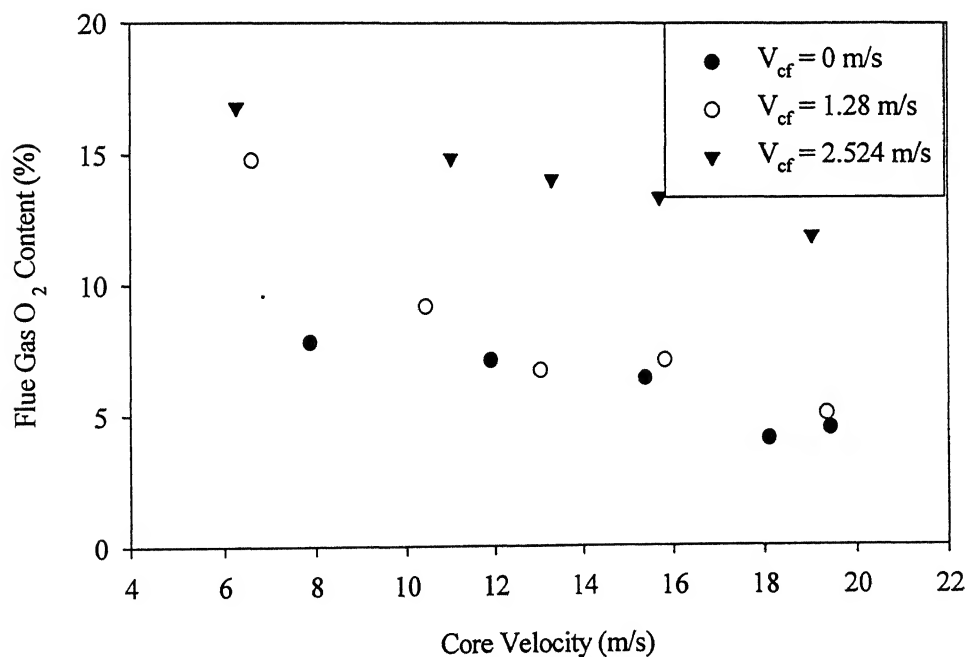


Fig 4.11. Exhaust gas O₂ content for $H/D_{core} = 5.0$ with coflow air only

core velocity, the flame is stabilized at higher equivalence ratio. Hence there will be an increase in combustion gas temperature. The decrease in flue gas oxygen content towards higher velocities may be due to consumption of oxygen during the process of CO conversion to CO₂. Similar trend of decreasing O₂ content with increase in core velocity can be observed in Fig.4.10 for other coflow velocity cases. It is mainly due to the fact that the flame holder is situated at well inside the potential core zone. There is no chance of mixing of core and coflow streams. As a result the oxygen in the coflow is not utilized and leads to increase in oxygen with increase in coflow air velocity.

The flue gas oxygen content for H/D_{core} = 5.0 is plotted in Fig.4.11 for three coflow velocities. It can be seen that the flue gas oxygen content is decreasing with increasing core velocity for case with no air in the coflow which resembles similar trend that of the case H/D_{core} = 0.61. The decreasing oxygen content with increase in velocity is mainly attributed to the better oxidation of fuel due to higher combustion gas temperature at higher equivalence ratio. For the coflow velocity of 1.28 m/s, the variation of oxygen content with core velocity maintains similar trend. However, the flue gas oxygen content seems to be very closer to the value of oxygen content for the case with no air in the coflow. This is attributed to better mixing of the coflow and core flow, as the flame stabilizer is located away from the potential core zone of core jet. The amount of oxygen present in the both core and coflow may be effectively utilized for complete combustion. But further increase in air velocity in coflow leads to increase in oxygen content maintaining similar trend as shown in Fig.4.6, which is due to excess availability of oxygen in the coflow.

4.2.4.2. Exhaust CO Emission

The results of the flue gas CO content are shown in Fig.4.12 for H/D_{core} = 0.61 against core velocity for three different coflow air velocities. It can be seen from Fig.4.12 that the flue gas CO content remains almost constant for zero coflow velocity with increase in core velocity. However, there is a slight increase in CO level when the coflow velocity is increased to 1.28 m/s. This kind of behavior is more pronounced when the coflow velocity is increased to 2.54 m/s. The level of CO emission is quite substantial for higher coflow velocity particularly at lower core velocity. Because the flames at lower core velocity is stabilized at lower

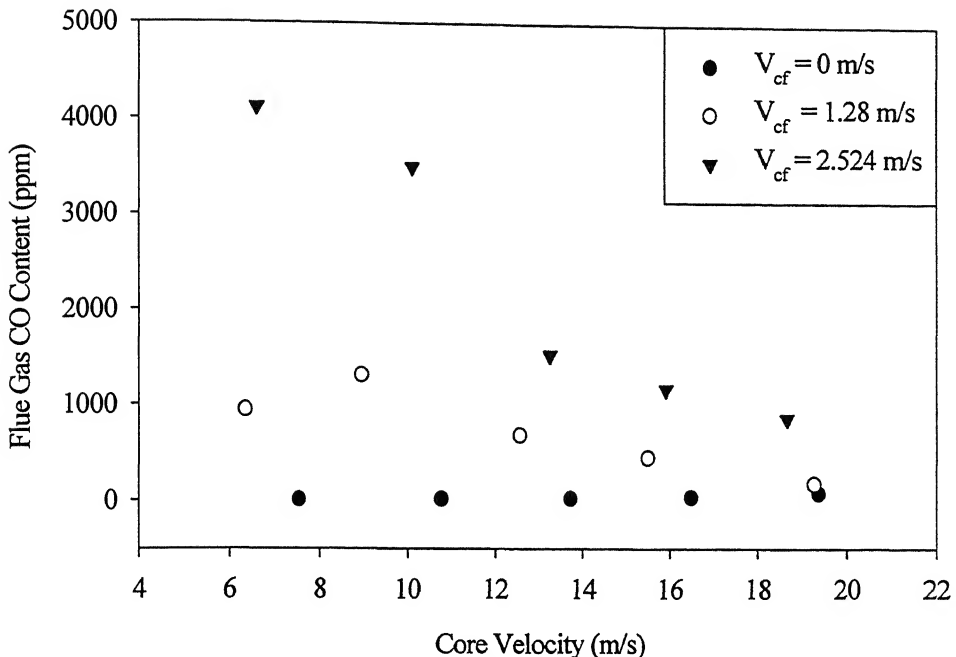


Fig 4.12. Exhaust gas CO emission for $H/D_{core} = 0.61$ with coflow air only

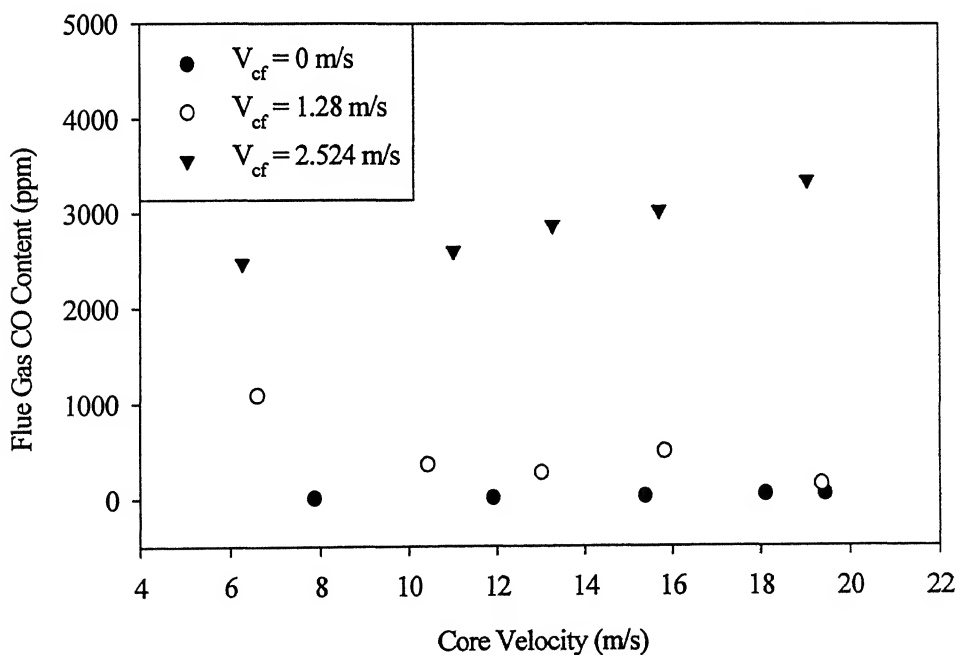


Fig 4.13. Exhaust gas CO emission for $H/D_{core} = 5.0$ with coflow air only

equivalence ratio, which can be seen from stability plot (see Fig.4.1). For this situation, the flue gas temperature is likely to be lower. Besides this, the flame stabilizer is located inside the potential core, which prevents any further mixing of coflow with the core flow. With further increase in coflow air velocity to 2.524 m/s, the CO content is decreasing with increase in core velocity. It can be observed that this variation seems to be having similar trend that of the case $H/D_{core} = 0.61$ with 1.28 m/s coflow velocity as shown in Fig.4.12. It can be noted that the CO emission level attains maximum value at lower core velocity. This may be occurred due to quenching of the combustion products in the downstream of the flame holder by the co flow air. Because, even the flue gas temperature attains a very low value (see Fig.4.8), which prevents further oxidation of CO to CO_2 .

The effects of the flame holder position on the CO emission level is investigated for which experimental data is generated for flame holder position $H/D_{core} = 5.0$. The results of CO emissions are plotted in Fig. 4.13 for three coflow velocities ($V_{cf} = 0$ m/s, 1.28 m/s and 2.52 m/s). It can be observed from this Fig. 4.8 that the CO emission level for lower coflow velocities ($V_{cf} = 0$ and 1.28 m/s) has a trend similar to the case of $H/D_{core} = 0.61$. However, for higher coflow velocity ($V_{cf} = 2.524$ m/s) the CO level increases slightly with increase in core flow velocity which is opposite to the trend that of $H/D_{core} = 5.0$ case. However, the increase in CO may be attributed to non-availability of enough time for the mixture to reside in the mixing zone due to both core and coflow velocities. As a result, the conversion of CO from CO_2 would take place leading to slight increase in CO emission level. Interestingly, there is substantial decrease in CO emission with increase in flame holder position to $H/D_{core} = 5.0$, particularly at lower core velocity flow. This observation can be attributed to better mixing of core flow with coflow particularly at lower core flow velocity, which is due to the presence of flame holder outside the potential core of the jets.

4.2.4.3 Exhaust CO_2 Content

The flue-gas CO_2 content data in terms of percentage are reported in Fig.4.14 and Fig.4.15 against core velocity for two flame holder locations with three different coflow velocities. It can be noted from Fig.4.14 that the flue gas CO_2 level is increasing with increase in core velocity for the all cases in the

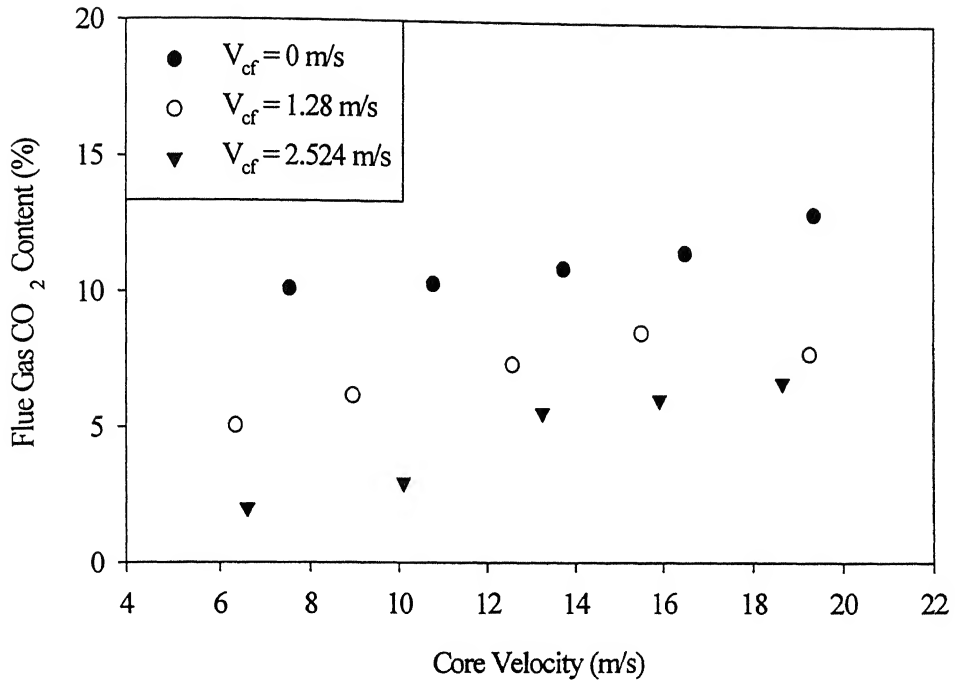


Fig 4.14. Exhaust gas CO₂ content for $H/D_{core} = 0.61$ with coflow air only

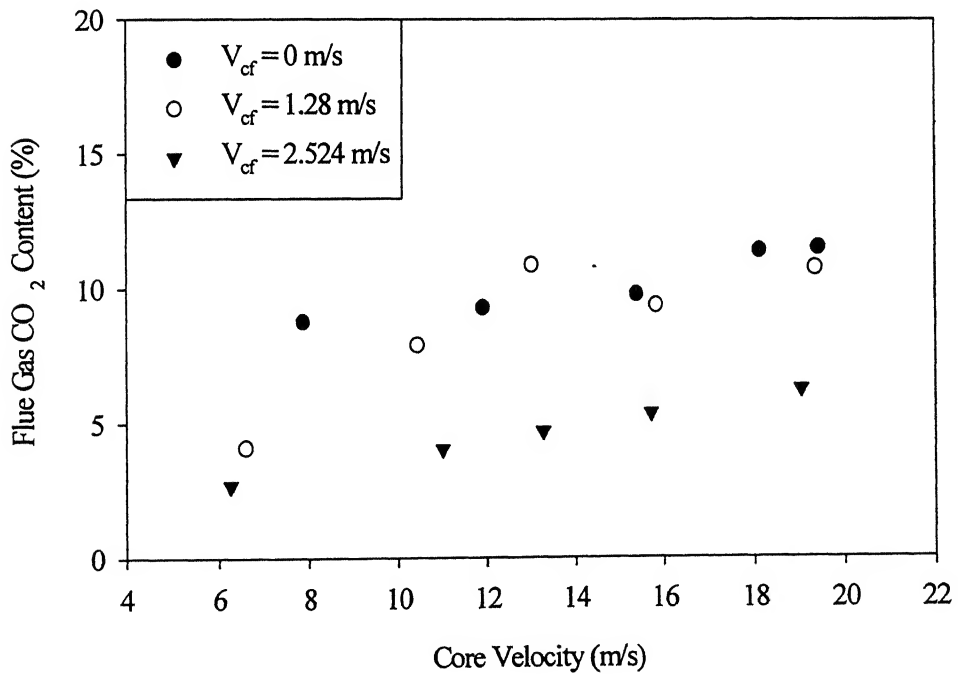


Fig 4.15. Exhaust gas CO₂ content for $H/D_{core} = 5.0$ with coflow air only

$H/D_{core} = 0.61$. The increase in CO_2 is mainly related to the combustion of fuel and conversion of CO to CO_2 in the higher combustion gas temperature. With addition of air to the coflow similar trends of increasing CO_2 level with core velocity can be noticed from Fig.4.14. However there is a decrease of the CO_2 level for higher coflow velocity in comparison to zero coflow velocity. It may be attributed to less oxidation of CO to CO_2 due to flame quenching by coflow air. Indeed, the mixing of the coflow with core flow in the downstream of the flame holder leads to decrease in the temperature level due to quenching of the combustion products by coflow air. The flue gas CO_2 level for $H/D_{core} = 5.0$ is plotted in Fig.4.15 for three different coflow velocities which seems to have similar trend to that of $H/D_{core} = 0.61$. Interestingly, the flue gas CO_2 level for coflow velocity = 1.28 m/s is having value almost similar to the case with zero coflow velocity. This may be due to the better mixing between the coflow and core flow, which helps in increasing the combustion gas temperature as shown in Fig 4.9. However, for further increase in coflow velocity, i.e., 2.52 m/s the CO_2 value is decreasing in comparison to the previous two coflow velocity cases. This may be due to the fact that hot combustion gas gets quenched by the excess coflow air, which prevents further conversion of CO to CO_2 .

4.2.4.4. Exhaust NO Content

The results of flue gas NO level are reported in Fig.4.16 against core velocity for flame holder conditions of $H/D_{core} = 0.61$ with three different coflow velocities. It can be observed from Fig.4.16 that the NO is increasing with increase in core velocity. For the zero airflow rate in coflow, the NO level increases with increase in core flow velocity. Such behavior may be due to the fact that flue gas temperature increases with core velocity since the flame is stabilized at higher equivalence ratio. This fact is evident in the plot of flue gas temperature vs. core velocity as shown in Fig.4.8. However, for the coflow air velocity of 1.26 m/s, the NO emission decreases substantially particularly at higher core velocity. Due to mixing of coflow with combustion product, the temperature of flue gas decreases which is resulted in decrease in NO. However, NO level first decreases marginally to certain value and again seem to opposite in comparison to the zone coflow velocity. The mixing of coflow with hot combustion product in the

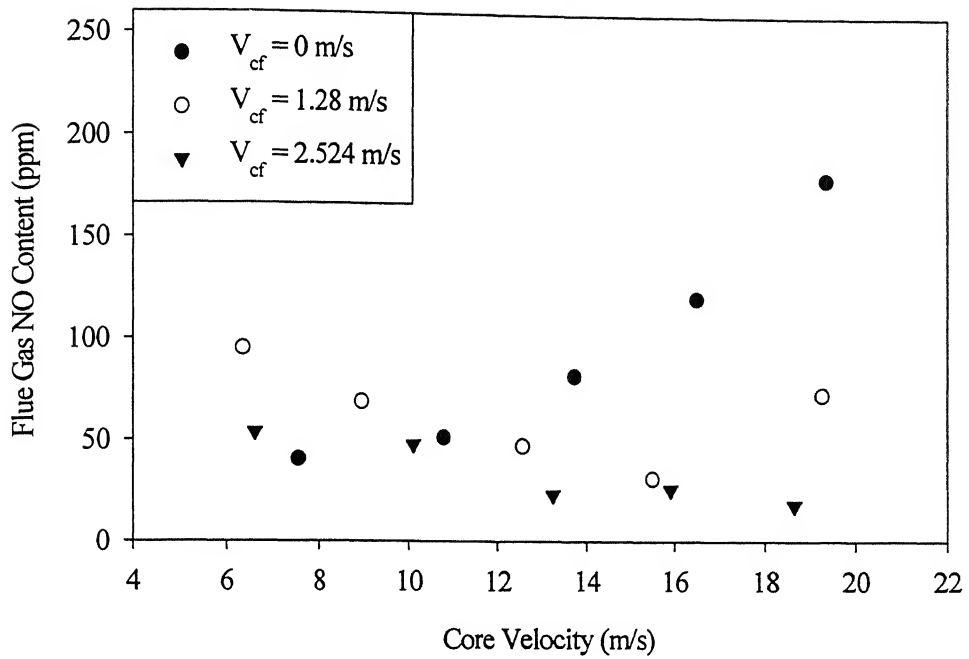


Fig 4.16. Exhaust gas NO emission for $H/D_{core} = 0.61$ with coflow air only

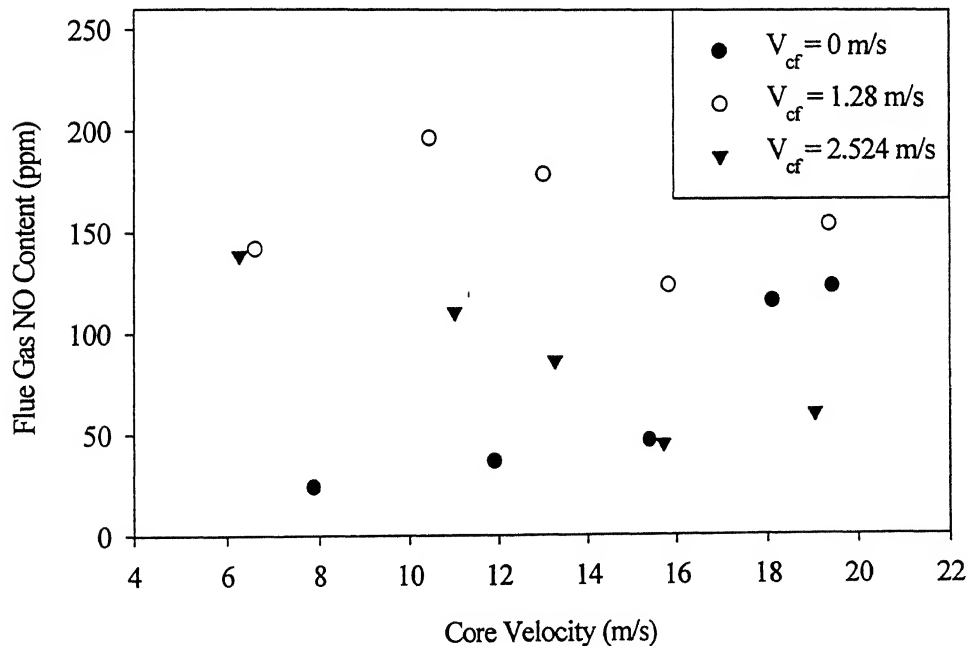


Fig 4.17. Exhaust gas NO emission for $H/D_{core} = 5.0$ with coflow air only

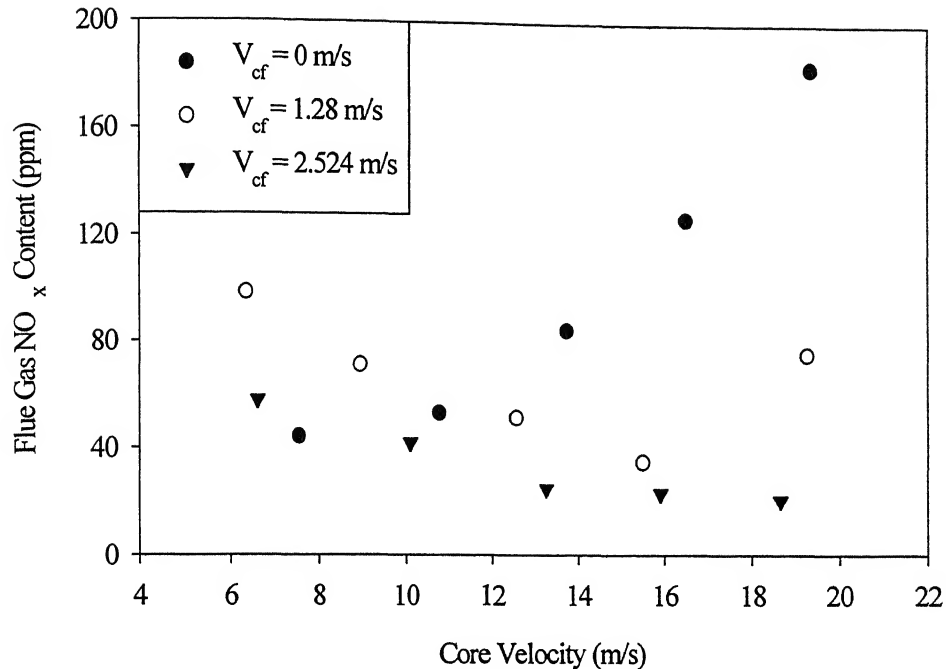


Fig 4.18. Exhaust gas NO_x emission for $H/D_{core} = 0.61$ with coflow air only

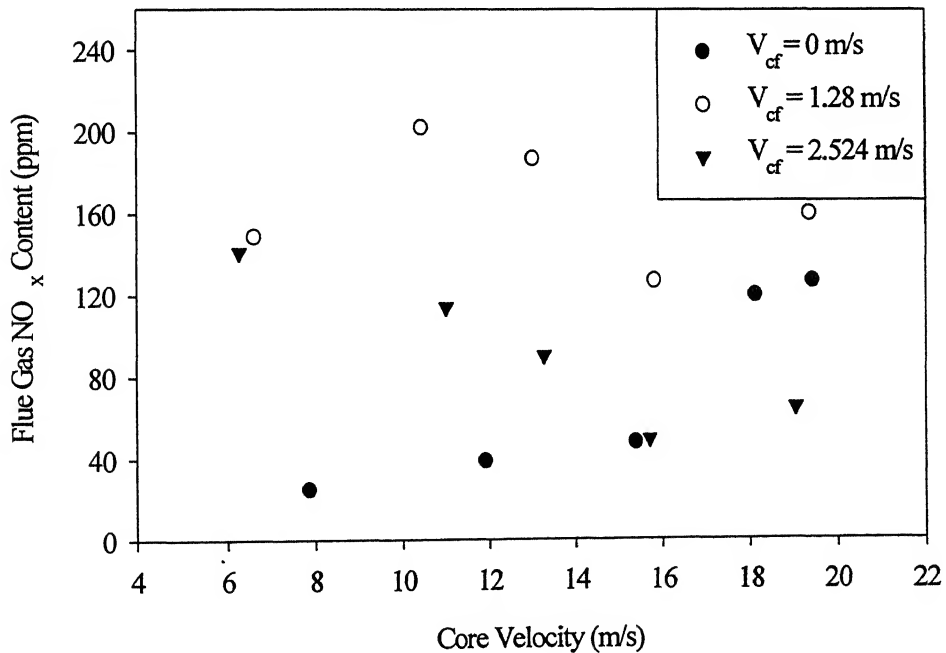


Fig 4.19. Exhaust NO_x emission for $H/D_{core} = 5.0$ with coflow air only

downstream of the flame holder may prevent the formation of hot spots particularly at higher core velocity. At the same time, with addition of air to the coflow results in similar trend to that of $H/D_{core} = 0.61$ with 1.28 m/s coflow velocity, and also there might be slight decrease in NO formation level. However, it required further studies in understand the mechanism of NO formation at high core flow velocity.

While going through the NO formation in the case of $H/D_{core} = 5.0$, the NO is increasing with increase in core velocity for the case with no air in the coflow as shown in Fig 4.17, which is also having trend similar to the case $H/D_{core} = 0.61$ with no air in the coflow. As the velocity increases, the combustion gas temperature is increasing as shown in Fig.4.9. The increase in NO formation is mainly attributed to higher combustion gas temperature. At the same time, the addition of air to the coflow leads to decrease in NO with increase in core velocity except at the higher core velocities. However, the increase in temperature due to the mixing of coflow with core flow in the case of $H/D_{core} = 5.0$ with coflow air leads to higher level of NO when compared to the $H/D_{core} = 0.61$ with coflow air. But, at the higher core velocities, the increase in NO needs further studies to understand that phenomena.

4.3. Bluff Body Stabilized Flame With Fuel-Air Coflow Mixture

The lean stability and emission levels are studied for two flame holder locations with premixed coflow in order to explore the possibility of enhancement of stability limit while reducing emission level. Efforts are made to keep the co-flow equivalence ratio below the lean flammability limit.

4.3.1 Lean Stability Limit

The stability limit is studied for premixed coflow velocity ($V=1.28$) similar to air coflow velocity as discussed in Section 4.2. The results of the lean stability limit with core velocity are shown in Fig 4.20 for $H/D_{core} = 0.61$. The overall equivalence ratio shows an increasing trend with increasing core flow velocity for all cases. The lean stability limit with premixed coflow shows a similar trend like $H/D_{core} = 0.61$ with no coflow. The data of the lean stability limit with core velocity for $H/D_{core} = 5.0$ are plotted in Fig 4.21 for a premixed coflow velocity of 1.28 m/s. The lean stability limit with fuel-air mixture in the coflow is compared

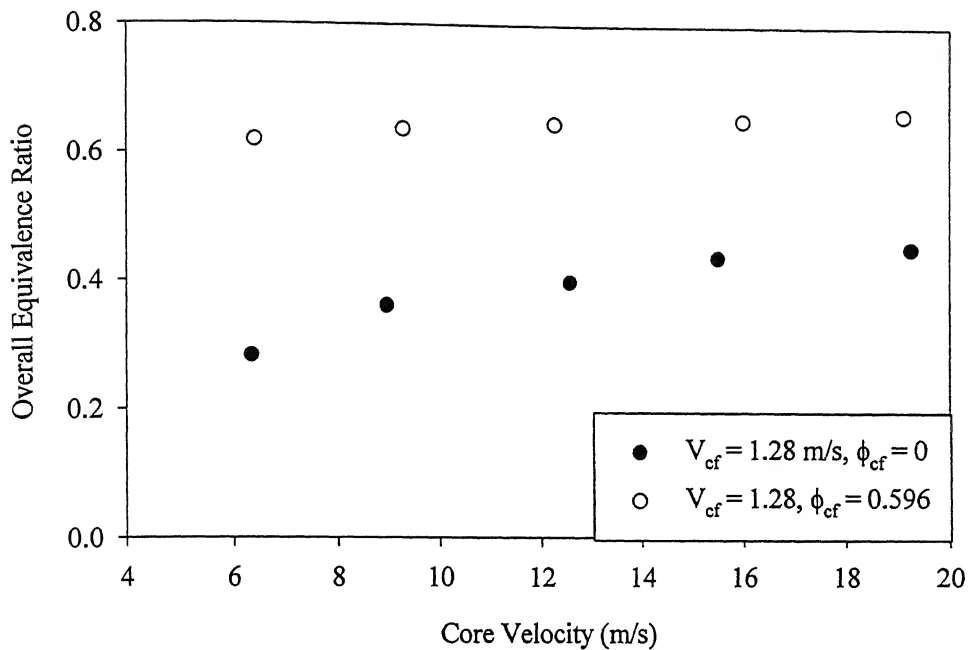


Fig 4.20. Lean stability limit for $H/D_{core} = 0.61$ with coflow air velocity = 1.28 m/s

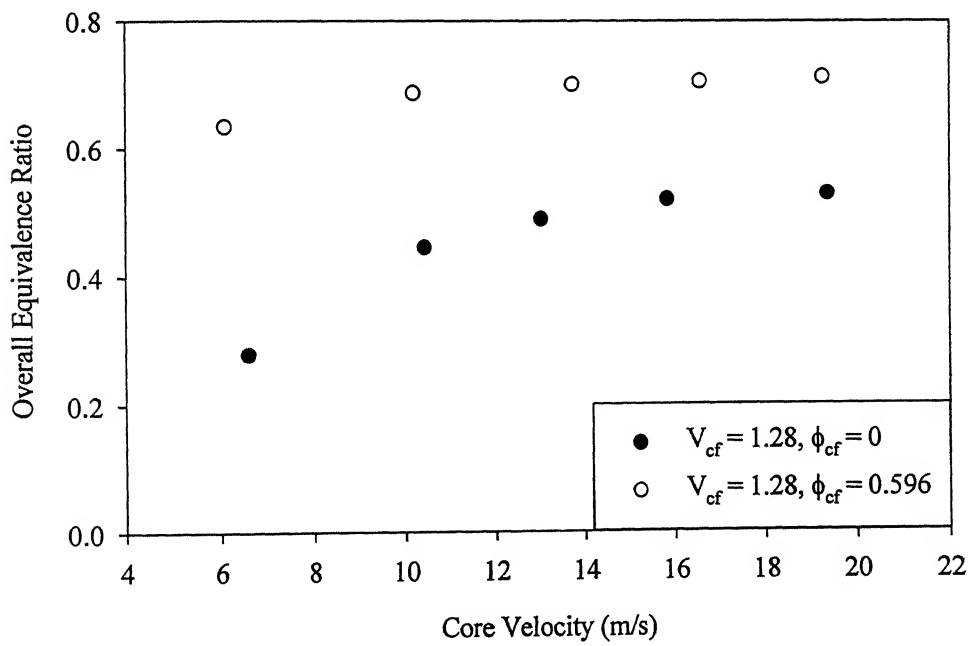


Fig 4.21. Lean Stability Limit for $H/D_{core} = 5.0$ with coflow air velocity = 1.28 m/s

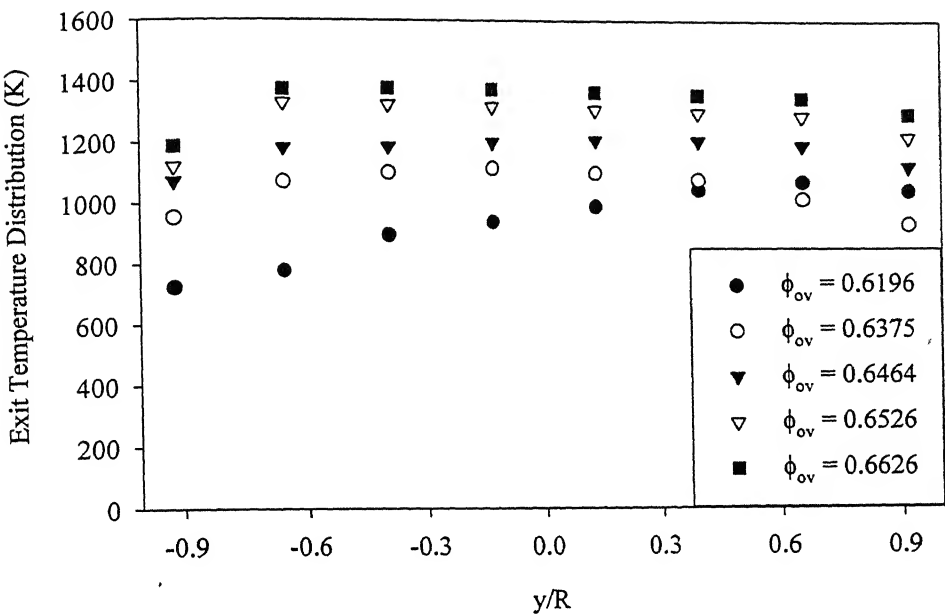


Fig 4.22. Exit gas temperature distribution for $H/D_{core} = 0.61$ with coflow fuel premixed with air ($\phi_{cf} = 0.596$ & $V_{cf} = 1.28$ m/s)

with that of air in the coflow for a particular coflow velocity indicates similar trend although the flame is stabilized at higher equivalence ratio. While comparing the results of stability limit of the $H/D_{core} = 0.61$ case with that of 5.0 with coflow fuel-air mixture, the stability limit seems to be closer to each other.

4.3.2. Exit Gas Temperature

The combustion gas exhaust temperature is plotted against core velocity as well as radial locations (y/R) as shown in Fig 4.22. All the cases of $H/D_{core} = 0.61$ and 5.0, the temperature is increasing with increase in core velocity as shown in Fig 4.23 & 4.24. For a coflow of 1.28 m/s, the combustion gas temperature level for the case $H/D_{core} = 0.61$ with coflow fuel- air mixture is almost similar than that of coflow with air only. This may be because of absence of mixing between the coflow and core flow due to the presence of flame holder within the potential core. While adding fuel-air mixture to the coflow, the exit temperature level for the case $H/D_{core} = 5.0$ with a coflow velocity of 1.28 m/s is increasing than that of the case with air only. The increase in temperature level may be due to the

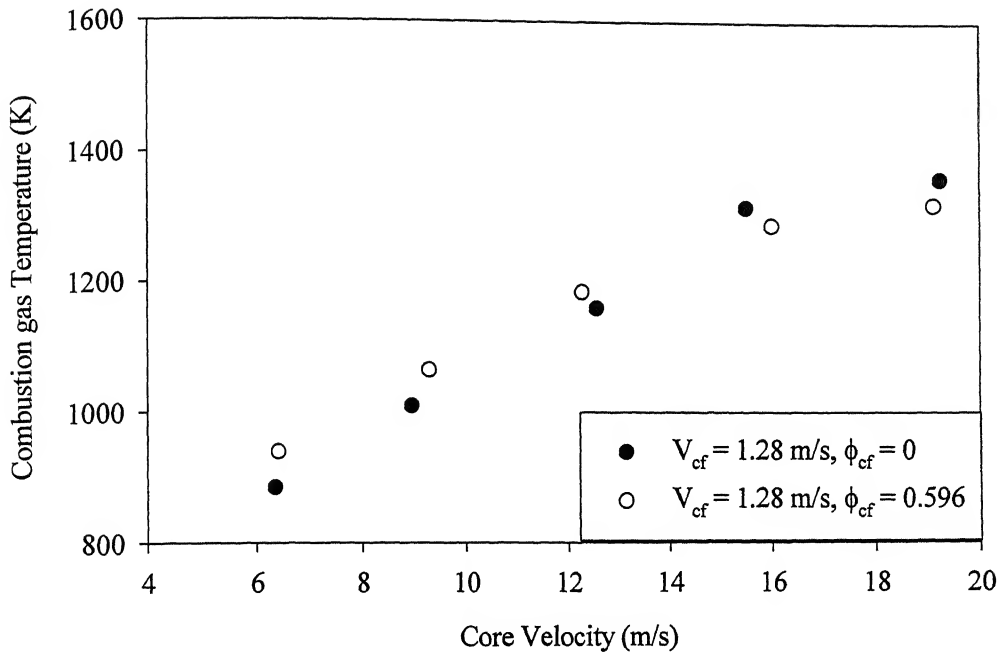


Fig 4.23. Average combustion gas temperature for $H/D_{core} = 0.61$ with coflow fuel premixed with air

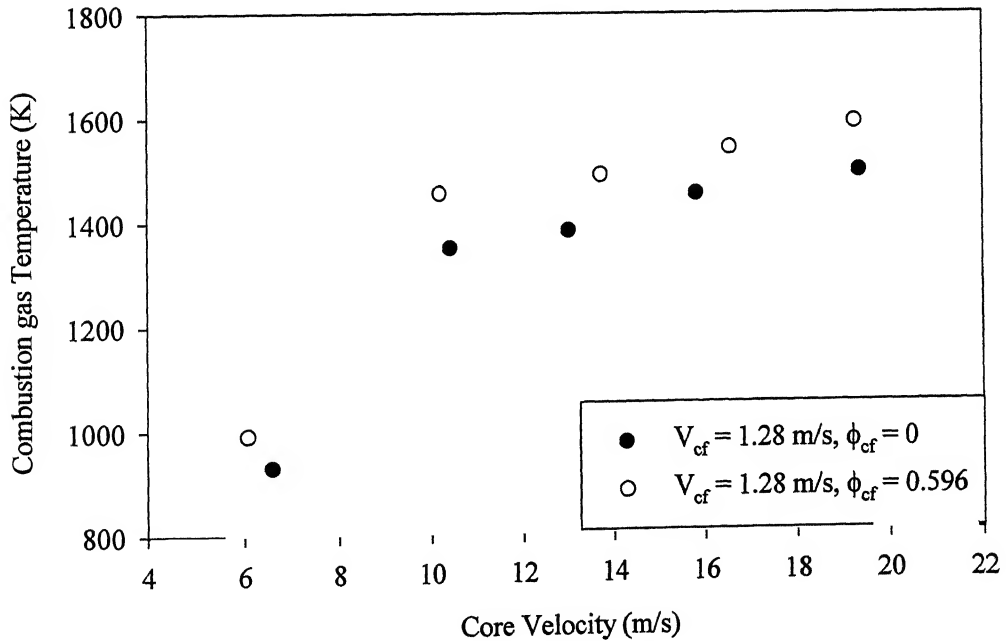


Fig 4.24. Average combustion gas temperature for $H/D_{core} = 5.0$ with coflow fuel premixed with air

presence of mixing between the coflow and core flow and also the uniform distribution of the fuel.

4.3.3. Exhaust O₂ content

The results of the flue gas O₂ content with core velocity are shown in Fig 4.25 for H/D_{core} = 0.61 for both fuel-air coflow mixture and coflow air cases. The exhaust O₂ content is decreasing with increase in the core velocity for both cases as shown in Fig 4.25. The flue gas O₂ content with core velocity is shown in Fig 4.26 for H/D = 5.0, which indicates similar trend than that of H/D = 0.61. However, there is a slight improvement in O₂ utilization in comparison to H/D = 0.61 case. This may be attributed to the uniform distribution of the mixture between coflow and core flow streams due to higher flame holder position.

4.3.4. Exhaust CO Content

The results of the flue gas CO content with core velocity are reported in Fig. 4.27 for H/D_{core} = 0.61 for both fuel-air coflow mixture and coflow air cases. For a coflow velocity of 1.28 m/s, the CO emission level is decreasing with increase in the core velocity for both cases. However, the CO emission level trend remains almost similar for both cases indicating that the adding fuel to the co-flow for H/D_{core} = 0.61 does not show much more effect on decreasing CO emission due to the location of the flame holder within the potential core. The flue gas CO emission with core velocity for H/D_{core} = 5.0 are shown in Fig. 4.28 for both fuel-air coflow mixture and coflow air cases which also indicates a similar trend of decreasing the CO emission level with increase in the core velocity. However, there is an increase in CO emission level with addition of mixture in the coflow stream particularly at lower core velocity. At lower core flow velocity, the shear layer is smaller as compared to higher core velocity. As a result, mixing will be less at lower core velocity and the mixture in the flame zone would not be very much affected by the coflow constituents. However, for higher core velocity, the flame zone equivalence ration will be very much influenced by the coflow constituents. Hence, there is an increase of CO emission level for fuel-air co flow case at lower core flow velocity while there is a decrease in CO emission level at higher core flow velocity case.

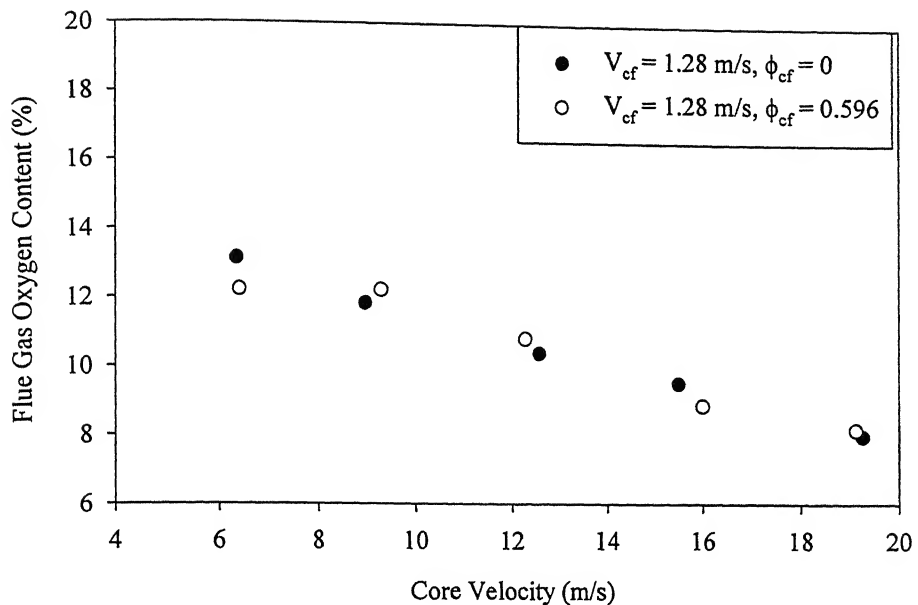


Fig 4.25. Exhaust gas O_2 for $H/D_{core} = 0.61$ with coflow air velocity = 1.28 m/s

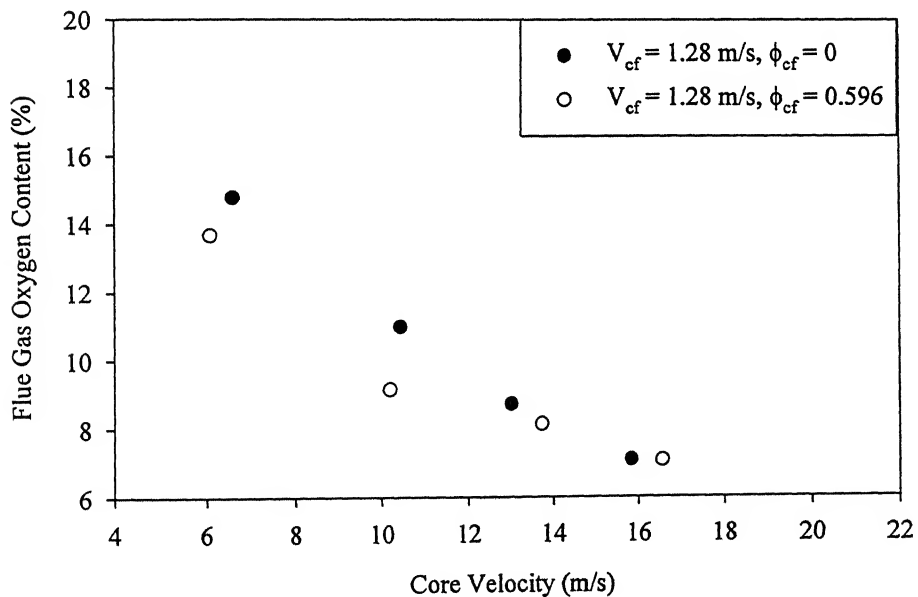


Fig 4.26. Exhaust O_2 content for $H/D_{core} = 5.0$ with coflow air velocity = 1.28 m/s

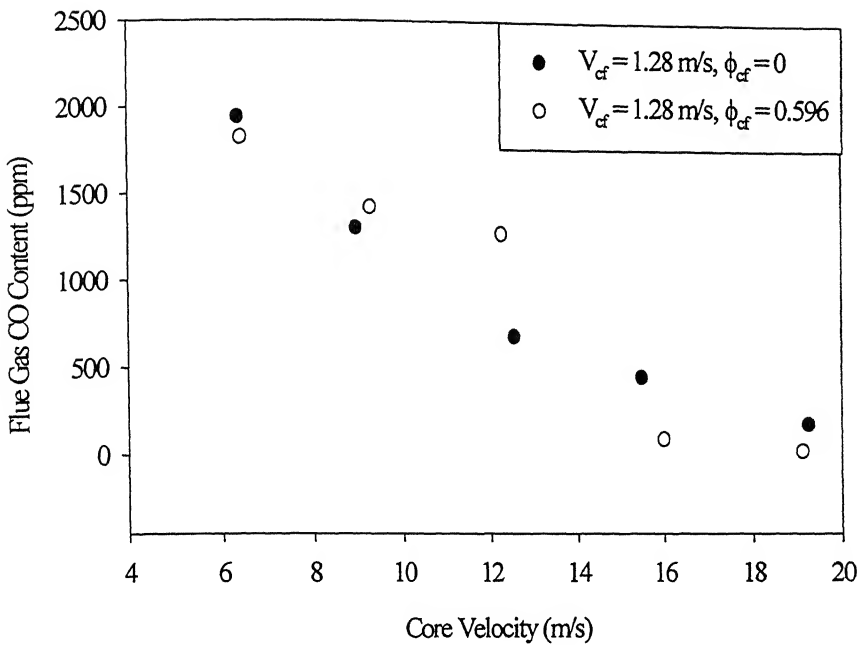


Fig 4.27. Exhaust gas CO for $H/D_{core} = 0.61$ with coflow air velocity = 1.28 m/s

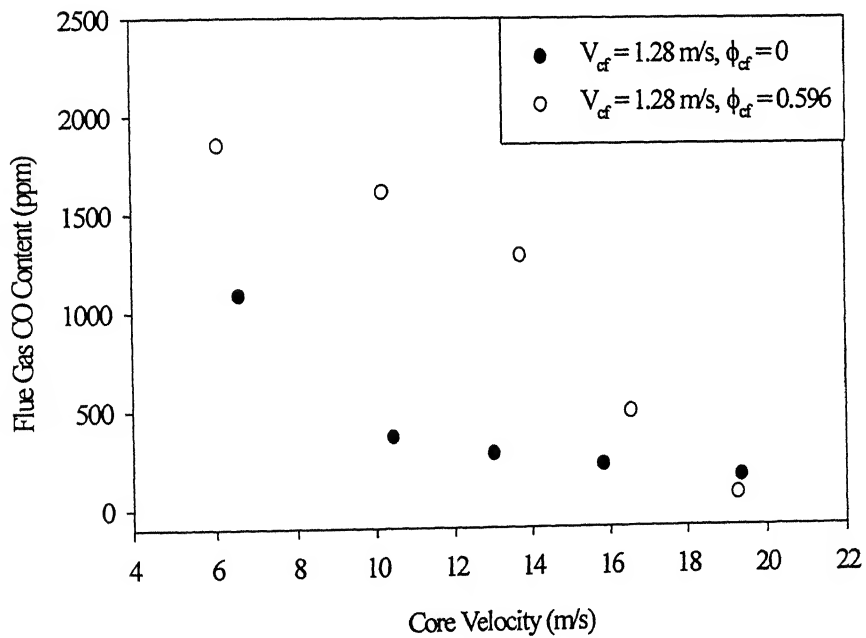


Fig 4.28. Exhaust CO content for $H/D_{core} = 5.0$ with coflow air velocity = 1.28 m/s

4.3.5. Exhaust CO₂ emission

The results of the CO₂ emission with core velocity is shown in Fig 4.29 for H/D_{core} = 0.61 for both fuel-air coflow mixture and coflow air cases. The CO₂ emission shows increasing trend in the direction of increasing velocity for both cases. The CO₂ emission for both fuel-air coflow mixture and coflow air cases of a particular coflow velocity shows similar trend. This may be due to the absence of mixing between the coflow and core flow in the down stream of the flame holder. The increase in CO₂ level is mainly attributed to increase in combustion gas temperature with increase in velocity at the lean stability limit.

The CO₂ emission level for H/D_{core}=5.0 is show in Fig. 4.30 for both fuel-air coflow mixture and coflow air cases which shows similar trend like that of H/D_{core}=0.61 case. It can be noted that the CO₂ level does not show any significant variation for both fuel-air coflow mixture and coflow air cases.

4.3.6. Exhaust NO emission

The results of NO level for H/Dcore=0.61 with core velocity is plotted in Fig. 4.31 for both fuel-air coflow mixture and coflow air cases. It can be observed that the NO level decreases with increases in core velocity and attains a minimum value at core velocity of 16 m/s and again shoots up with increase in core velocity. The hot spot due to temporal unmixedness behaviour of air and fuel is the main factor for the formation of NO. Both cases seem to produce similar level of NO emission.

The NO emission level for the flame holder position (H/D_{core} = 5.0) is plotted in Fig 4.32. Interesting to note from this Fig. 4.32 that there is substantial decrease in NO level with addition of fuel-air mixture instead of air alone in the coflow stream. It may be attributed to the mixing of coflow with core flow. The hot spot formation due to fuel pockets is less probable in the former case compared with later and can be avoided by premixing the coflow stream. It needs further insight to understand the physics of this interesting phenomenon.

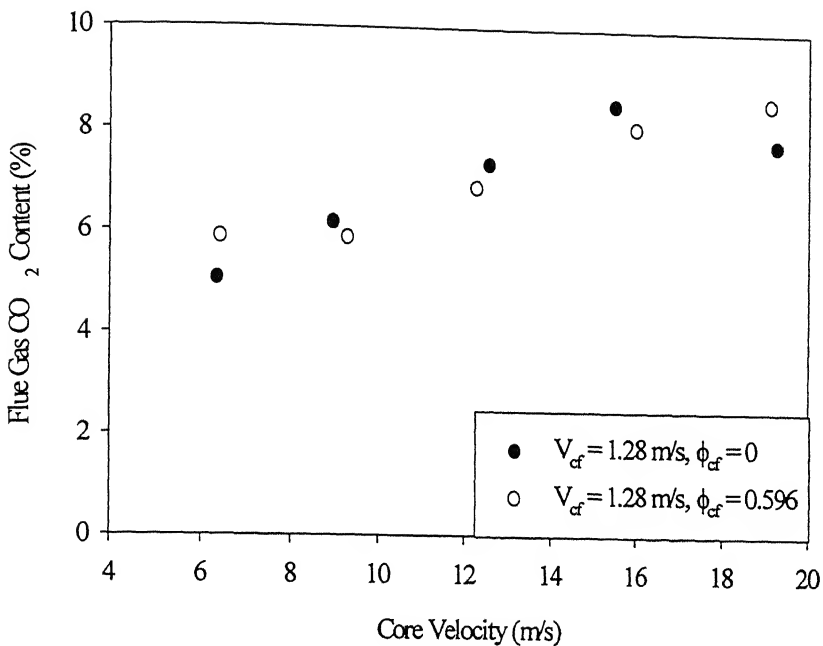


Fig 4.29. Exhaust CO_2 content for $H/D_{\text{core}} = 0.61$ with coflow air velocity = 1.28 m/s

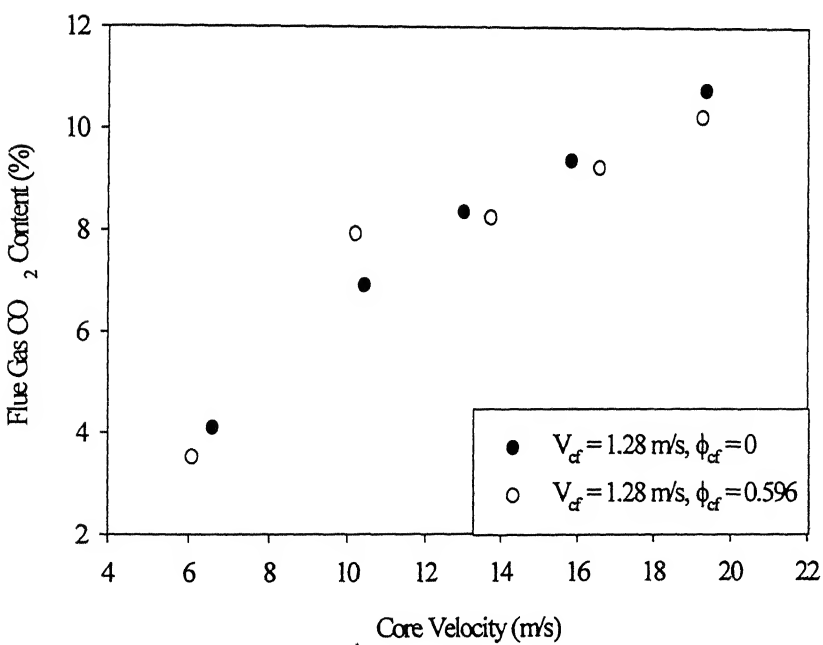


Fig 4.30. Exhaust CO_2 content for $H/D_{\text{core}} = 5.0$ with coflow air velocity = 1.28 m/s

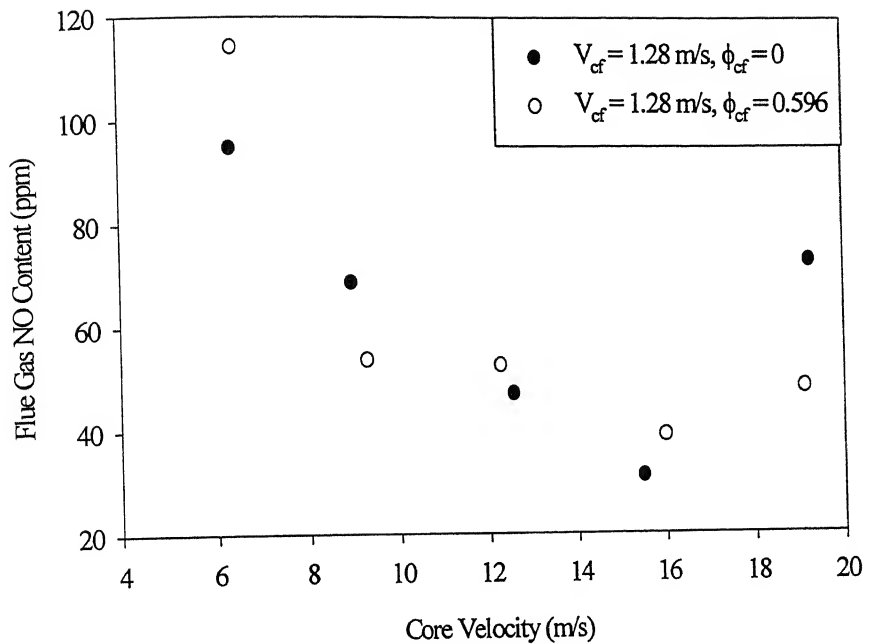


Fig 4.31. Exhaust NO content for $H/D_{core} = 0.61$ with coflow air velocity = 1.28 m/s

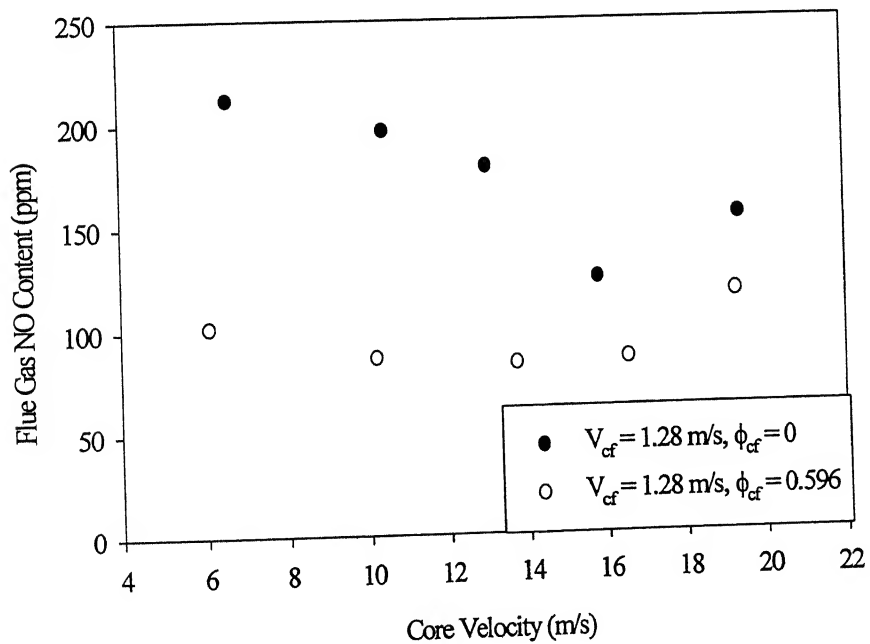


Fig 4.32. Exhaust NO content for $H/D_{core} = 5.0$ with coflow air velocity = 1.28 m/s

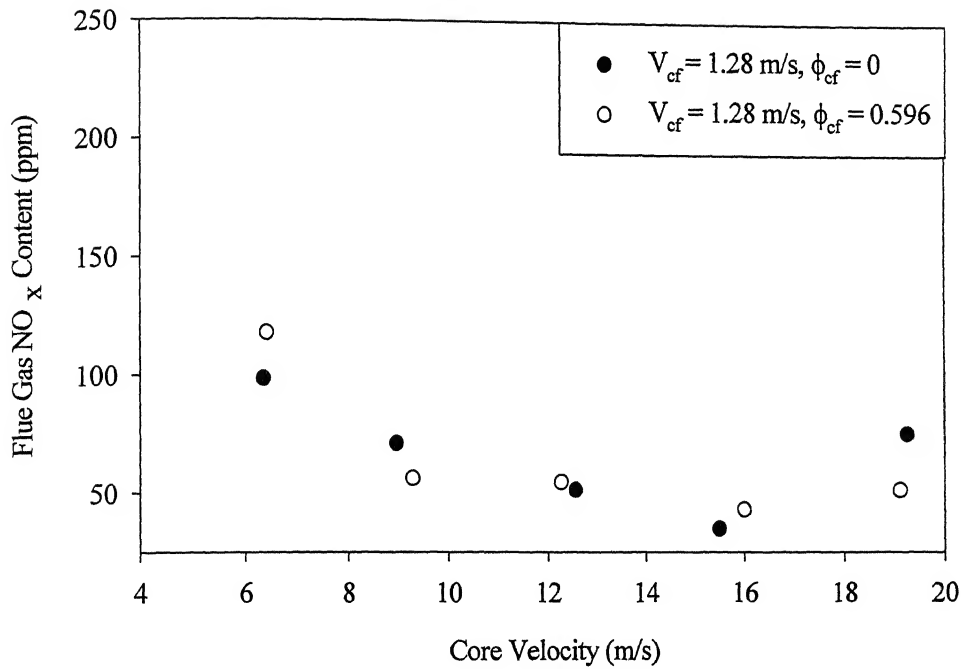


Fig 4.33. Exhaust NO_x content for $H/D_{core} = 0.61$ with coflow air velocity = 1.28 m/s

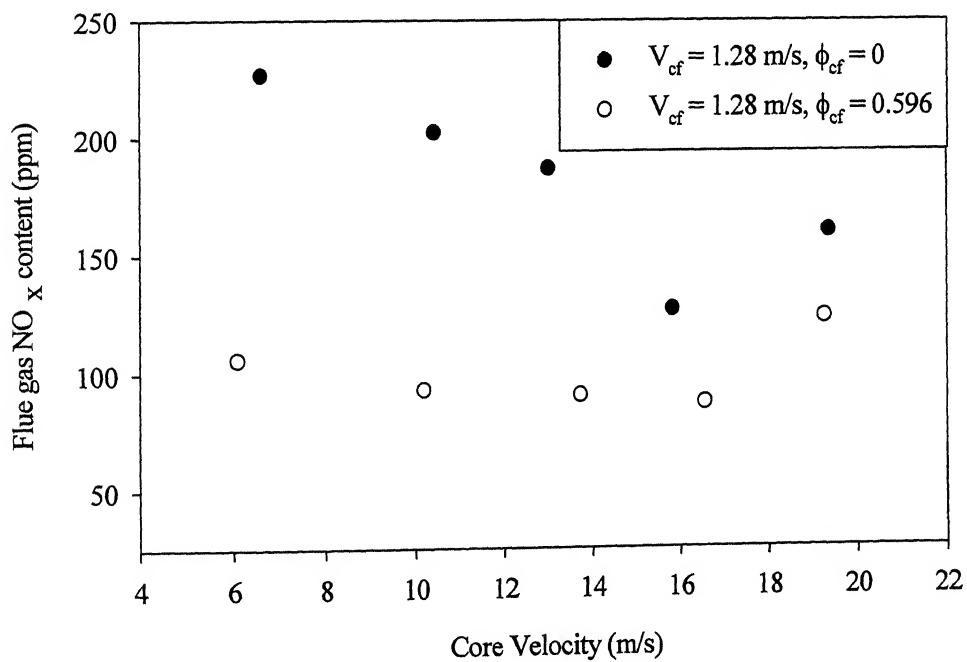


Fig 4.34. Exhaust NO_x content for $H/D_{core} = 5.0$ with coflow air velocity = 1.28 m/s

4.3.7. NO_x emission

The NO_x emission and NO emission resembles almost same for all cases as shown in Fig 4.33 and 4.34. The small difference between the NO and NO_x are due to the some other constituents of NO_x like NO₂, N₂O and etc.

4.4. Swirl Stabilized Flame Analysis

It has been reported in the literature that swirl flow helps in stabilizing the flame. In the present work, effort is being made to stabilize the flame by imparting swirl to the coflow stream with the help of vane swirler as show in Fig 3.3b (Sec3.6, page 20). The amount of swirl can be quantified by the swirl number as defined in Section 3.9.3. The swirl number having value less than 0.5 is called as low swirl and the swirl number more than 0.5 is called as strong swirl according to Beer and Chigier [30] and Chigier and Chervinsky [8]. Hence, the lean stability limit using swirl flame stabilizer is studied in present work with help of two swirl numbers, such as 0.13 (low swirl) and 0.667 (strong swirl). The swirl effects are studied for two swirl velocity viz., 1.5 and 2.56 m/s. The sound level is also measured. And also the emissions levels are measured and analyzed. The results of the swirl stabilized flame analysis are discussed in the following sub headings:

1. Lean stability limit
2. Exit gas temperature distribution
3. Exhaust O₂ content
4. Exhaust CO emission
5. Exhaust CO₂ emission
6. Exhaust NO emission
7. Exhaust NO_x emission
8. Overall Sound Pressure Level Measurement (OSPL)

4.4.1. Lean Stability limit

Several experiments are conducted in order to check the repeatability of the readings. The lean stability limit is found out by the procedure explained in the Sec 3.9.2. The results of lean stability limit for swirl number of 0.13 are shown in Fig 4.35 for both fuel-air coflow mixture and coflow air cases. The overall equivalence ratio is increasing with increase in core velocity for all cases. In order to explore the effects of premixed mixture in the coflow stream on the core flow stream, the variation of core equivalence ratio for swirl number of 0.13 case

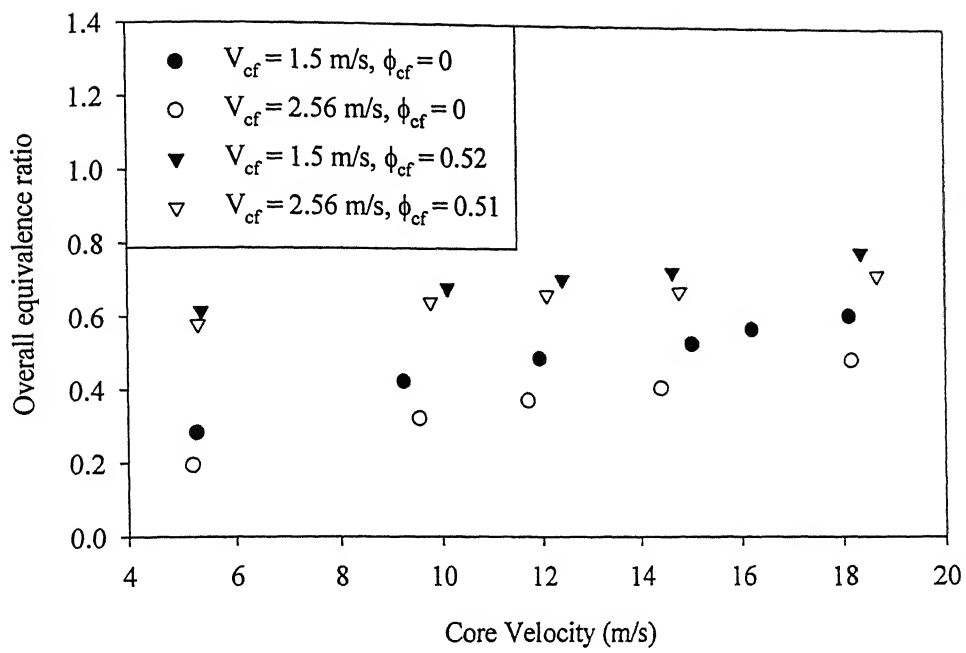


Fig 4.35. Lean stability limit for the Swirl No. 0.13 with coflow air or fuel premixed with air

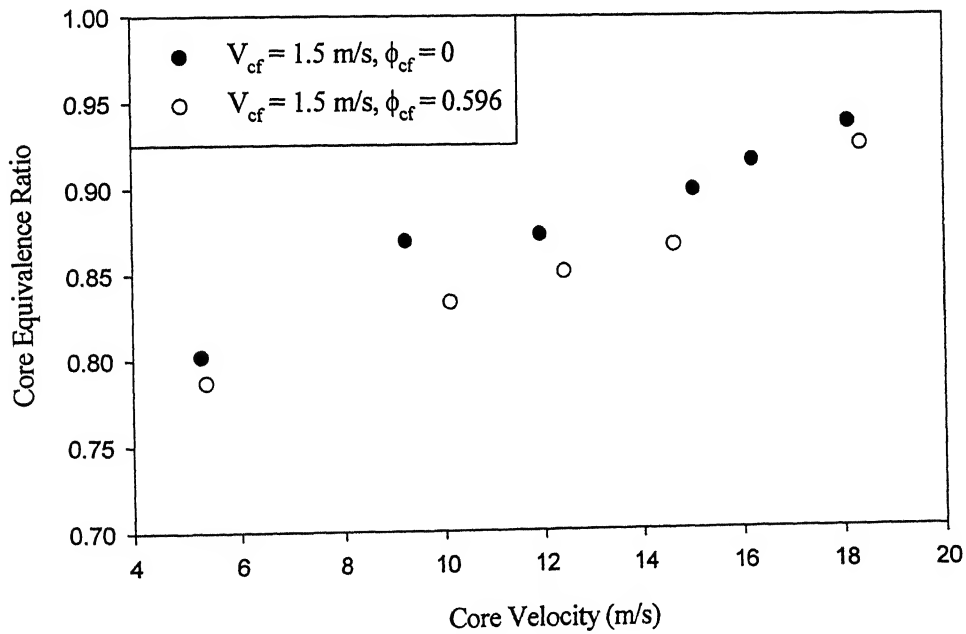


Fig 4.36. Effect of core equivalence ratio for Swirl No. 0.13 with coflow velocity of 1.5 m/s

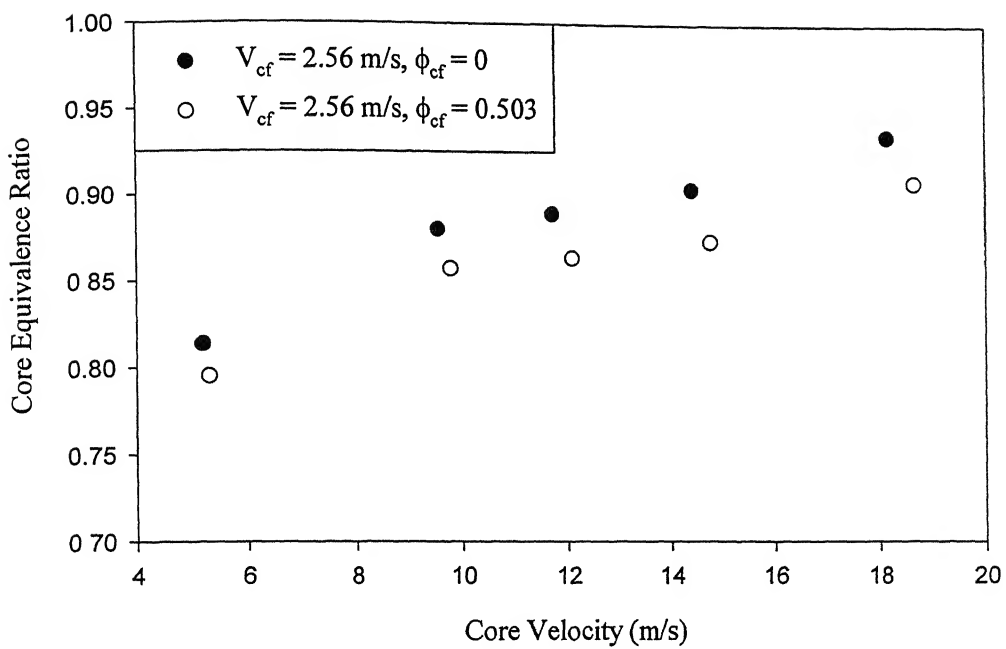


Fig 4.37. Effect of core equivalence ratio for Swirl No. 0.13 with coflow velocity of .56 m/s

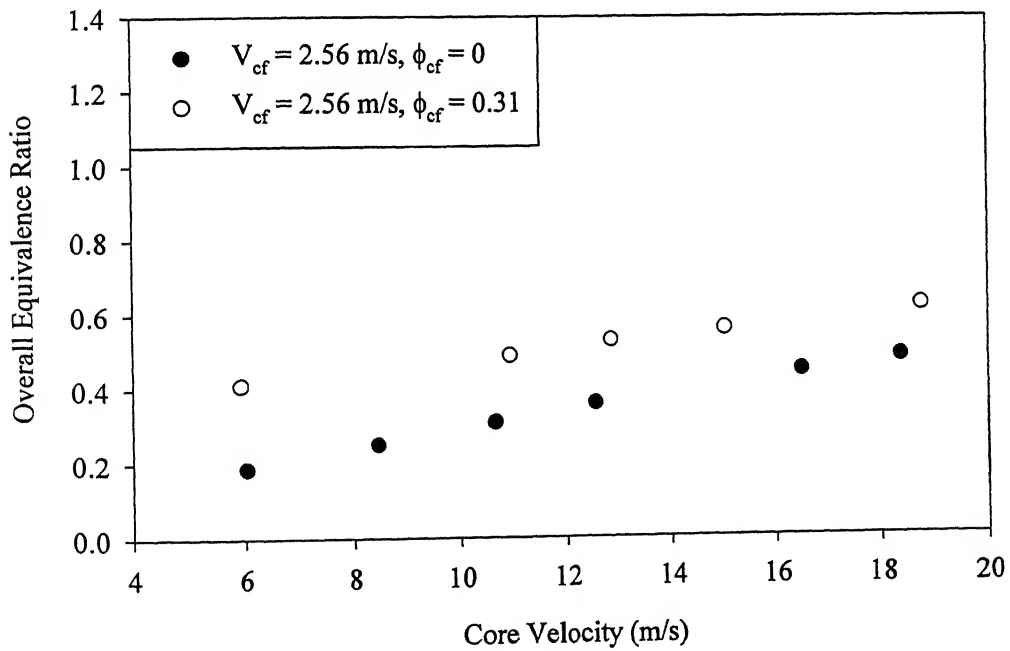


Fig 4.38. Lean stability limit for Swirl No. 0.67 with coflow air or fuel premixed with air

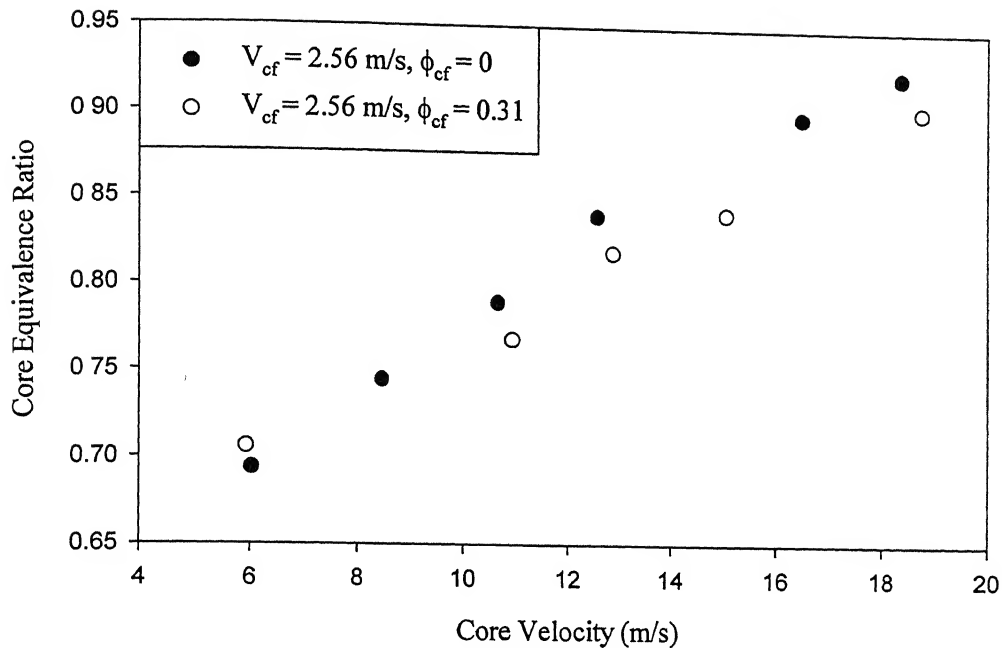


Fig 4.39. Effect of core equivalence ratio for Swirl No. 0.67 with coflow velocity of 2.56 m/s

is plotted against the core velocity. Interesting to note from this Fig 4.36 that the flame is stabilized at lower core equivalence ratio level with addition of fuel-air mixture to the coflow stream. This may be due to enhanced mixing between the core flow and swirl coflow streams. At the higher coflow velocity, the stability limit (see Fig 4.37) for coflow air come closer to the case for fuel-air coflow mixture. This may be attributed to the high swirling coflow velocity ($V_{cf} = 2.56 \text{ m/s}$), which leads to lower residence time.

In order to study the effect of strong swirl number on lean stability limit, the 40° vane angle swirler is used to generate a Swirl number of 0.67. The results of overall equivalence ratio for swirl number 0.67 are plotted against core velocity in Fig 4.38. It can be observed that the overall equivalence ratio is increasing with increase in core velocity. However, the stability limits for higher swirl number is improved in comparison to low swirl number. Besides this, the flame height decreases with increase in swirl number, which will be helpful for designing a compact combustor. This may be due to the presence of flow entrainment set up

by toroidal vortex type recirculation zone as observed in the cold flow studies of Chigier and Chervinsky [8]. It is conjectured that the presence of recirculatory in the central zone of the jet is playing the important role in flame stability limit, which may be explored in future. With addition of premixed mixture in the coflow stream, similar trend of enhanced stability limits with respect to core equivalence ratio is observed for higher swirl number case as shown in Fig 4.39.

4.4.2 Exit Gas Temperature Distribution

The exhaust combustion gas temperature measured with Pt-Pt13%Rh thermocouple is plotted in Fig 4.40 against core velocity for swirl Number of 0.13. With the addition of air to the coflow for velocity of 1.5 m/s, the temperature shows an increasing trend with increase in core velocity. As the velocity increases, the overall equivalence ratio will increase. This will lead to an increasing trend of exit gas temperature with core velocity. While increasing the coflow air from 1.5 m/s to 2.56 m/s, the combustion gas temperature level is decreasing due to the presence of quenching of combustion products by excess air present in the coflow. But at the same time, adding fuel-air premixture to the coflow does not show any significant change in temperature. The combustion gas temperature for a swirl number of 0.67 is plotted in Fig 4.41 with core velocity for both fuel-air coflow mixture and air only coflow cases with a coflow velocity of 2.56 m/s. The combustion gas temperature is increased for the swirl number of 0.67 than the swirl number of 0.13 with same coflow velocity ($V_{cf} = 2.56$ m/s) because of the better mixing between the coflow and core flow due to the presence of toroidal vortex type recirculation zone.

4.4.3 Exhaust gas O₂ content

The results of the flue gas O₂ content with core velocity for swirl number of 0.13 are plotted in Fig 4.42 for both premixed mixture and air in the coflow stream. The flue gas O₂ content is decreasing with increase in core velocity for two coflow velocities (1.5 m/s and 2.56 m/s). While comparing the flue gas O₂ content for fuel-air coflow mixture and air only of two coflow velocity such as 1.5 m/s and 2.56 m/s, the flue gas O₂ content does not show considerable difference.

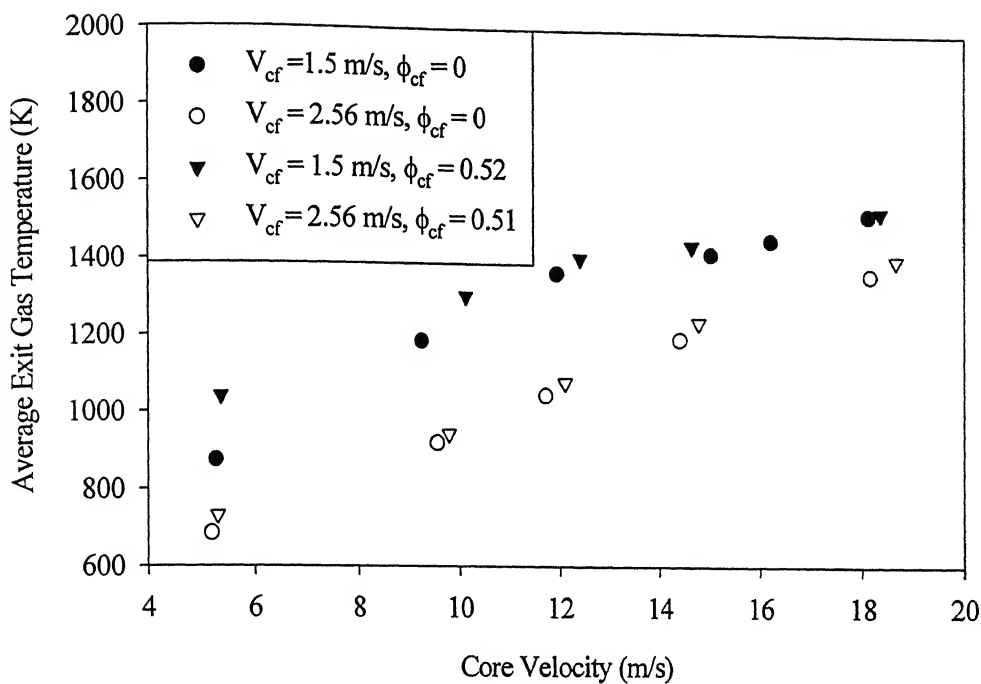


Fig 4.40 Exhaust gas combustion temperature for Swirl No. 0.13 with coflow air or fuel premixed with air

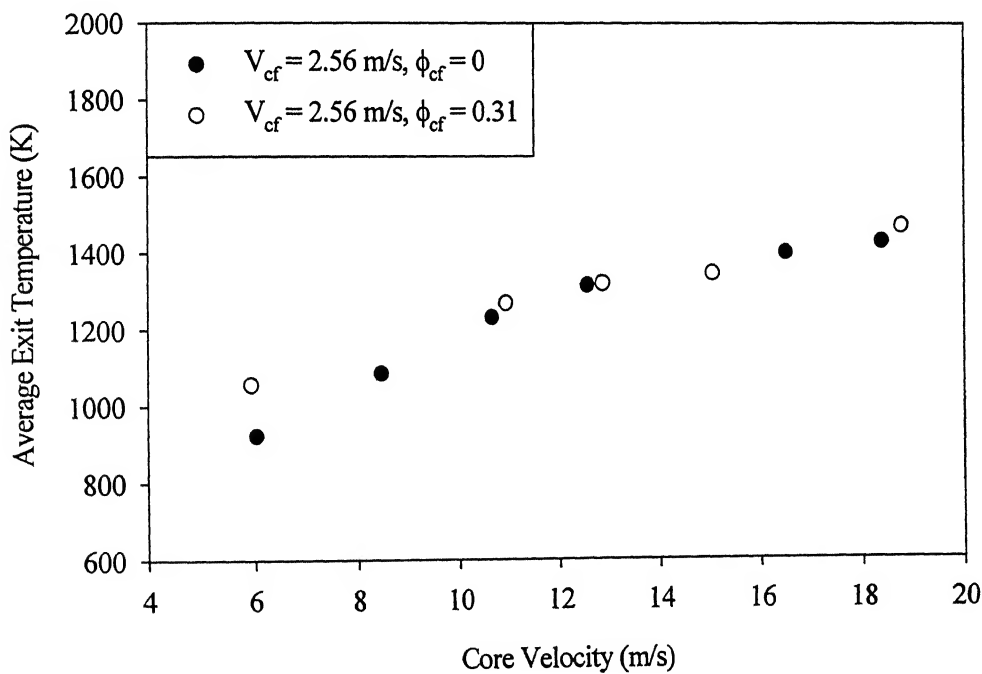


Fig 4.41 Exhaust gas combustion temperature for Swirl No. 0.67 with coflow air or fuel premixed with air

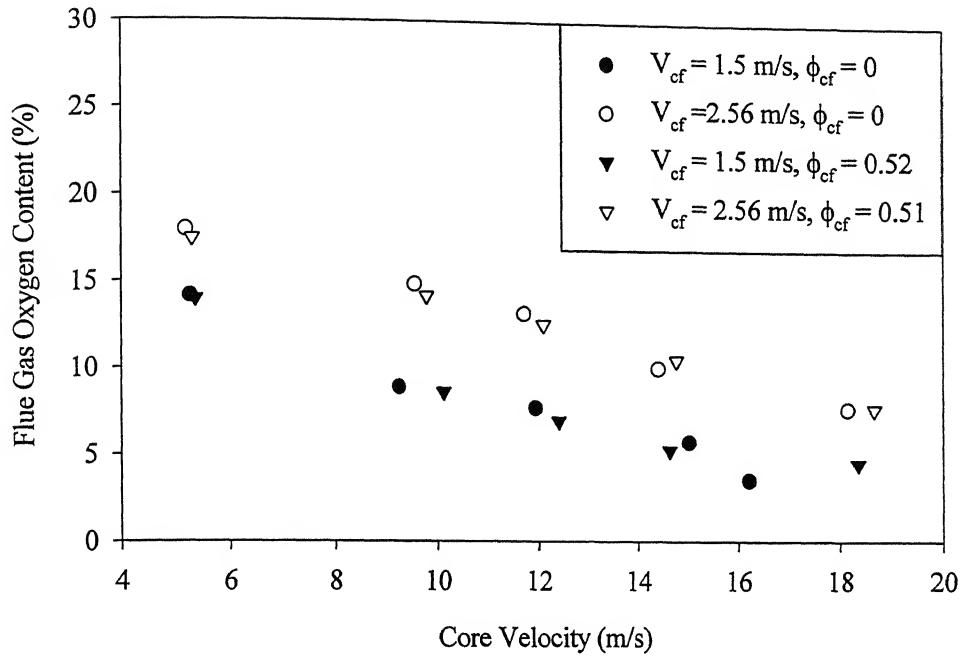


Fig 4.42 Exhaust gas Oxygen content for Swirl No. 0.13 with coflow air or fuel premixed with air

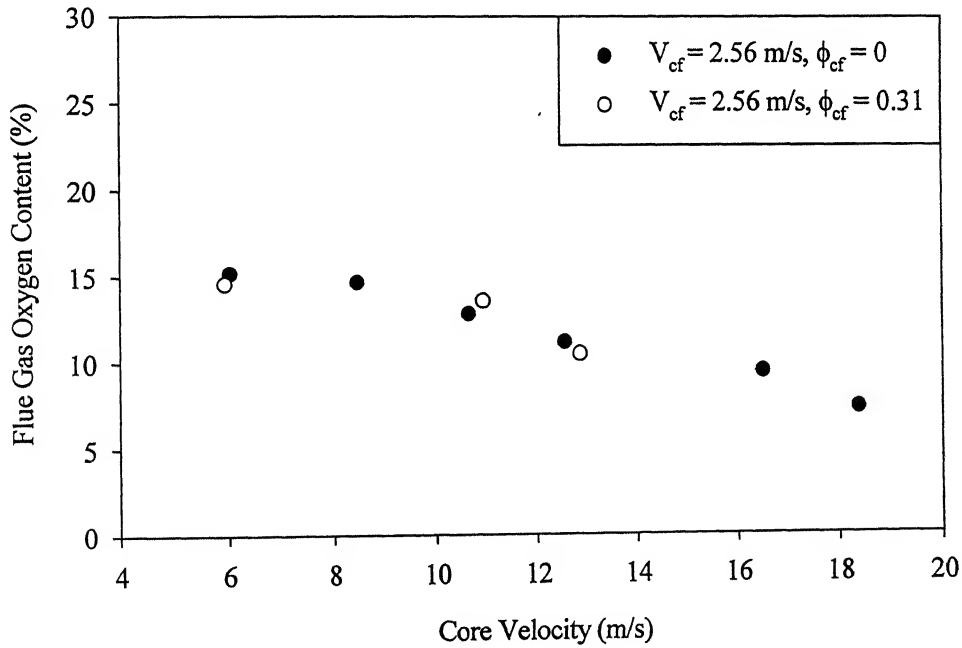


Fig 4.43 Exhaust gas Oxygen Content for Swirl No. 0.67 with coflow air or fuel premixed with air

The flue gas O₂ content with core velocity for swirl number 0.67 is having similar trend to that of swirl number of 0.13 case as shown in Fig 4.43 but exhibits lower value for swirl number 0.67 in comparison to low swirl number, 0.13. This sort of better O₂ utilization is mainly due to the presence of the toroidal type recirculation vortex created by the strong swirl of 0.67. But, it is observed that exorbitant amount of CO are being produced when the coflow velocity is lower than 2.56 m/s. Interestingly, large amount of CO are produced for premixed coflow stream, particularly when the core velocity increases beyond 13 m/s even for coflow velocity of 2.56 m/s. This may be due to the non-availability of sufficient amount of O₂ for oxidization of CO to form CO₂, which needs further studies to overcome this problem.

4.4.4 Exhaust gas CO emission

The results of flue gas CO for the swirl number 0.13 are plotted in Fig 4.44 for both premixed coflow mixture and air only cases. It shows a decreasing trend with increase in core velocity. For lower coflow velocity ($V_{cf} = 1.5$ m/s), the CO emission level is almost same for both cases. This may be due to the higher residence time and higher temperature created due to better mixing of the low swirling coflow with axial core flow. When the coflow increases to higher velocity of 2.56 m/s, there is an increase in CO emission level, which increases further with addition of premixed mixture in the coflow stream. This sort of nature may be attributed to the low temperature and lower residence time. But, the CO level starts decreasing rapidly in the high core velocity due to increase in gas temperature and better mixing.

The CO emission level for swirl number 0.67 for both fuel-air coflow mixture and air only cases show similar trend to previous one for the coflow velocity of 2.56 m/s (see Fig 4.45). There is a decrease of CO emission level as much as 40 % in the lower core velocity region in comparison to swirl number of 0.13.

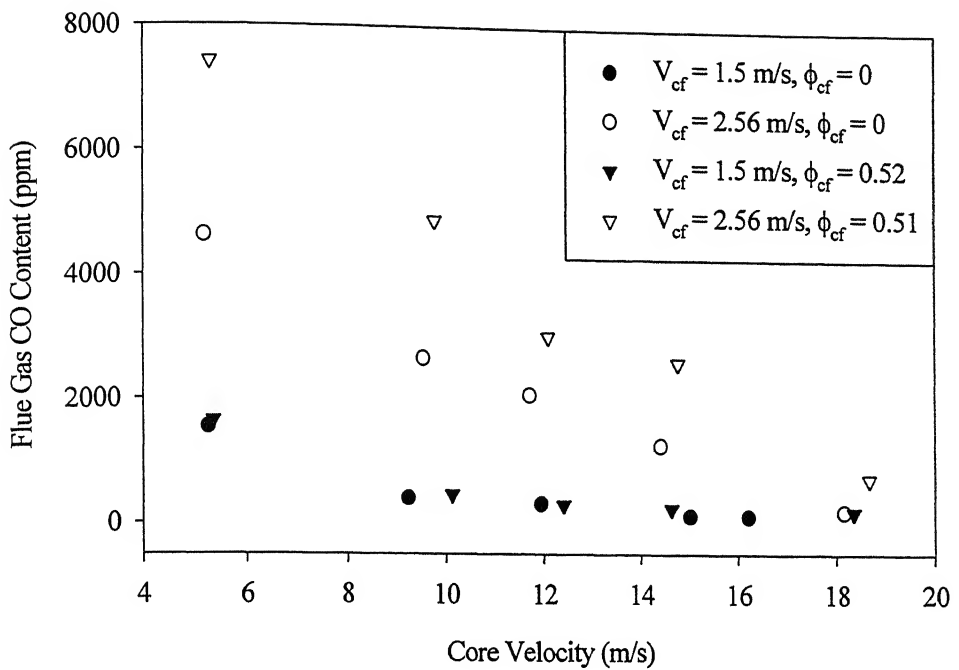


Fig 4.44. Exhaust gas CO content for Swirl No. 0.13 with coflow air or fuel premixed with air

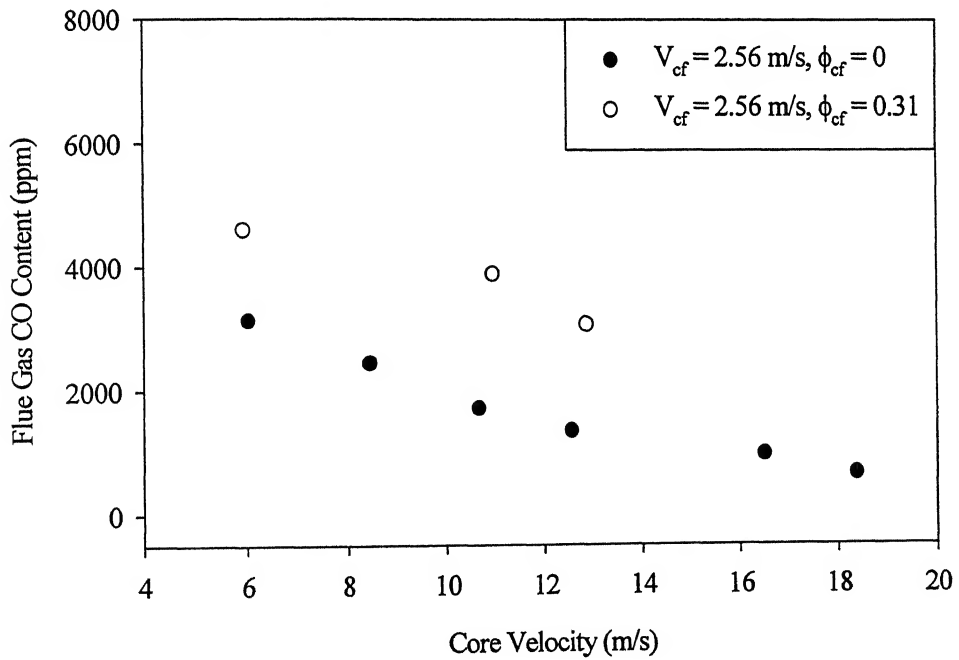


Fig 4.45. Exhaust gas CO content for Swirl No. 0.67 with coflow air or fuel premixed with air

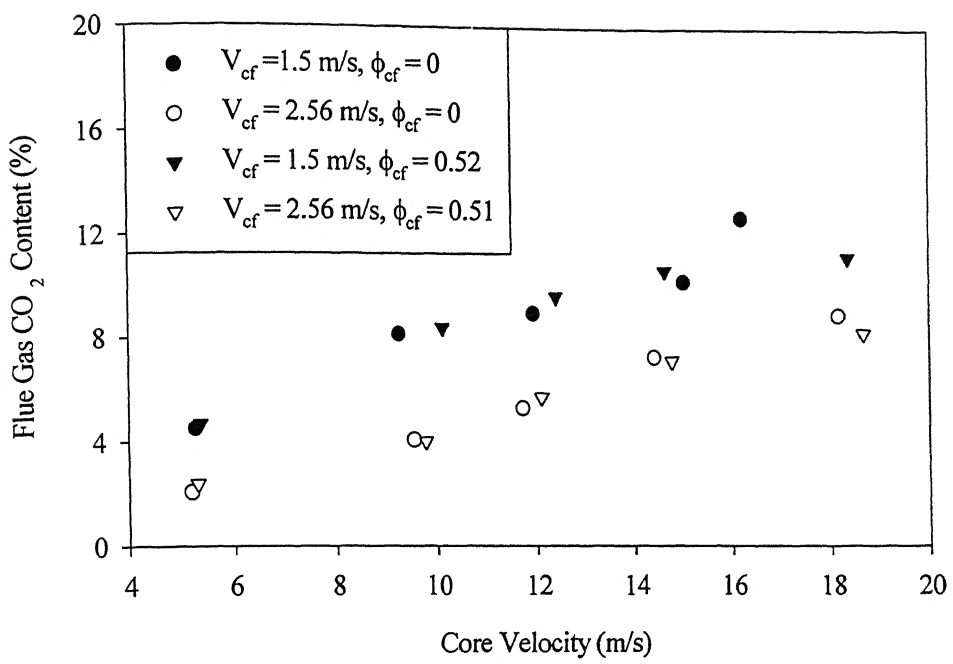


Fig 4.46. Exhaust gas CO₂ content for Swirl No. 0.13 with coflow air or fuel premixed with air

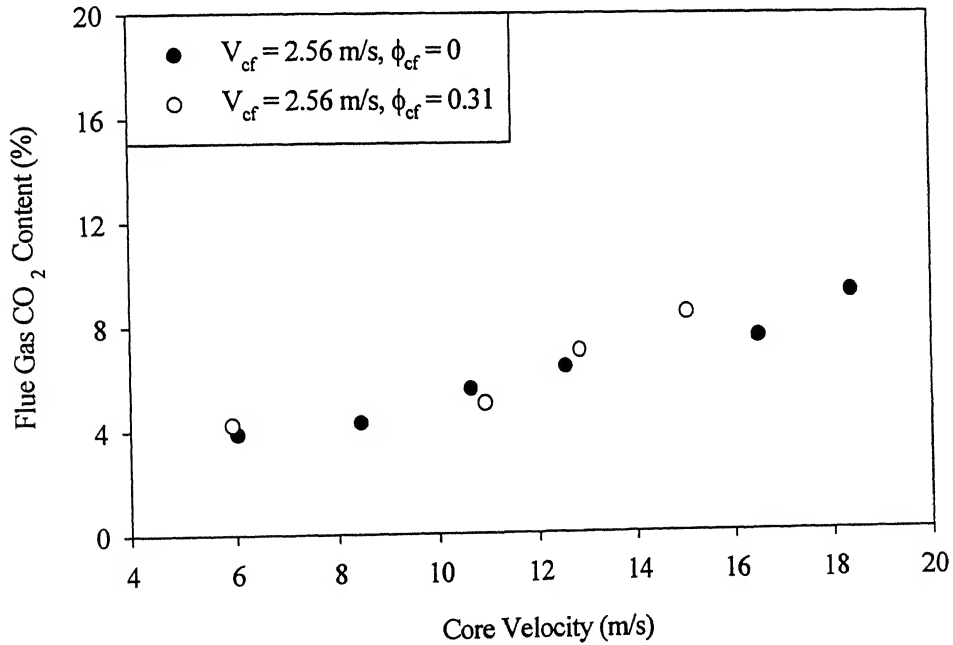


Fig 4.47. Exhaust gas CO₂ content for Swirl No. 0.67 with coflow air or fuel premixed with air

4.4.5 Exhaust CO₂ Emission

The results of the flue gas CO₂ emission for swirl number of 0.13 with core velocity in Fig 4.46 is showing increasing trend for both fuel-air coflow mixture and air stream. However, the CO₂ emission level is decreased for higher coflow velocity ($V_{cf} = 2.56$ m/s) since large amount of CO cant be converted into CO₂ due to lower temperature and residence time prevailing in the burner. Interestingly the adding fuel-air premixture to the coflow seems to have no impact on the CO₂ emission level. The CO₂ emission for a swirl number of 0.67, shown in Fig 4.47 exhibits a similar trend that of earlier case. But the higher swirl number have higher CO₂ level indicating the beneficial effects of higher swirl number in enhancing the combustion process of fuel. This may be due to the presence of the toroidal vortex type recirculation zone, which enhances mixing level.

4.4.6. Exhaust NO Emission

The results of the flue gas NO level with core velocity for a swirl number of 0.13 in Fig 4.48 shows an increasing trend for both coflow velocity ($V_{cf} = 1.5$ m/s, and 2.56 m/s) This type of trend may be attributed to the increase in gas temperature towards the direction of increasing core velocity (see Fig 4.40) since the flame is stabilized at higher equivalence ratio. When there is an increase in coflow air velocity, the NO level is decreased as much as 50%. This may be due to better mixing of the combustion products and also better mixing of coflow with core flow, which reduces the amount of hot spot formation. At the same time, adding fuel-air mixture to the coflow is not creating any significant effect to the NO emission reduction particularly at the lower coflow velocity ($V_{cf} = 1.5$ m/s). However, for higher coflow velocity, there is no change in NO emission level at lower core flow velocity and but for with increase in core velocity, the NO level is decreased as much as round 30% particularly at the higher core velocity region.

The results of the flue gas NO level for a swirl number of 0.67 is shown in Fig 4.49 with core velocity for both cases only for a coflow velocity of 2.56 m/s. Here, the flue gas NO level is having similar trend to the NO emission level for 0.13. But, there is an increase in the NO emission level in comparison to swirl number 0.13. Addition of fuel-air mixture to the coflow does not show any significant change in NO level.

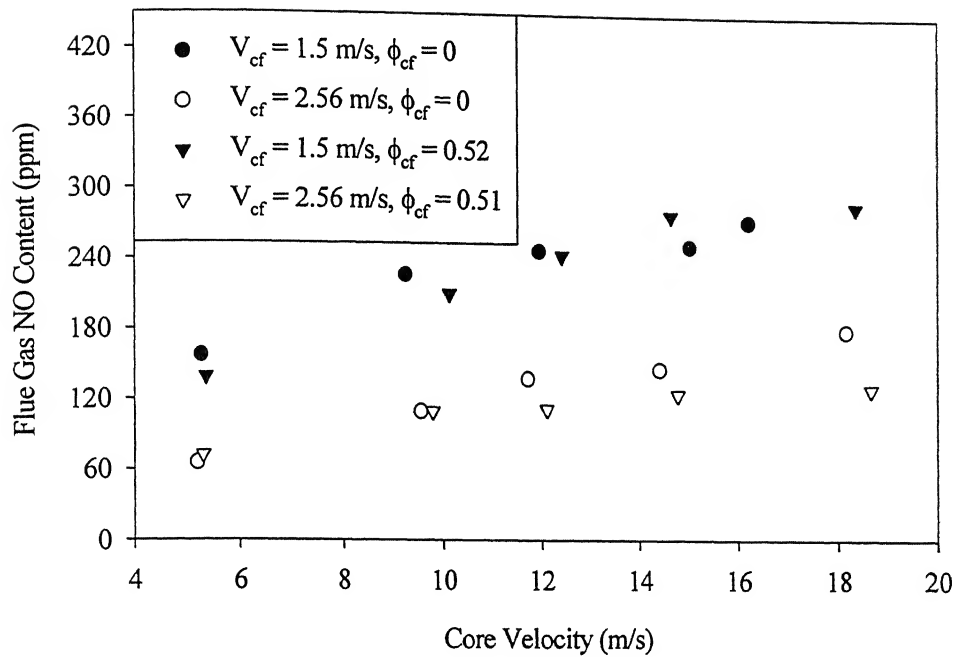


Fig 4.48. Exhaust gas NO content for Swirl No. 0.13 with coflow air or fuel premixed with air

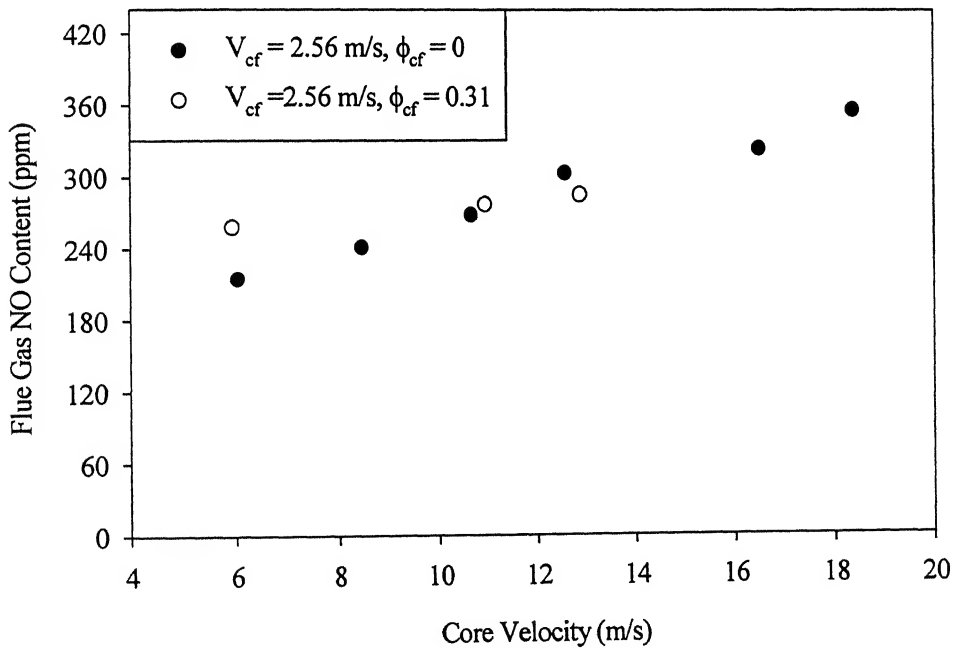


Fig 4.49. Exhaust gas NO content for Swirl No. 0.667 with coflow air or fuel premixed with air

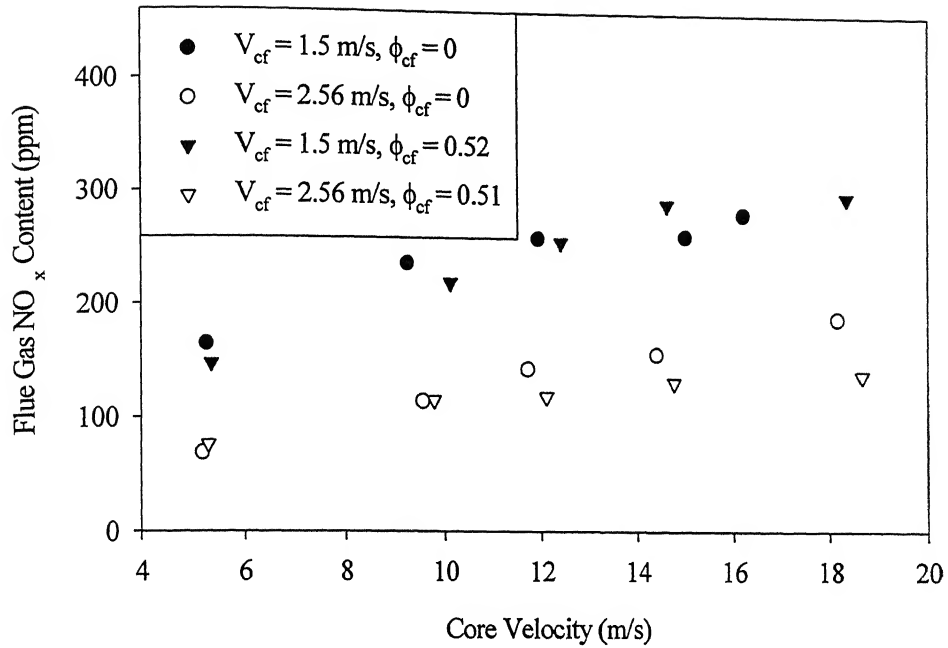


Fig 4.50. Exhaust gas NO_x content for Swirl No. 0.13 with coflow air or fuel premixed with air

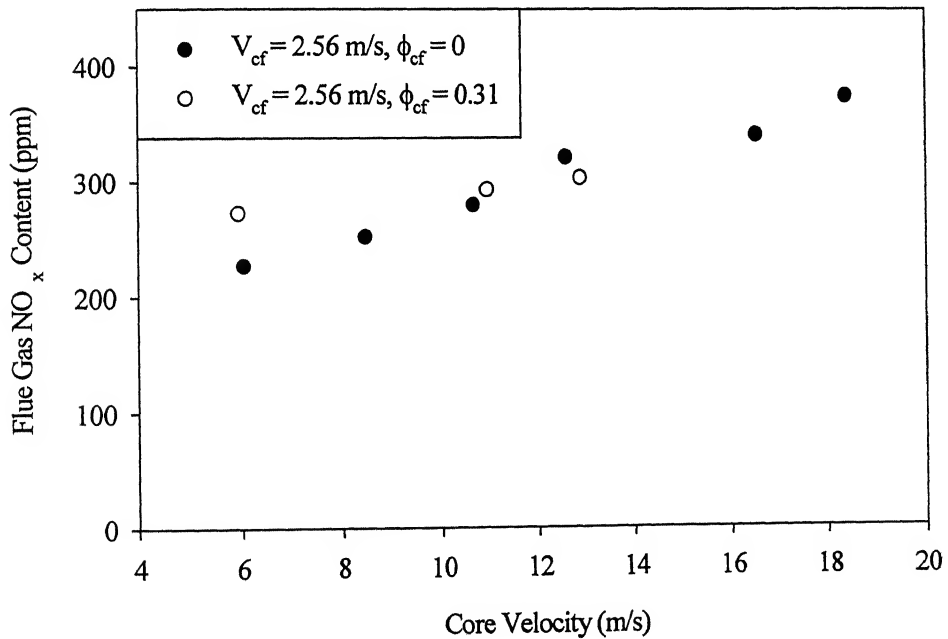


Fig 4.51. Exhaust gas NO_x content for Swirl No. 0.67 with coflow air or fuel premixed with air

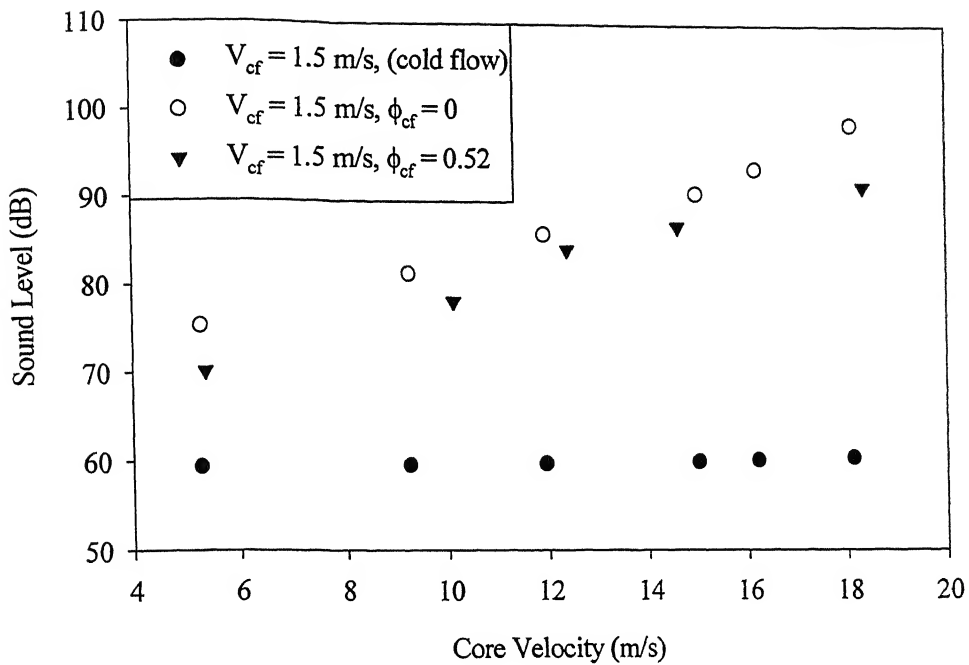


Fig 4.52. Overall sound level for Swirl No. 0.13 with coflow velocity = 1.5 m/s

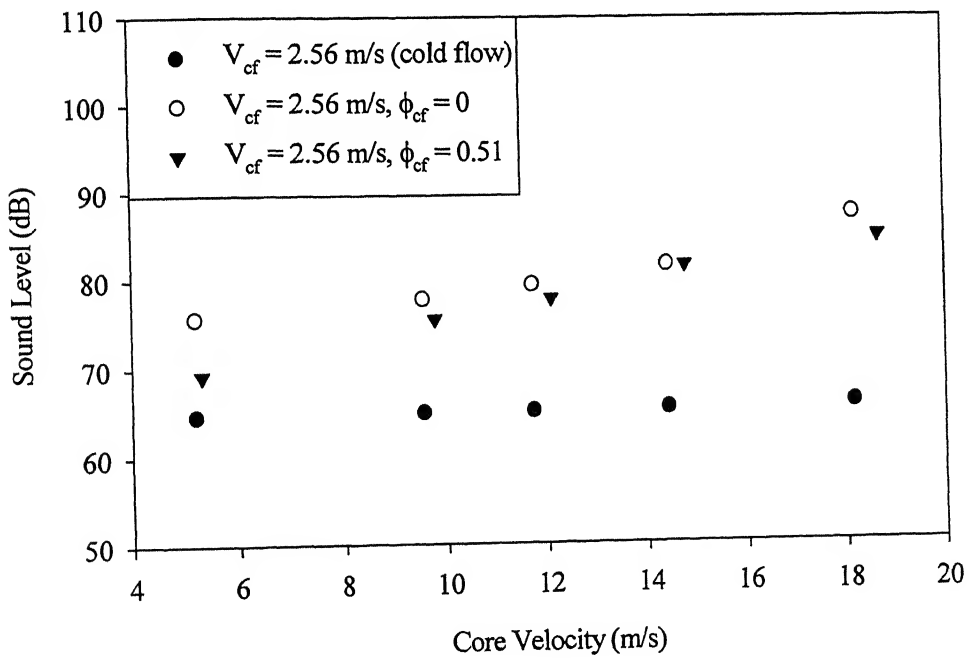


Fig 4.53. Overall sound level for Swirl No. 0.13 with coflow velocity = 2.56 m/s

4.4.7. Overall Sound Pressure Level Measurements

The overall sound pressure level (OSPL) measured at lean stability limit for a swirl number of 0.13 is shown in Fig 4.52 against core velocity for coflow velocity of 1.5 m/s. It can be noted that the sound level is increasing with increase in core velocity for reacting flow. The magnitude of OSPL in case of reacting flow is quite higher than that of cold flow. However, when the coflow velocity increases to 2.56 m/s (see Fig 4.53), the sound level is decreased by approximately 20dB in the region of higher core velocity. But when fuel air mixture is added to the coflow there is a decrease in the sound level.

The overall sound pressure level with core velocity for reacting flow is shown in Fig 4.54 for a swirl number of 0.67. The sound level is increasing with increase in core velocity for both premixed and air coflow streams. In comparison to low swirl number flow, the sound level seems to be decreased marginally. This observation seems to be very interesting which needs to be studied thoroughly in future.

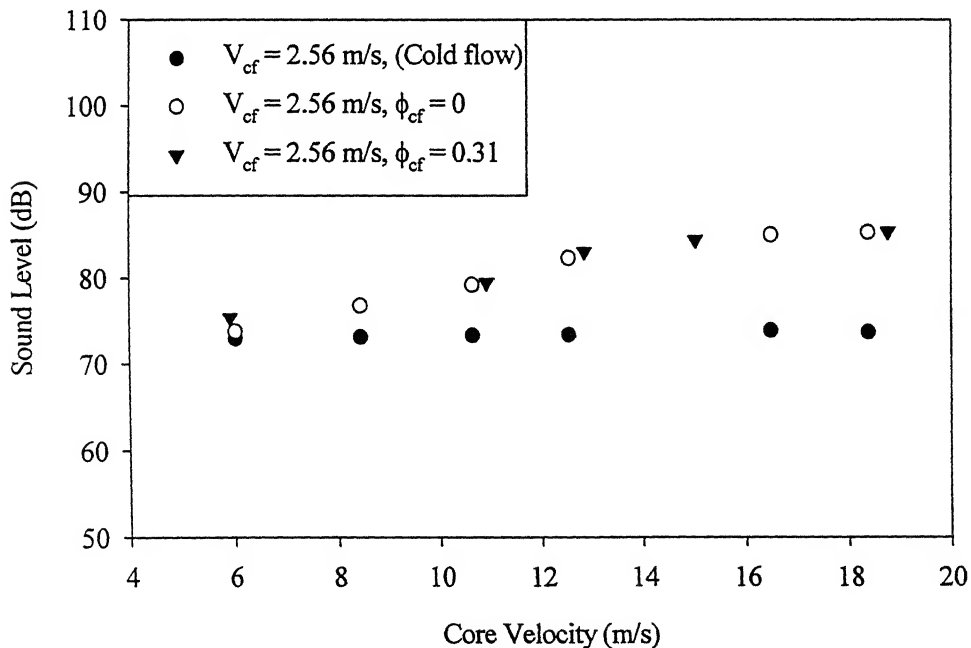


Fig 4.54. Overall sound level for Swirl No. 0.67 with coflow velocity =2.56 m/s

4.5. Uncertainty Analysis

All the measurements are not perfectly accurate; so, some means for describing inaccuracies are needed. A generally agreed and appropriate concept for expressing inaccuracies is an “Uncertainty”. This value should be provided by uncertainty analysis. An uncertainty is not the same as an error. An error in measurement is the difference between the true value and the recorded value; an error is a fixed number and cannot be a statistical variable.

The general procedure for estimating the uncertainties in the calculated quantities using measured data as described below [29,30,31].

Let $x_1, x_2, x_3, \dots, x_i, \dots$ be the independent parameters (variables) in the experimental measurement, and $u_1, u_2, u_3, \dots, u_i, \dots$ be their relative uncertainties. Let, R be the experimental result calculated from the measured data.

The quantity R can be expressed as,

$$R = R(x_1, x_2, x_3, \dots, x_i, \dots, x_n)$$

The effect of error in measuring individual x_i on R may be estimated by analogy to derivative of function.

A small change δx_i in x_i would cause R to vary according to

$$\delta R_i = \frac{\partial R}{\partial x_i} \delta x_i, \quad \text{----- (1)}$$

For applications, it is convenient to normalize the above equation by dividing throughout by R to obtain

$$\frac{\delta R_i}{R} = \frac{1}{R} \frac{\partial R}{\partial x_i} \delta x_i = \frac{x_i}{R} \cdot \frac{\partial R}{\partial x_i} \cdot \frac{\delta x_i}{x_i}, \quad \text{----- (2)}$$

Eq. (2) might be used to estimate the uncertainty intervals in the result R , due to variation in x_i , by substituting the certainty interval for x_i ,

$$u_{x_i} = \frac{x_i}{R} \cdot \frac{\partial R}{\partial x_i} \cdot u_{x_i}, \quad \text{----- (3)}$$

It can be shown that the best representation for the uncertainty interval of the results is

$$u_R = \pm \left[\left(\frac{x_1}{R} \frac{\partial R}{\partial x_1} u_1 \right)^2 + \left(\frac{x_2}{R} \frac{\partial R}{\partial x_2} u_2 \right)^2 + \dots + \left(\frac{x_n}{R} \frac{\partial R}{\partial x_n} u_n \right)^2 \right]^{1/2} \quad \text{---(4)}$$

For stability criteria, Q_{A1} , Q_{A2} , Q_{F1} , Q_{F2} be the variables for determining overall equivalence ratio.

For finding core velocity Q_{A1} , Q_{F1} are the variables.

For $\phi_{ov} = 0.511243$

$$Q_{A1} = 20.8118 + (520.994 * X) - (1114.83 * X * X) + (1760.45 * X * X * X) - (1530.85 * X * X * X * X) + (672.481 * X * X * X * X * X) - (116.421 * X * X * X * X * X) \quad (X \text{ is manometric deflection in m})$$

$$X = 0.717 \text{ m}$$

$$Q_{A1} = 177.1766 \text{ litre/min}$$

$$Q_{A2} = 38.8218 + (1253.88 * X_1) - (3943.35 * X_1 * X_1) + (9602.04 * X_1 * X_1 * X_1) - (12843.5 * X_1 * X_1 * X_1 * X_1) + (8690.64 * X_1 * X_1 * X_1 * X_1 * X_1) - (2317.22 * X_1 * X_1 * X_1 * X_1 * X_1) \quad (X_1 \text{ is manometric deflection in m})$$

$$Q_{A2} = 245.735 \text{ litre/min}$$

$$Q_{F1} = 6.0 \text{ litre/min}$$

$$Q_{F2} = 8.0 \text{ litre/min}$$

It is estimated that the maximum possible error in the measurement of the airflow rate would be,

For Core flow,

$$\text{Air flow rate } (Q_{A1}) \text{ X is } = 0.02 \text{ m}$$

$$\text{Fuel flow rate } (Q_{F1}) = 0.2 \text{ litre/min}$$

For Coflow,

$$\text{Airflow rate } (Q_{A2}) \text{ X}_1 \text{ is } 0.002 \text{ m}$$

$$\text{Fuel flow rate } (Q_{F2}) = 0.3 \text{ litre/min}$$

$$u_{\phi_{ov}} = \pm \sqrt{\left(\frac{Q_{A_1}}{\phi_{ov}} \cdot \frac{\partial \phi_{ov}}{\partial Q_{A_1}} \cdot u_{A_1} \right)^2 + \left(\frac{Q_{A_2}}{\phi_{ov}} \cdot \frac{\partial \phi_{ov}}{\partial Q_{A_2}} \cdot u_{A_2} \right)^2 + \left(\frac{Q_{F_1}}{\phi_{ov}} \cdot \frac{\partial \phi_{ov}}{\partial Q_{F_1}} \cdot u_{F_1} \right)^2 + \left(\frac{Q_{F_2}}{\phi_{ov}} \cdot \frac{\partial \phi_{ov}}{\partial Q_{F_2}} \cdot u_{F_2} \right)^2} \quad (5)$$

$$\phi_{ov} = \frac{(Q_{F_1} + Q_{F_2})}{(Q_{A_1} + Q_{A_2})} / 0.0647517 = 0.511243$$

$$\frac{\partial \phi_{ov}}{\partial Q_{A_1}} = 0.0647517 \cdot (Q_{F_1} + Q_{F_2}) \cdot \frac{(-1)(1)}{(Q_{A_1} + Q_{A_2})^2} = -5.0685138 * 10^{-6}$$

$$\frac{\partial \phi_{ov}}{\partial Q_{A_2}} = 0.0647517 \cdot (Q_{F_1} + Q_{F_2}) \cdot \frac{(-1)}{(Q_{A_1} + Q_{A_2})^2} = -5.0685138 * 10^{-6}$$

$$\frac{\partial \phi_{ov}}{\partial Q_{F_1}} = \frac{0.0647517}{(Q_{A_1} + Q_{A_2})} \cdot (1+0) = 1.5310941 * 10^{-4}$$

$$\frac{\partial \phi_{ov}}{\partial Q_{F_2}} = \frac{0.0647517}{(Q_{A_1} + Q_{A_2})} \cdot (1) = 1.5310941 * 10^{-4}$$

$u_{A_1} = \pm (\text{expected error in } Q_{A_1} \text{ due to } x) / (\text{measured } Q_{A_1}) = 4.33 \%$

$u_{A_2} = \pm (\text{expected error in } Q_{A_2} \text{ due to } x) / (\text{measured } Q_{A_2}) = 3.51 \%$

$u_{F_1} = \pm (\text{expected error in } Q_{F_1} \text{ due to } x) / (\text{measured } Q_{F_1}) = 3.33 \%$

$u_{F_2} = \pm (\text{expected error in } Q_{F_2} \text{ due to } x) / (\text{measured } Q_{F_2}) = 3.75 \%$

The uncertainty in ϕ_{ov} can be obtained with help of Eq. (5)

$$u_{\phi_{ov}} = 0.0157321 = 1.57321 \%$$

4.6. Concluding Remarks

In this thesis, an experimental study on turbulent lean premixed flame based combustor has been carried out extensively. The coaxial premixed flame burner is designed and developed in the laboratory. The measurement systems such as flow meters, temperature and species sampling probe are developed and calibrated. Two types of flame holders such as inlet mounted inverted cone and vane swirlers are employed to stabilize the flame in this burner.

The core velocity is varied from 4 to 20 m/s for a particular coflow velocity. It has been found out that the flame is stabilized at higher equivalence ratio. The effects of coflow velocity on the lean stability limit are explored considering three coflow velocity ($V_{cf} = 0, 1.28$ and 2.56 m/s). It has been observed that the flame is stabilized at lower overall equivalence ratio when coflow velocity is increased. But the emission level is increased with higher coflow velocity. Besides this, the effects of flame holder locations (H/D_{core}) on lean stability limit and emission levels are studied for two $H/D_{core} = 0.61$ and 5.0 . It has been found out that higher flame holder position improves the flame stability, but with increase in NO emission level. In order to reduce the emission level, the fuel-air mixture is injected in the coflow stream instead of air. The stability limit is improved marginally for $H/D_{core} = 5.0$ when the premixed mixture is used in the coflow stream. Interestingly, this partially premixed fuel injection in the coflow stream although reduces the NO emission level, but produces little more CO emission.

In the case of swirl burner, the vane swirler is placed in the coflow stream for stabilizing the flame. The vane angle such as $10^\circ, 40^\circ$ have been employed for generating a swirl number of 0.13 and 0.67 respectively. The effect of swirl flow on the lean stability as well as emission levels have been explored for two coflow velocities ($V_{cf}=1.5$ & 2.56 m/s). It has been found that there is an improvement of the stability limit and CO emission level for high swirl number (0.67) case as compared to low swirl number (0.13). On the contrary, the NO emission level is increased considerably due to the higher temperature prevailing in the burner. In order to improve the flame stability and emission level further, fuel-air mixture

instead of air is injected into the coflow port. For lower coflow velocity, the stability and CO emission level for lower swirl number show slight improvement due to presence of improved fuel distribution. The CO emission level is increasing in the case of lower swirl number with higher coflow velocity ($V_{cf} = 2.56$). In the case of low swirl number, the NO emission is improved with addition of fuel-air mixture to the coflow. But, the NO emission does not show any significant change in the higher swirl number. However, the CO emission level is improved for the case of higher swirl number with higher coflow velocity. Besides this, efforts are made to measure overall sound pressure level using microphone based sound level meter for both cold and reacting flow. Interestingly, the sound level is increased significantly when combustion takes place. With increase in coflow velocity, the sound level decreases significantly particularly at higher core flow velocity. However, it seems that the swirl number does not have much effect on the sound level. It has also been found out that the swirl flames generates more NO emissions as compared to the bluff body-stabilized flame.

4.7. Suggestions For Future Work

The following investigations may be suggested for future work.

1. Suitable flow visualization can be employed in order to unravel the actual mechanism of flame stabilization.
2. The effects of turbulence level on the flame stability can be explored.
3. Lean stability and emission can also be studied for higher swirl number.
4. Instead of bluff body, opposed reacting jet can be used for flame stabilization.
5. The effect of lean stability and emission level can be explored with the help of the preheated air as well as prevaporized combustor.
6. The coflow velocity can be varied with core velocity in a fixed ratio to the core flow to study the lean stability limit as well as the emission level.
7. Combustion instability analysis for the swirl stabilized flame.

REFERENCES

1. R.E.Jones, "Gas Turbine Engine Emissions-Problems, Progress and Future", Progress in Energy and Combustion Science, Vol-4, 73-113, 1978
2. Strahle, Warren. , "Introduction to Combustion", Combustion and Science Technology Book Series, Vol-1, 1993.
3. J.M.Beer and N.A.Chigier, "Combustion Aerodynamics", John Wiley & Sons, Inc., 1972.
4. R.W.Schefer and R.F.Sawyer, "Lean premixed recirculating flow combustion for control of oxides of Nitrogen", Sixteenth Symposium (International) on Combustion, The Combustion Institute, pp119-134, 1977.
5. G.C.Williams, H.C.Hottel, and A.C.Scurlock, " Flame Stabilization and Propagation in high velocity gas streams", Third Symposium (International) on combustion Flame and Explosion Phenomena, pp 21-49,Williams and Wilkins and Baltimore, 1949.
6. F. H. Wright and E. E. Zukoski, " Flame spreading from bluff body flame holders" Fifth Symposium (International) on Combustion, The Combustion Institute, pp 933-978, 1955.
7. E.E.Zukoski and F.E.Marble, "The Role of Wake Transition in the process of Flame Stabilization on Bluff bodies", Combustion Researches and Reviews, AGARD, Butterworth, London, pp 167-180, 1955.
8. T.A.Bovina, "Studies of Exchange between Recirculation zone behind the flame holder and Outer flow", Seventh Symposium (International) on combustion, The Combustion Institute, pp 692-696, 1959.
9. R.A.Jeffs, "The flame stability and heat release rates of some can-type combustion chambers", Eighth Symposium (International) on Combustion, The Combustion Institute, pp 1014-1027, 1960.
10. F.Filippi and L.Fabbrovich-Mazza, "Control of bluff-body flame holder stability limits", Eighth Symposium (International) on Combustion, The Combustion Institute, pp956-963, 1960.
11. G.Winterfeld, "On process of Turbulent Exchange behind Flame holders", 10th Symposium (International) on Combustion, The Combustion Institute, pp 1265-1275, 1965.

12. N.A.Chigier and A.Chevinsky, "Experimental Investigation of Swirling Vortex motion in Jets", Journal of Applied Mechanics, Trans ASME, pp 443-451, June 1967.
13. N.Syred, N.A.Chigier, and J.M.Beer, "Flame stabilization in recirculation zones of jets with swirl", Thirteenth Symposium (International) on Combustion, The Combustion Institute, pp617-624, 1971.
14. N.Syred and J.M. Beer, "Effect of Combustion upon Precessing Vortex Cores generated by Swirl Combustors", Fourteenth Symposium (International) on combustion, The Combustion Institute, pp 537-540, 1973.
15. A.Mestre and A.Benoit, "Combustion in Swirling Flow", Fourteenth Symposium (International) on combustion, The Combustion Institute, pp 719-725, 1973.
16. Andre Mestre, "Efficiency and Pollutant formation studies in a swirling flow combustor", Fluid mechanics of combustion; Joint fluids Engineering and CSME conference, Montreal, pp 89-96, 1974.
17. G.A.Karim, I.Wierzba, M.Metwally and K.Mohan, "The combustion of a fuel jet in a stream of lean gaseous fuel-air mixtures", Eighteenth Symposium (International) on Combustion, The Combustion Institute, pp 977-991, 1981.
18. N.Negishi, "Lean premixture combustion on a coaxial burner", Nineteenth Symposium (International) on Combustion, The Combustion Institute, pp 441-447, 1982.
19. Yukio Mizutani and Masashi Satomura, " Combustion of ultra-lean combustible mixture in a heat recirculation type cyclone furnace system ", Nineteenth Symposium (International) on Combustion, The Combustion Institute, pp599-536, 1982.
20. Ruey-Hung Chen, and James F.Driscoll, " The role of the recirculation vortex in improving Fuel-air Mixing within Swirling flames", Twenty-second Symposium (International) on combustion, The Combustion Institute, pp 531-540, 1988.
21. Thomas F.Fric, "Effect of Fuel-Air Unmixedness on NO_x emissions", Journal of Propulsion and Power, Vol.9, No.5, pp 708-713, Sep-Oct, 1993.
22. Nils A.Rokke, John E.Hustad and Otto K.Sonju, "A study of partially premixed unconfined propane flames", combustion and flame vol-97, pp88-1069, 1994.

23. Yoshiaki Onuma, Masaharu Morikawa, Tsuyoshi Takeuchi and Susumu Noda,” “The stabilization of fuel-lean premixed combustion by a cyclone combustor”, Eighth International Symposium on Transport phenomena in combustion, vol-1, pp617-628, 1995.
24. Wataru Fujisaki, Masaru Takei, Toshiji Amano and Koji Hase, “Combustion characteristics of an ultra low NO_x two stage premixed combustor”, Eighth International Symposium on Transport phenomena in combustion, vol-2, pp1238-1249, 1995.
25. Lin Xie, Shigeru Hayashi and Kohichi Hirose, “ NO_x Formation in turbulent lean-premixed combustion with minimum heat losses”, Twenty-Sixth Symposium (International) on combustion, The Combustion Institute, pp2155-2160, 1996.
26. Zhuang Shu, Suresh K. Aggarwal, Viswanath R. Katta, and Ishwar K. Puri, “Flame-Vortex Dynamics in an inverse Partially Premixed Combustor: The Froude Number Effects”, Combustion and Flame, Vol-111, pp 276-295, 1997.
27. J.C. Hermanson, M.B. Coklet and J.J. Sangiovanni, “Stability and Emissions of lean turbulent premixed flames with very lean coflow”, AIAA journal, Vol-35, No-11, pp1705-1711, November 1997.
28. J.M. Samaniego and T. Mantel, “Fundamental mechanisms in premixed turbulent flame propagation Via Flame-Vortex Interactions, Part I: Experiment”, Combustion and Flame, vol-118, pp537-556, 1999.
29. E. Rathakrishnan, “Instrumentation Measurements and Experiments in Fluids”, to be published.
30. S.J. Kline, “The Purpose of Uncertainty Analysis”, Trans ASME, Journal of Fluids Engineering, Vol-107, pp153-160, June 1985.
31. R.J. Moffat, “Using Uncertainty Analysis in the Planning of an Experiment”, Trans ASME, Journal of Fluids Engineering, Vol-107, pp173-178, June 1985.

137903



A137903